UNIVERSITÀ DEGLI STUDI DI MILANO

PhD course in Environmental Science

XXXI Cycle

Laminopathies : pathology, cell mechanics and environmental induction

Supervisor: Prof. Caterina LA PORTA

PhD Candidate:
Maria Chiara LIONETTI
Matr. R11292

Academic years 2015 / 2018

ABSTRACT

The nuclear lamina (NL) is a fibrillary protein network lining the inner surface of the nuclear envelope. It is mainly composed by type V intermediate filaments called lamins and lamin-associated proteins. Three lamin genes are present in Mammals: LMNA, which encodes lamin A and lamin C (A-type lamins), as well as, LMNB1 and LMNB2 that encode lamin B1 and B2 (B-type lamins) respectively. Lamins and LAPs associate to form a dense and dynamic three-dimensional matrix that establishes a huge number of stable and transient interactions with different classes of molecules: DNA, transcription factors, nuclear pore complexes and structural proteins of the cytoskeleton. All of these interactions are essential to provide nuclear structural stability and integrity, to physically and functionally link nuclear lamina to the cytoskeleton and to organizes chromatin. Thus NL, in addition to play a fundamental structural role, it is also a key player in cellular mechanotransduction processes and gene expression and epigenetic regulation.

Mutations in genes encoding for lamins are associated with a wide a range of diseases, named laminopathies. Among these, the most interesting one is Hutchison-Gilford Progeria Syndrome (HGPS), a rare fatal genetic disorder due to do a point mutation in LMNA. This mutation results in the production of a truncated version of lamina A, lacking 50 amino acids, known as Progerin. HGPS is mainly characterized by morphological changes in the nucleus and premature aging. HGPS patients indeed, from their first years of life, develop pathological conditions typical of the elderly such as cataracts, diabetes and osteoporosis while preserving the normal cognitive functions. These patients typically die from cardiovascular complications around 14 years of age, on average.

Considering Hutchinson-Guilford Progeria Syndrome as an extreme example of what nuclear lamina aberration entails, during my PhD I investigated many aspects of nuclear lamina biology with particular regard to the impact of nuclear lamina structural perturbations on cell functions, mechanics, gene expression regulation and the interconnection existing between nuclear lamina integrity, ageing process and oxidative stress.

Indeed, to gain a comprehensive picture of nuclear lamina biology in health and disease, it has been adopted interdisciplinary and integrative research strategies able to take into account structural, mechanical and molecular aspects.

Bioinformatics study has been performed: public available transcriptomic data of HGPS patients have been analysed with respect of those of healthy matched controls. This analysis allowed to delineate the typical global gene expression profile of HGPS patients and to identify all the deregulated pathways in the presence of the pathology.

Moreover, impacts of lamina alterations on its physical and functional connections with extra-nuclear and nuclear elements have been studied in an inducible expression cellular model of the mutated form of Lamin A responsible for HGPS. This cellular model faithfully recapitulates the peculiar cellular phenotype of the HGPS patients resulting to be a valid alternative to primary cell lines deriving from the patients.

Finally, the interdependence between oxidative stress, ageing and lamins has been investigated in a novel oxidative stress cellular model developed in our laboratory, that is also efficient in recapitulating typical ageing profile.

RIASSUNTO

La lamina nucleare (NL) è un reticolo di proteine fibrillari che riveste la superficie interna della membrana nucleare. Essa è principalmente composta da filamenti intermedi di tipo V , chiamati lamìne, e proteine ausiliari ad esse associate (lamin-associated proteins, LAPs). Nei mammiferi le lamìne sono codificate da tre geni : LMNA, che codifica per la lamìna A e lamìna C (lamìne di tipo A), LMNB1 e LMNB2 che codificano rispettivamente per la lamìna B1 e B2 (lamìne di tipo B). Lamìne e LAPs si associano a formare una matrice tridimensionale densa e dinamica che stabilisce numerose interazioni, sia stabili che transitorie, con diverse classi di molecole biologiche: DNA, fattori di trascrizione, proteine strutturali. Tutte queste interazioni sono essenziali per fornire stabilità strutturale e preservare l'integrità nucleare, per collegare fisicamente e funzionalmente la lamina nucleare al citoscheletro e per organizzare la cromatina. In questo modo, oltre a svolgere un ruolo strutturale fondamentale, la lamina nucleare risulta ricoprire ruoli chiave anche nei processi di meccanotrasduzione del segnale e nella regolazione dell'espressione genica ed epigenetica.

Mutazioni a carico dei geni che codificano per le lamìne nucleari sono associate ad un'ampia ed etogenea classe di patologie note come laminopatie. Tra queste, una delle più controverse ed interessanti è la Hutchison-Gillford Progeria Syndrome (HGPS), una malattia genetica rara dovuta a una mutazione puntiforme nel gene LMNA. Tale mutazione risulta nella produzione di una versione tronca della lamìna A, mancante di 50 amminoacidi, conosciuta come Progerina. HGPS è principalmente caratterizzata da alterazioni morfologiche del nucleo e invecchiamento precoce. I soggetti affetti da Progeria, infatti, fin dai primi anni di vita sviluppano condizioni patologiche tipiche dell'età senile quali cataratta, diabete e l'osteoporosi pur preservando le normali funzioni congnitive. Questi pazienti muoiono tipicamente per complicanze cardiovascolari intorno ai 14 anni di età, in media.

Considerando la sindrome di Hutchinson-Guilford come un esempio estremo di ciò che alterazioni della lamina nucleare comportano, durante il mio dottorato di ricerca ho investigato diversi aspetti riguardanti la biologia della lamina nucleare con particolare interesse all'impatto che perturbazioni strutturali della lamina nucleare possono avere sulle normali funzioni cellulari, la meccanica cellulare, la regolazione dell'espressione genica e l' interconnessione esistente tra integrità della lamina nucleare, processo di invecchiamento e stress ossidativo.

Per ottenere una visione d'insieme del contributo della lamina nucleare sia in condizioni fisiologiche che patologiche, sono state adottate strategie di ricerca basate su approcci interdisciplinari e integrativi in grado di tenere conto degli aspetti strutturali, meccanici e molecolari.

Per fa questo, in prima instanza sono state effetuate delle analisi bionformatiche: tutti i dati di trascrittomica relativi a pazienti HGPS, presenti in database pubblici e in letteratura, sono stati raccolti e analizzati rispetto a dati equivalenti ottenuti da controlli sani.

Tale analisi ha permesso di delineare profilo di espressione genica tipico di pazienti HGPS e di individuare i pathways deregolati in presenza della patologia.

È stato inoltre studiato l'impatto che alterazioni della lamina nucleare hanno sulle connessioni fisiche e funzionali che questa stabilisce sia con elementi nucleari ed extra-nucleari, in un modello cellulare in cui è possibile indurre sperimentalmente, in modo controllato, l'espressione della forma mutata di Lamìn A responsabile dell' HGPS. Tale modello cellulare ricapitola fedelmente il peculiare fenotipo cellulare dei pazienti risultando essere una valida alternativa all'utilizzo di linee primarie derivanti dai pazienti.

Infine, l'interdipendenza tra stress ossidativo, invecchiamento e lamìne nucleari è stata investigata in un nuovo modello cellulare di stress ossidativo sviluppato nel nostro laboratorio, efficiente nel ricapitolare il processo di invecchiamento, *in vitro*.

Contents

Introduction **2**

I. 1 Nuclear Lamina : an overview 2

I. 2 Laminopathies 10

I. 3 Nuclear Lamina, Oxidative Stress and Ageing 14

Outline **17**

1 Pathway deregulation analysis in Hutchinson-Gilford Progeria Syndrome **19**

Figures 25

2 Effects of Progerin on nuclear cell plasticity **36**

Figures 46

3 Sulforaphane can not protect the cells to a repeated, short and sublethal treatment with hydrogen peroxide **56**

Figures 63

Concluding remarks and future perspectives **70**

Final report **72**

Bibliography **77**

Introduction

I. 1 Nuclear Lamina : an overview

The nuclear lamina (NL) is a well conserved cellular structure, present in all nucleated cells of metazoa. NL is a thin, filamentous protein meshwork composed of nuclear lamins (Lamin A, C and B) and lamin-associated proteins (LAPs), that line the inner surface of the nuclear envelope (NE) forming a sort of 3D nuclear matrix which basically acts both as nuclear scaffold, providing to the nucleus mechanical stability, and as a dynamic interface between the NE and the residing DNA. Firstly characterized from the ultrastructural point of view in amphibian oocytes [31], NL has been more recently also widely investigated in mammalian cells (all reviewed in [20]). It is now well known that NL composition and architecture varies among various organisms, from one tissue to another and during time (i.e. cell development and differentiation). For example, while in amphibian oocytes NL is an ordered 10 nm filaments network arranged in a regular woven meshwork pattern, in mammalian cells it has an irregular pattern and resulted to be non-homogeneously distributed along nuclear inner surface but rather organised in alternate patches with high or low lamins concentration, with a thickness ranging from 30 to 100 nm. NL is crucial for several structural and functional cellular processes: it provides nuclear structural stability [88], it maintains nuclear shape and volume [56], preserves intranuclear protein localization, organizes nuclear pore complexes (NPCs) [31] and, since it serves as anchoring point for chromatin and transcription factors [21] at the nuclear periphery, it actively participates in chromatin modelling and gene regulation [94]. Moreover, NL is also involved in signal transduction between nucleus and cytoskeleton [44], cell cycle regulation [26], cell development and differentiation, cell migration, and apoptosis[6]. The first notions of the nuclear lamina functional and structural peculiarities derive from some studies in Xenopus laevis oocytes and Drosophila melanogaster. In the early 90's, it has been widely reported that NL can bind chromatin. In particular, it has been observed that a fraction of chromatin appears

to be in close proximity to the lamina during interphase [26] and that the binding of lamins to decondensing chromosomes after mitosis is an initial critical step in nuclear reassembly in both mammalian and Drosophila cell-free systems [65]. In addition, an intact lamina is required for DNA replication in nuclei formed from extracts of Xenopus laevis oocytes [15]. If the Xenopus oocyte nuclear lamin protein is removed from the extracts, nuclei still form but are unable to replicate DNA [15]. In addition, it has been isolated a Drosophila mutant which is defective in producing wild type lamin Dmo showing impaired viability, fertility, and locomotion. Ultrastructural analysis of these mutants central nervous system revealed that lamin Dm0 deficiency strongly affected structural integrity of the nuclear envelope and the proper integration of NPCs into the nuclear membrane [69]. Similar results have been obtained in Lmna knockout mice where it has been observed that Lmna-/- slower growth after birth if compared to the control group and mutant mice death by 5-6 weeks of age, with histologic evidence of muscular dystrophy, cell nuclei aberrations and structurally weakened nuclear envelopes [88]. The functional importance of lamins is further supported by the finding that structural changes in the lamina in human are among the most dramatic hallmarks of differentiation, cancer[6] and aging.

I. 1.1 Architecture and structural role

Lamins are the main components of nuclear lamina. These are 60 to 80 kDa proteins belonging to the superfamily of intermediate filament mainly consisting of a globular amino-terminal domain (head) followed by a long α-helical rod domain and a carboxy-terminal domain (tail) (Figure 1).

The central α-helical or rod domain represents approximately half of the lamin molecule (about 350 residues) and comprises four α-helical segments (1A, 1B, 2A and 2B), each one having a heptad-repeat periodicity and connected by short intervening subdomains (L1, L12 and L2). The C-terminal tail domain contains a nuclear localization signal (NLS) required for the transport of lamins into the nucleus, an immunoglobulin-like structural motif (Ig-fold) and a -CAAX box, fundamental for post-translational processing of lamins. Lamins are divided into A-type and B-type lamins based on sequence homologies. Mammalian genome contains three lamin genes: LMNA, LMNB1 and LMNB2. LMNA gene encode for Lamin A and for Lamin C, an alternative splicing gene product (A-type lamins) while B-type lamins (Lamin B1 and Lamin B2) are respectively encoded by LMNB1 and LMNB2 genes. A-Type Lamins are mainly expressed at later stages of development and in differentiated cells, B-types lamins are

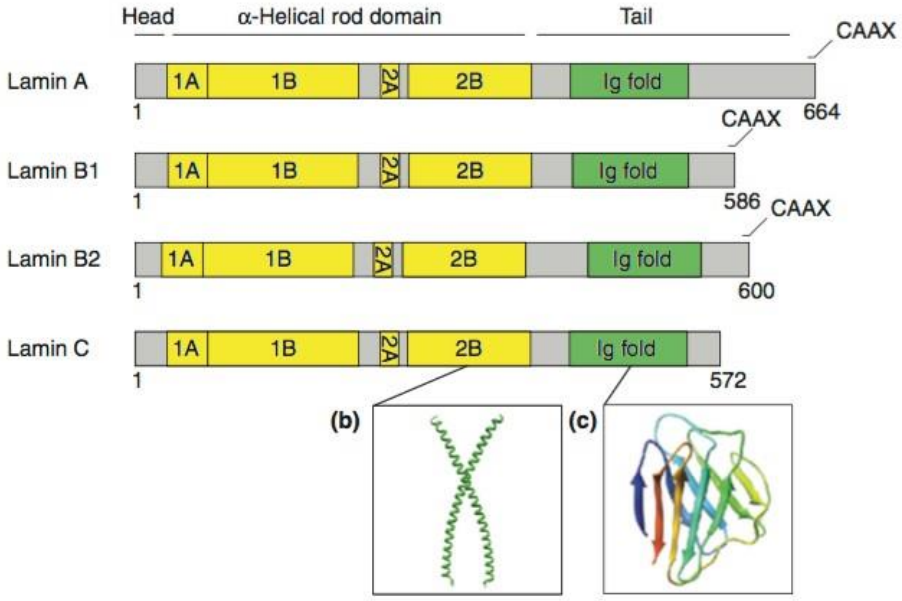

Figure 1: **Domain organization of Nuclear Lamins in human and molecular 3D structure of alfa-domain of Rod Domain and Ig Fold domain** [22]

constitutively expressed. There are also three minor lamins isoforms : AΔ10 [62], C2 (germ line specific) and B3 [81]. Initially expressed as pre-lamins, nuclear lamins need a cascade series of post-translational modification of their carboxy-terminal -CAAX motif to reach the mature form. Lamins processing takes place in a highly regulated temporal sequence starting with the farnesylation of the cysteine residue of the -CAAX box, followed by -AAX removal by an endopeptidase, most likely Rce1 (Ras-converting enzyme 1) and/or Zmpste24 (Zinc metalloprotease related to Ste24p)/FACE1 [99] and a cysteine residue carboxymethylation catalyzed by the enzyme isoprenylcysteine carboxyl methyltransferase (Icmt). While B-type lamins maturation terms at this processing stage, resulting in their permanent farnesylation and carboxymethylation, Lamin A needs further processing steps. Indeed, to form mature Lamin A the removal of additional 15 amino acids from its C-terminus, including the farnesylated/carboxymethylated cysteine residue is required. Lamin A and lamin C are exactly identical for 566 amino acids but lamin C lacks of 98 amino acids at the C-terminal domain respect to Lamin A. Thus, the main difference between these two A-type lamins is that Lamin C has no -CAAX box at its C-term domain.Once post-transcriptionally processed, lamins dimerize through their coiled-coil heptad repeat pattern present in the rod domain forming the basic building blocks of higher-ordered lamin assemblies. Then, lamins dimers associate one to another in a polar head-to-tail manner obtaining lamins polymers that in turn, through anti-parallel association of two of these form

lamin protofilaments. Finally, between three and four protofilaments associate laterally to form an intermediate filament of about 10 nm in diameter (Figure 2).

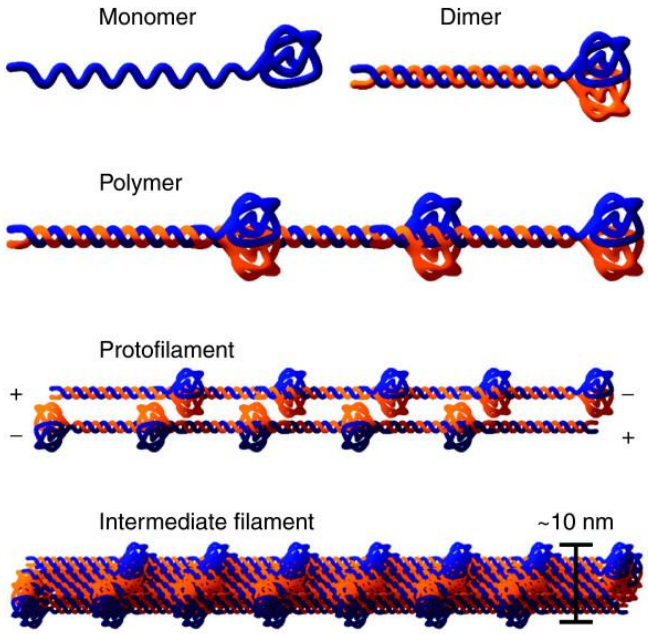

Figure 2: **Schematic representation of model of lamin polymerization process** [22]

The nuclear lamina assembly process has been widely studied. Some in vitro studies conducted in bacteria expressing full-length and truncated lamin isoforms have revealed that both the N- and C-terminal end domains are fundamental for the proper filament formation: N-terminal head domain seems to promote lateral association of protofilaments and ultimately 10-nm filaments, while the C-terminal tail domain controls lateral assembly of protofilaments. However in vivo significance is far from the light nowadays.

Interactions between A and B-type lamins are possible and necessary. As emerged from in vitro binding assay, pre-Lamin A, Lamin A, Lamin B1 and lamin C can form homo- and heterodimers when ectopically expressed in yeast [22]. Affinity chromatography with purified lamins protein experiments also confirmed this result revealing that Lamin A and C could directly interact with Lamin B in a heterotypic association occurring through a single binding site, present at the N-term domain of Lamins A/C. Interestingly, some heterotypic lamins dimers associations, such as B-A and B-C lamins, are stronger than heterotypic C-A, and homotypic B-B and C-C. Some post-translational modification may strongly influence this strength of interaction. For instance, phosphorylation of Lamin B causes a decrease in affinity for Lamin A/C and, at the same time, an increased affinity for itself. This peculiar kind of lamins affinity regulation by phosphorylation events has a strong impact on NL architecture and dynamics.

Indeed, since phosphorylation events can manage and regulate the degree of heterotypic versus homotypic association, they play a pivotal role in Nuclear Envelope break down process and re-assembly that typically occurs during cell division.

I. 1.2 Functional roles

Nuclear Lamina and chromatin interaction

Tight apposition of a layer of condensed chromatin adjacent to the NL has been observed with early electron microscopy [25]. Following, DNA fluorescence in situ hybridization (FISH) revealed the presence of some genomic loci at the nuclear periphery, as also confirmed by DNA adenine methyltransferase identification (DamID) experiments on several different cell types. In particular, DamID technique gave as result a global chromatin association profiles of NL components revealing that about 40% of the human genome is organized into about 1300 lamin-associated domains (LADs), ranging from 10 kb to more than 10 Mb (Figure 3). Interestingly, while some hundreds of genome regions change their association with NL in time (facultative LADs) [61], most LADs are permanently associated with NL ("constitutive LADs"), in all the analysed cell types [67].

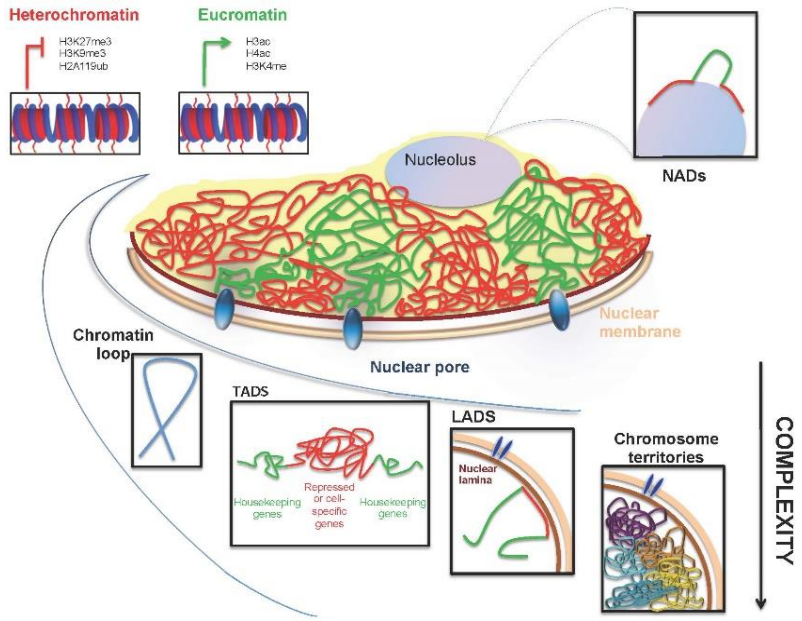

Figure 3: **Schematic representation of nuclear architecture and different levels of complexity of NL-chromatin interactions** [4]

In the light of these early experimental observations, LADs caught the researchers' attention for two main reasons. First, NL-LADs association may help in establish proper chromosome

topology. Second, several different genes found in LADs show very low expression levels suggesting LADs involvement in gene expression regulation, mainly gene repression. Indeed, it has been widely reported that LADs exhibit several molecular feature typical of transcriptionally inactive chromatin, such as histone modifications H3K9me2 and H3K9me3 typical of heterochromatin [35], the facultative heterochromatin mark H3K27me3 and telomeric region markers typical of the so-called pericentromeric heterochromatin. As expected, LAD are also not enriched in DNA methylation [3]. Accordingly, it has also been referred that chromatin detachment from the NL is frequently accompanied by gene activation while attachment to the NL is frequently accompanied by gene inactivation [75]. Thus, NL proteins must be involved in NL - LAD interactions and lamins are the more obvious candidates for this function. Some ChIP studies have suggested that Lamin A/C have binding sites in inter-LAD regions [29, 61] and some other experimental evidences show that B-type lamin depletion, in Drosophila, causes chromatin detachment from the NL [85]. Nevertheless, although A- and B-type lamins differ in their subcellular distribution, Lamin A and Lamin B1 DamID profiles are almost identical [47]. Accordingly, Lamin A knockdown leads to increased interaction of LADs with Lamin B [84]. Moreover, concerning lamins involvement in gene expression regulation, it has been recently reported that the Polycomb group (PcG) proteins directly interact with Lamin A/C [64]. PcG proteins are transcriptional repressors, present predominantly in the nucleus as multimeric protein complexes named Polycomb repressive complexes (PRCs) [82]. These complexes are able to post-translationally modify histones and silence target genes acting as key epigenetic regulators of the most important cellular processes. Notably, what it has been show is that Lamin A/C is fundamental for correct PcG protein nuclear compartmentalization and functioning since Lamin A depletion resulted in impaired PcG mediated transcriptional repression (Figure 4) [13].

However, since deletion of all lamins in mouse embryonic stem cells has no evident effects on DNA-NL association, this suggest that not only lamins mediate NL-LADs association but there are also some other NL components involved. Among these, Nuclear Envelope Transmembrane proteins (NETs) whose depletion or overexpression can alter chromosome localization [95] [60]. For instance, it has been discovered that Lamin B receptor (LBR), one of the most important member of the NET proteins family, can directly bind to heterochromatin via its Tudor domain and that Emerin, another member of the NET family, is required as cofactor in Lamin A/C-DNA association to efficiently anchor chromatin to the NL [52] In particular, Emerin has been reported to interact with LADs [48][35]tethering chromatin to the NL since it interacts with NL proteins as well as chromatin components [2]. Interestingly, epidermal stem cells expose

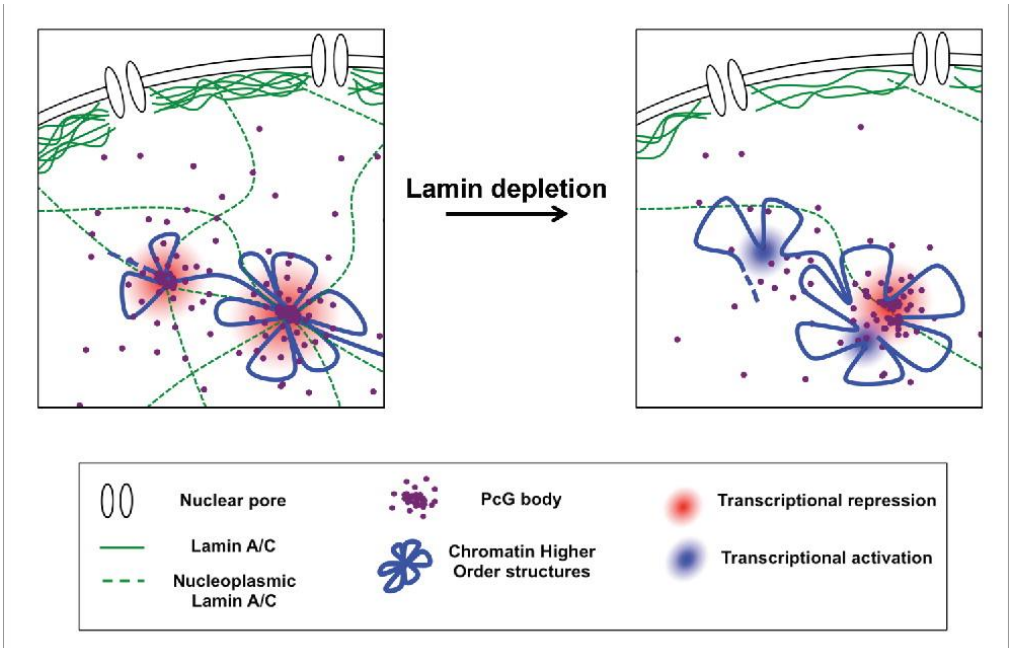

Figure 4: **Schematic rapresentation of the molecular mechanism underlying PcG/Lamin A interplay [13]**.

to mechanical strain showed Emerin redistribution from the inner nuclear membrane to the endoplasmic reticulum [76], followed by partial replacement of H3K9me2/3 by H3K27me3 histone modification and changes in chromosome positioning inside the nucleus suggesting emerin involvement in mechanosensory pathway signalling to heterochromatin [98]. Thus, several NL proteins such as lamins, LBR, and emerin are components of a scaffold to which LADs are anchored and that actively contribute to gene expression regulation [1].

Nuclear lamina role in cell mechanics

Cells are flexible building blocks of tissues that interact with each other in a dynamic fashion and are continuously subjected to various kinds of mechanicals stress that mainly include deformations by compression and stretching [44]. In the light of this, it appears clear that cells must be able to face up to these various mechanical stimuli and adapt to them in order to sustain their living functions.

Mechanotransduction is the process through which environmental mechanical stimuli generate cellular signalling events. The main mediator of this process is the cytoskeleton that, because of its structural qualities, acts as a conductive-viscoelastic material transmitting force and propagating stress within and between cells [46]. In this scenario, cell nucleus should not be thought as an independent entity, rather it is closely linked to the cytoskeleton both me-

chanically and functionally through NL and LINC complex (Linker of the Nucleoskeleton and the Cytoskeleton)(Figure 5).

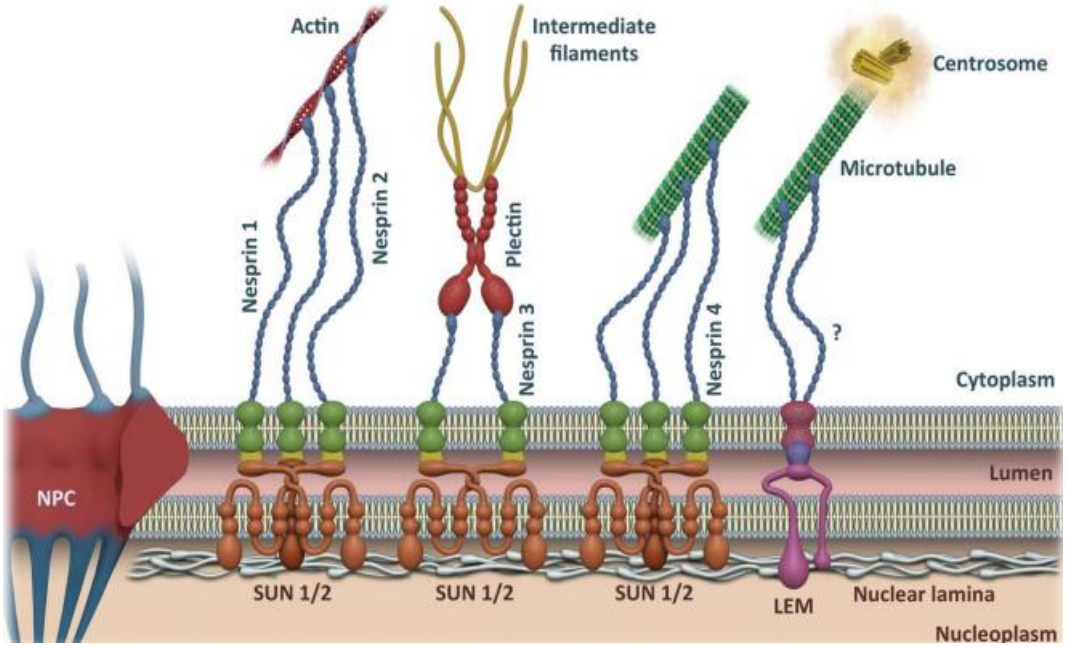

Figure 5: **LINC complex representation** [23]

Morphological changes to the nucleus in response to force were observed over 80-years ago [36, 63]. It has been widely reported that external mechanical stimuli impact on nuclear positioning [37], nuclear morphology [36, 70], and gene activity suggesting the presence of a cell's mechanotransduction pathways that orchestrate nuclear responses [33]. The LINC complex links nucleoskeleton and cytoskeleton and it mainly consists of two major lamin-interacting transmembrane proteins SUN1/SUN2 and Nesprin family proteins [16, 39]. Nesprins are high molecular weight proteins associated with the nuclear membrane [103]. There are 4 different nesprin proteins isoforms currently described: Nesprin-1 [101], Nesprin-2 [102, 54], Nesprin-3 [97] and Nesprin-4. These associate with the inner or outer nuclear membrane depending on their size. In particular, the larger isoforms, nesprin-1 and -2, associate with the outer nuclear membrane exposing the N-term domain towards the cytoplasm and binds to microfilaments [16], and intermediate filaments [44]. In this way, they ensure nucleus-to-cytoskeleton connection providing a strong anchorage of the nuclear membrane to the cytoskeleton that is essential for migration and correct localization of the nucleus inside the cell. At the same time, smaller Nesprin-1isoform is present at the inner nuclear membrane where directly binds to Lamin A/C and emerin [43], a nuclear envelope transmembrane protein involved in NL-chromatin interaction [53]. SUN-proteins associated with the inner nuclear membrane, with

their carboxy-terminus in the perinuclear space, and their amino-terminus in the nuclear interior [58] SUN proteins are necessary for the correct localization of nesprins to the nuclear envelope, and can directly bind to lamins A/C [44]. Notably, The LINC complex has been implicated in serving functions important for nuclear migration[27], positioning and morphology. This evidence aligns with the current idea that lamina is essential for maintenance not only of nuclear shape but also nuclear stiffness and structural integrity. NL and lamins play also another crucial role in cell and tissue mechanics since cellular, and thus tissue stiffness depends on A-type: B-type lamins stoichiometry [90] This can be derived from the fact that different mutations in the genes for lamina proteins such as A- and B-type lamins, and emerin are associated with a series of pathologies that are, among others, characterized by a reduced resilience to mechanical stress[73]. Proteomic analysis revealed that Lamin A is 30 fold more abundant in stiff tissue, such as cartilage, in comparison with soft tissue as brain or adipose tissue where Lamin B is the dominant isoform [90, 89]. Consistently, micropipette aspiration experiment performed on knocked down lamin-A human cells showed that knockdown nuclei are softer [17]. Collagens in the extracellular matrix (ECM) are a key determinant of tissue stiffness and scale with tissue stiffness whereas Lamin A levels respond to changes in tissue elasticity [89]. Accordingly, when experimentally expose to mechanical stress stimuli on longer time scales (hours-days), the nucleus can alter its stiffness to reflect the stiffness of the cellular microenvironment [89]. This stiffness regulation seems to be mainly due to Lamin A solubilisation which is mediated by stress-dependent phosphorylation events: low mechanical stress favours Lamin A phosphorylation and possibly Lamin A solubilisation.

I. 2 Laminopathies

Nuclear lamina is an essential component of metazoan cells since it is involved in most nuclear activities including DNA replication, RNA transcription, nuclear and chromatin organization, cell cycle regulation, cell development and differentiation, nuclear migration and mechanotransduction, as previously reported. In the last three decades, the interest for NL and its components has exponentially grown because of the discovery of several mutations in genes encoding for lamins which are responsible for the onset of the so called laminopathies [5, 83, 8, 68]. Laminopathies are 17 genetic disorders with a broad clinical spectrum, all caused by mutations in lamins or in lamins functional-related genes. Laminopathies can be classified depending on the affected tissue and depending on the gene in which the causative mutation occurs. Indeed,

laminopathies can be tissue-specific, if the mutation affects somatic cells belonging to a certain tissue, or systemic, if mutation affects all or almost all cell types [100]. Moreover, they can be classified as primary laminopathies, referred to those caused by mutations on Lamin A or secondary laminopathies, those due to mutations in B-type lamins genes, prelamin processing proteins (such as Zmpste24) or lamin binding proteins (i.e. emerin). Notably, about 90% of the mutations causing laminopathies occurs in LMNA gene and more than 400 mutations in the Lamin A gene have been identified from patients [93]. Each mutation has a very wide range of phenotypes, and the genetic features vary such that in some cases function is gained, while in others function is lost. However, what is common among all these pathologies is that the cell nuclei of affected people have abnormally shaped nuclear envelopes showing herniations or honeycomb structures of the lamina and the lamin-associated proteins [11], resulting in mechanically weakened nuclei that rupture more easily under mechanical loading [80] [50]. These effects on the nuclei however, are not sufficient to completely explain the general cell functions impairment observed in affected tissues. Three models have been proposed to explain the link between the mutation of the LMNA gene and the observed pathologies:

- The 'gene regulation' hypothesis according to which, in particular A-type lamins play a regulatory role in specific DNA-transcription by activating mechanosensitive genes [91].
- The 'structural' hypothesis which states that lamins play an essential role in the structural integrity of the nucleus and thus in the structural integrity of the whole cell, via connections between nuclear lamina, cytoskeleton and extracellular matrix [80, 50] taking in account that nuclear lamina aberration not only influence cell mechanics but can also result in disturbed signaling cascades.
- The "DNA-damage hypotesis" according to which lamina alterations cause DNA repair mechanism impairment, leading to premature aging of cells and tissues [32, 87]. Presumably, given the relevance of NL both in structural and in functional cellular aspects, these three hypotheses do not exclude each other.

Although mutations on Lamin A induce various types of diseases, the most interesting feature is their promotion of premature aging. Since the aging process is believed to be the result of a series of complex overlapping physiological mechanisms, it is astonishing that a single mutation on Lamin A is able to promotes the aging process [100]. Firstly described in 1886 by Jonathan Hutchinson that reported some clinical informations about " a 31 years-old boy with congenital absence of hair and mammary glands with atrophic condition of the skin and

its appendages" [45], Hutchinson-Gilford Progeria Syndrome (HGPS) was better described by Hastings Gilford in 1897. He decided to name this syndrome "Progeria" from the greek words "pro", meaning "premature", and "gèras", meaning "old age" [30], because all the affected patients displayed, since childhood, all the peculiar features typical of the elderly (Figure6) such as sarcopenia, osteoporosis, diabetes, cataracts, and atherosclerosis except cancer and neuro-degenerative diseases [30, 19], however preserving cognitive functions [71, 14].

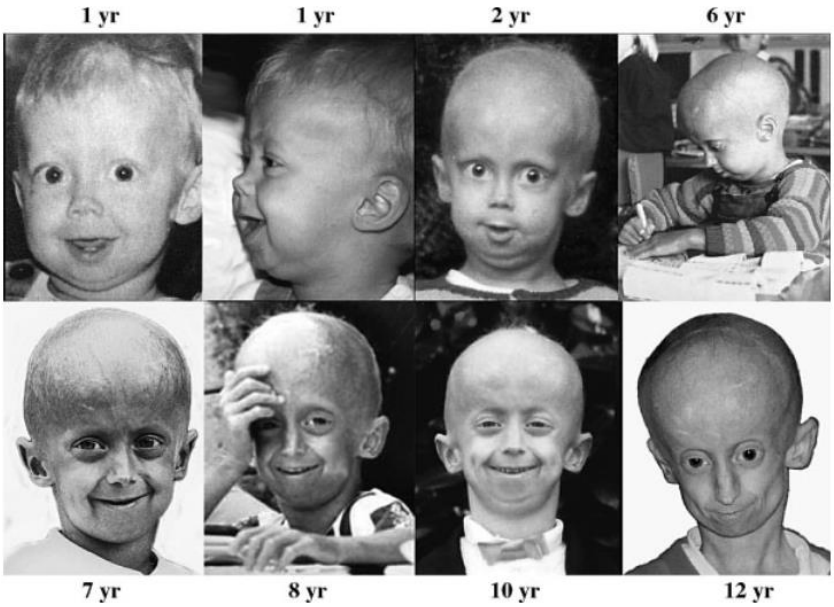

Figure 6: **Dutch HGPS patient in its growth and arising of typical phenotype (figure from [41])**

HGPS patients usually die from cardiovascular complications at around 14 years of age [14]. HGPS is a very rare (1: 20,000,000)[14], fatal genetic disorder due to a base pair substitution at exon 11 of the Lamin A gene (c.1824C>T, p.G608G), at least in 90% of all HGPS cases [79]. Mutation is spontaneous and typically occurs, de novo, during gametogenesis or in fertilization period. Nowadays, there are 154 HGPS affected patients all around the word [source:Progeria Research Foundation], with a similar sex ratio between two genders. Interestingly, even though this de novo heterozygous silent mutation does not change the aminoacidic sequence of the wild type Lamin A protein, it generates a donor cryptic splicing-sites that causes the production of a mutated form of Lamin A lacking of 50 amino acids, known as Progerin [18]. Since this 50 amino acid deletion results in Zmpste24-cleavage sites loosening, Δ50Lamin A cannot undergo the physiological post-translational processing thus remaining permanently farnesylated. This property tethers Progerin to cell's inner nuclear membrane, likely permanently thus preventing its proteasome-mediated elimination (Figure 7). As a consequence, Progerin accumulates into

the nucleus leading to nuclear morphologic alterations, shortened telomere length, increased DNA damage foci, a decrease of heterochromatin levels [7] and general impairment of all the processes in which NL is actively involved [9] [57] [72].

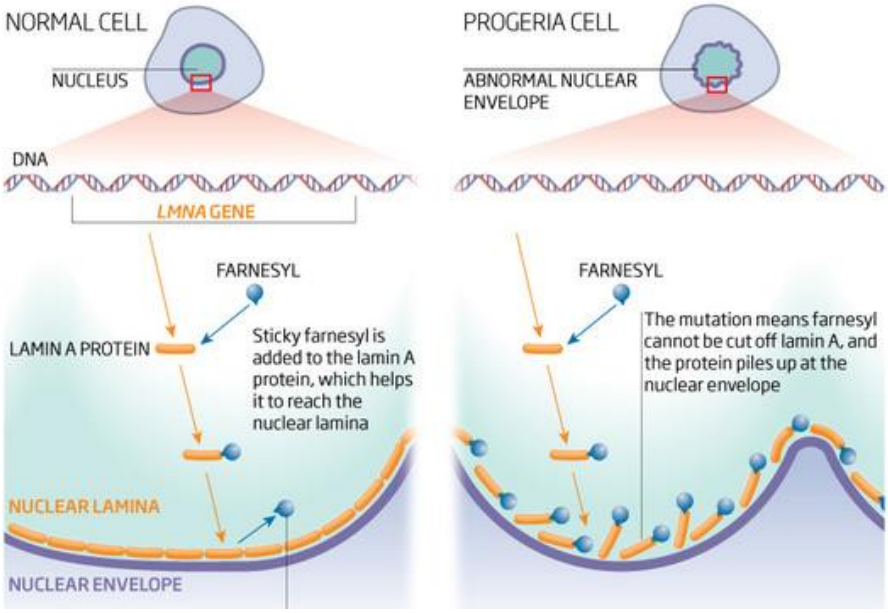

Figure 7: **On the left, Lamin A physiological processing and insertion in nuclear lamina. On the right, what happens in presence of mutated Lamin A.** [49]

Notably, also normal aged cells show Lamin A aberrant localization, low levels of heterochromatin, nuclear blebbing and increased levels of Progerin [78] which it has been reported to be sufficient itself to induce all the nuclear abnormalities characteristic of HGPS. These support the raising belief according through which the accelerate aging displayed in HGPS is a phenocopy of the physiological aging process [59]. Despite strenuous efforts have been made to understand molecular mechanisms underlying the onset of the pathology, progeria is still an incurable disease.Basically, all the therapeutic strategies target post-translational modifications of Progerin. Initial preclinical studies identified farnesyltransferase inhibitors (FTIs) [92, 12] and prenylation inhibitors (statins and aminobisphosphonates) as potential beneficial treatments for HGPS. Unfortunately, the first clinical trials for children with progeria utilizing the FTI lonafarnib lone and lonafarnib, pravastatin and bisphosphonates in combination reported no significant improvements in patients quality of life and lifespan. More recently, additional therapeutic strategy are emerging consistently with the notion that reduced expression of ICMT, the enzyme responsible for carboxymethylation of the farnesylcysteine of Lamin A/Progerin, has a dramatic effect ameliorating the phenotype of progeria mice, significantly increasing lifespan. In

addition, other reports have shown a beneficial effect of rapamycin [34, 10] and sulphorafane [28], a chemotherapeutic and a natural antioxidant respectively, on the phenotype of HGPS patient cells by increasing Progerin clearance by autophagy. Moreover, resveratrol, an enhancer of SIRT1 deacetylase activity, alleviates progeroid features and extends lifespan in progeria mice model, although the effect on survival is relatively modest [55, 23].

I. 3 Nuclear Lamina, Oxidative Stress and Ageing

Oxidative stress refers to a cell state during which there is an unbalance between the production of reactive oxygen species (ROS), physiological by-products of mitochondria metabolism, and ROS elimination. Living cells have developed several defence mechanisms, both enzymatic and non-enzymatic, through which ROS amount is kept at tolerable levels. However, there are some cases in which the balance between ROS production and elimination is shifted so much in favour of ROS production, that these defence systems fail to counterbalance the adverse effects of ROS on cellular macromolecules. Indeed, while moderate physiological increase in ROS levels results in cell proliferation and differentiation promotion [77], ROS overload causes DNA, proteins, and lipids damages leading to cell proliferation and longevity impairment [86].In the last 60 years, ROS have been one of the most addressed topics in biomedical research mainly because of the widely reported relation existing between oxidative stress and aging. While in the common vision aging is just the natural process of becoming older, in the biomedical research field aging is defined as a complex, continuous and irreversible process that affects all cell type and organs, during which most of the crucial physiological functions are impaired and lost. Firstly proposed by Denham Harman, "the free radical theory of ageing" [40] claims that ageing is the cumulative result of oxidative damage. Since this theory came out in '50s, several thousand of studies reported that ROS levels and oxidative damage increase with increasing age [66, 38] and that reducing oxidative damage extends the lifespan of various animal models (i.e. : yeast, fruit flies, mice, etc.) [42]. Exogenous Hydrogen peroxide (H_2O_2) exposure, is sufficient to induce premature cellular senescence in wild type fibroblasts recapitulating aging process profile [24]. More recently, several studies also referred the presence of a strong interdependence between oxidative stress and lamins. More specifically, it has been observed that lamins depletion and lamins genes mutation negatively impact on oxidative stress response and adaptation mechanism which in turn are tightly coupled to cell proliferation, longevity, cellular senescence, apoptosis and autophagy. Conversely, oxidative stress influences lamins expression

and stability by interfering in physiological lamins post-translational modification processing. For instance, increased ROS lead to the oxidation of cysteine residues in the Lamin A tail domain which promotes the formation of Lamin A inter- and intramolecular disulphide bonds [74]. Interestingly, high levels of ROS, such as superoxide radical (O2 -), hydrogen peroxide (H_2O_2), singlet oxygen, and hydroxyl radical (OH) have been detected in HGPS fibroblasts, as well as in normally aged fibroblasts, contributing to increase levels of DNA damage and nuclear shape alterations (Figure 8) [51, 96].

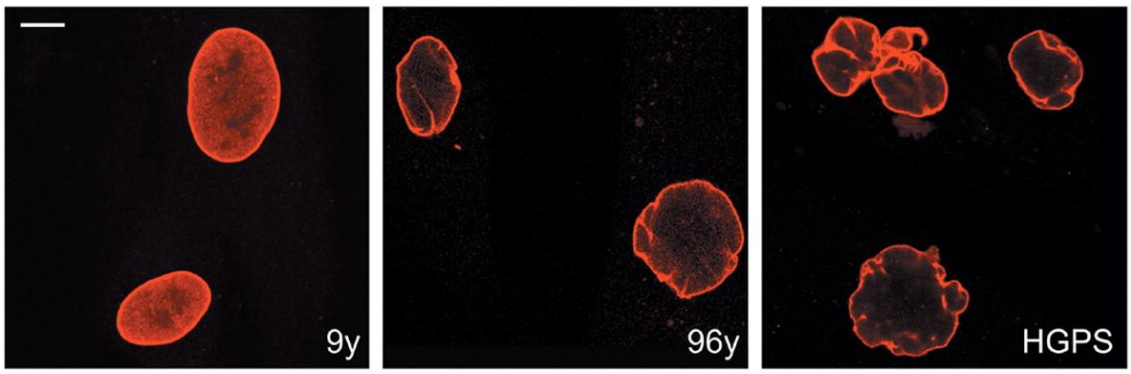

Figure 8: **Shape similarity between aged healthy fibroblasts of 96y patients (B) and HPGS fibroblasts (C), young healthy fibroblast (A) as control. Lamin A/C in red. [78]**

This, seems to be due to the Progerin capability to sequester NRF2, a transcription factor that regulates genes harbouring antioxidant response elements (ARE) and that activate antioxidant response signalling pathway. The sequestration of NRF2 by Progerin prevents NFR2 transcriptional activity resulting in increased chronic oxidative stress (Figure 9). In addition, Progerin was also found to be expressed in old wild type fibroblasts, that exhibit an altered dimorphic nuclear profile as in progeria patient-derived fibroblasts [78].

Since physiologic ageing process and HGPS share some clinical features (Figure 9), it would be of great relevance better understand and characterize the molecular mechanism underling Progeria onset in order to shade light on normal aging and viceversa.

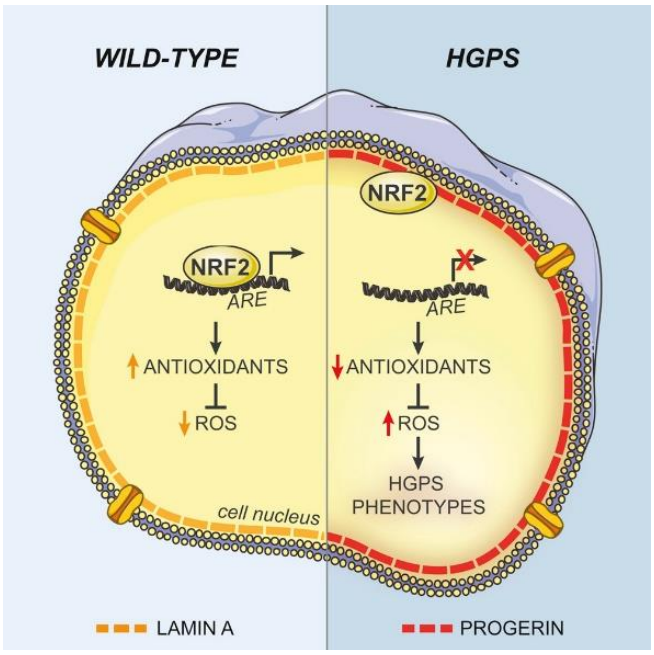

Figure 9: **Schematic representation of a wild type cell nucleus and HGPS one, showing Progerin capability to sequester NFR2 thus ROS accumulation [78].**

Outline

During my PhD I investigated many aspects of nuclear lamina biology with particular regard to the impact of nuclear lamina structural perturbations on cell functions, mechanics and gene expression regulation. Moreover, I also investigated the effect of "chemical environmental" on nuclear lamina structure and functions in a cellular model that faithfully recapitulates, in vitro, aging process.

The present thesis is divided into three chapters whose contents result into three scientific publications:

- **Chapter 1**: Since nuclear lamina interacts with DNA and it has been reported to be actively involved in gene expression regulation we evaluated the effect Progerin on global gene expression regulation. To do this, our group performed a bioinformatics study in which all public available transcriptomic data of HGPS patients have been analysed with respect of those of healthy matched controls. As result we obtained a list of the most deregulated genes and we identified the pathways deregulated in presence of the pathology, to which these genes belong.

  Title : "Pathway deregulation analysis in Hutchinson-Gilford Progeria Syndrome."
  Authors : Francesc Font-Clos, Maria Chiara Lionetti, Stefano Zapperi and Caterina A.M.La Porta.
  Journal : Scientic Reports, under revision.

- **Chapter 2**: Herein, I report the results obtained while studying the impacts of nuclear lamina alterations on nuclear plasticity and nucleus interaction to cytoskeleton, in an inducible cellular model of mutated Lamin A.

  Title : "Effects of Progerin on nuclear cell plasticity"
  Authors : Maria Chiara Lionetti, Federico Mutti, Maria Rita Fumagalli, Francesc Font-

Clos,Giulio Costantini Stefano Zapperi and Caterina A.M.La Porta.
in preparation

- **Chapter 3**: In this last chapter, I report the results obtained studying the interdependence between ROS, ageing and lamins in a novel oxidative stress cellular model developed in our laboratory. In particular, I studied the impact of "chemical" environment on nuclear lamina structure and related functions, and the possible reversibility of the oxidative stress effects by anti-oxidant supplementation.

Title : "Sulforaphane can not protect the cells to a repeated, short and sublethal treatment with hydrogen peroxide"
Authors : Maria Chiara Lionetti, Federico Mutti, Erica Soldati, Maria Rita Fumagalli, Graziano Colombo, Emanuela Astori, Aldo Milzani, Isabella Dalle Donne, Emilio Ciusani, Giulio Costantini, Caterina A. M. La Porta,
Journal : Journal of Nutrition Biochemistry, under revision

Pathway deregulation analysis in Hutchinson-Gilford Progeria Syndrome

Francesc Font-Clos[a], Maria Chiara Lionetti[b], Olga Vasieva[f], Stefano Zapperi[c,1,1,1], Caterina A.M. La Porta[b]

[a]*ISI Foundation, Via Chisola 5, Torino, Italy*
[b]*Center for Complexity and Biosystems, Department of Environmental Science and Policy, University of Milano, via Celoria 26, 20133 Milano, Italy*
[c]*Center for Complexity and Biosystems,, Department of Physics, Via Celoria 16, 20133 Milano, Italy*
[d]*CNR - Consiglio Nazionale delle Ricerche, Istituto di Chimica della Materia Condensata e di Tecnologie per l'Energia, Via R. Cozzi 53, 20125 Milano, Italy*
[e]*Department of Applied Physics, Aalto University, P.O. Box 14100, FIN-00076, Aalto, Finland*
[f]*Functional and Comparative Genomics, University of Liverpool, UK*

Abstract

Hutchinson-Gilford progeria syndrome (HGPS) is an autosomal dominant aging disease involving lamin A, a protein that plays a crucial role in the nuclear scaffold. The cause of the disease is still unknown although it was recently proposed that it could involve an impairment of mesenchymal lineage differentiation. We have tackled this problem by performing a pathway deregulation analysis of HGPS transcriptomes with the aim of identifying a characteristic gene expression signature that might shed light on the most important features of the disease and suggest possible prognostic/therapeutic targets. Our findings highlight two new and interesting aspects: first we found that the most deregulated pathway in HGPS subjects is the epithelial-mesenchymal transition (EMT), suggesting that this pathway should be targeted by therapeutic intervention or used for prognosis. The second interesting possible target emerging from our analysis is PTX and CCL2 which play a critical role during inflammation and therefore could be involved in many of the clinical consequences of this complex disease.

Introduction

Hutchinson-Gilford progeria syndrome (HGPS) is an autosomal dominant, rare, fatal pediatric segmental premature aging disease [1] belonging to a family of genetic diseases called laminopathies [2]. The diagnosis is based on common clinical features and detection of heterozygous lamin A (LMNA) pathogenic variants either within exon 11 (classical) or at the intronic border of exon 11 (atypical). LMNA is the only gene in which pathogenic variants are known to cause HGPS. The lamin proteins are the principal components of the nuclear lamina, a complex molecular interface located between the inner membrane of the nuclear envelope and chromatin [3]. In HGPS, a mutation produces a shortened abnormal protein, called progerin, with a 50 aminoacid deletion near its C-terminal end. This deletion does not affect the ability of progerin to localize into the nucleus or to form a complex with the normal Lamin A protein, but the sites for the proteolytic cleavage of the terminal 18 amino acids and the farnesyl side group of prelamin A

*Caterina A. M. La Porta
Email address: caterina.laporta@unimi.it (Caterina A.M. La Porta)

along with the phosphorylation site involved in the dissociation and re-association of the nuclear membrane at each cell division are removed in progerin [4, 5].

HGPS patients show characteristic craniofacial features and cardiovascular disease that constitute the major cause of morbidity and mortality. The disease progression displays many of the symptoms of normal aging, such as progressive atherosclerosis, while other symptoms such as neural degeneration, diabetes, malignancies and cataracts are absent. Samples from biopsy and autopsy are limited due to the rarity of the disease and therefore most information comes from studies on patient-derived skin fibroblasts, wild type and mutant lamin A overexpression in established cell lines [2, 3]. The clinical strategy up to now is based on the use of farnesyltransferase inhibitors and anti aging treatment with rapamycin and resveratrol [6]. The cause of the disease is still unclear and many hypothesis are under investigation: progerin-mediated stem cell pool exhaustion [7], mesenchymal lineage differentiation defects [8], a diminished DNA-damage repair response [9] and nuclear fragility in mechanically stressed cells such as cardiomyocytes [10].

In this paper, we approach this problem using pathway deregulation analysis of progeria transcriptomes to identify a characteristic gene expression signature associated with progeria that sheds light on the most important features of the disease with the ultimate goal of identifying interesting key targets.

Results

Transcriptomic signature of HGPS

We collect from the existing literature a set of six experiments reporting transcriptomic data from HGPS patients, matched with healthy controls. The latter are human dermal fibroblasts obtained from healthy subjects. We could not find enough data from parents of HGPS patients. Altogether the data contain 34 HGPS samples and 38 healthy controls. In dealing with samples coming from different experiments, we are faced with the thorny issue of batch effects. It is not possible to naively merge all the data sets into a unique pool, since each experiment has its characteristic features that must be removed in order to uncover the biological signal. We have successfully addressed this problem in the context of obesity by using the method of singular value decomposition. We apply the same strategy here (see the Methods section) and find a set of 62 differentially expressed genes (FDR 10^{-4}) when comparing HGPS and healthy subjects.

Figure 1 reports the 62 genes and displays the fold change in the expression level and a measure of statistical significance (the p-value according to the Kolmogorov-Smirnov test) for each batch separately.

The 62 genes can be subdivided into two groups: the group of down-regulated genes (colored in blue in Figure 1) and the group of up-regulated genes (colored in red in Figure 1). The down-regulated genes group includes genes involved in microtubule dynamics (STMN2), genes involved in vascular remodeling (CTHRC1, S1PR1, MMP3, HAS2, MXRA5), in Wnt-pathway (SFRP1), in protein folding (CLEC2B) and erytrocytes (EPB41L3). On the other hand, among the up-regulated genes we find genes involved in neuronal excitability (SCN3A),in cardiac conduction (KCNE-4), in the migration and differentiation of muscle cells (ITGA7, MYOCD, MEOX2, ANKRD1, PPP1R14A), in inflammation (PTX3, CCL2) and finally a gene involved in the connectivity of neurons (PCDH10). The overall picture reveals an impairment of specific functions related to endothelial and muscle cells as well as a general state of inflammation that could help explain the most important symptoms displayed by HGPS subjects such as atheroscelrosis and cardiovascular disease. On the other hand, it is possible to point out a general preservation of the brain functions.

Pathway deregulation in HGPS with respect to healthy subjects

We use Pathway Deregulation Scores (PDS) to estimate the overall deregulation of each pathway in each sample (for the computational details, see Methods). Figure 2a shows boxplots of HGPS samples (colored from red, strong deregulation, to pale blue, no deregulation) and of control samples (thinner, colored in gray). It is apparent that a number of pathways are appreciably deregulated. We assess the statistical significance of these clear differences by means of fold-change of median group values, comparing HGPS to control samples, and sort the pathways accordingly. Pathways marked with gray circles have $FDR < 10^{-3}$. Remarkably, the pathway with highest deregulation is the epithelial mesenchymal transition (EMT) pathway. KRAS signaling is also significantly deregulated as well as TNFα signaling, both possibly related to EMT and inflammation processes. Impairment of coagulation is also among the significantly deregulated pathways and is involved in many biological processes including inflammation. Figure 2b shows an example of the PDS projection for the EMT pathway: the segregation of HGPS samples with respect to healthy ones is clear. The data is further projected onto its first 3 principal components to allow for visualization. The axis display the proportion of explained variance. Figure 2c gives an overall view of pathway deregulation in HGPS transcriptomes by displaying a heatmap of PDS values.

Role of farnesyltransferase inhibitors

We have checked if the observed deregulation depends on the effect of treatment with farnesyltransferase inhibitors (FTI). One of the batches studied (E-MEXP-2597, see Datasets section) contains 10 samples treated with FTI. When we remove those samples from the analysis we find an HGPS signature that is very similar the original one (it is composed of 56 genes, 54 of which are part of the original signature). Furthermore, the ranking of the pathways obtained without the samples treated with FTI is again very similar and the top five pathways (including EMT and KRAS) are the same. Hence, we conclude that the pathway deregulation we observe is not an effect of the treatment with FTI but is associated with HGPS.

Experiments

We experimentally validate the deregulation of the EMT pathway assessing the level of expression of some known markers of mesenchymal state such as β-catenin and vimentin by immunofluorescence. We use fibroblasts derived from one HGPS subject and from his/her healthy parents. As shown in Figure 3, both β-catenin and vimentin mesenchymal markers are mainly expressed in the healthy father with respect to HGPS. In fact, β-catenin is mainly expressed in the cytoplasm and at the edge of the plasma membrane while in the healthy father it is expressed in the nucleus, where this factor translocates when active. Accordingly, vimentin is down regulated in the HGPS subject.

Interaction between lamins and HGPS signature

We perform a centrality analysis of the interaction network between lamins and the HGPS signature, see Methods for details on how the network was constructed. Figure 4a shows the interaction network, with seed nodes colored in pale green (LMNA), dark green (LMNB1) or red(HGPS); and the rest of nodes colored in gray and positioned according to which clusters of seed nodes they connect to.

Figure 4b is a coarse-grained representation of the same network: nodes represent clusters in panel a, and connections are aggregated so that the width of the arrows is proportional to the number of directed connections between two clusters. The panel shows a characteristic group of central nodes that facilitates the cross-talk between lamins and HGPS-related genes. To further

asses the centrality of such nodes, we compute 4 well-know centrality measures (see methods for details).

Figure 4c displays a heatmap of centrality values, with nodes ranked according to their average ranked centrality. This ranked list should highlight the nodes that are more central in the interaction between lamin related genes and our HGPS signature. The most central nodes according to this analysis include factors involved in the control of the cell cycle such as CCND1, CDK1, Cyclin A and YAP, factors which play an important role in kinetochore such as AURKB, SPC25, NDC80, MAD2L2, transcription factors such as NFkB, E2F, SOX9,CREB that control many functions from the proliferation to differentiation and development, factors involved in controlling apoptosis such as BIRC5, AkT, ERK1/2, chemokines or such as CCL2, IER3 and factors regulating the extracellular matrix MMP3, HAS2. Therefore, this kind of analysis allow to highlight the most important functions impaired in HGPS subjects that are involved in their severe phenotype.

Discussion

HGPS is a rare disease that is at present impossible to cure. The most common form of HGPS is caused by a de novo heterozygous point mutation in the human lamin A gene. Progeria is usually diagnosed in the first year or two of life and is characterized by a rapid progression of aging phenotypes. In spite of a severe atherosclerosis, cardiac or cerebrovascular disease, these subjects show a normal motor and mental development. The analysis of data contains 34 HGPS samples and 38 healthy controls by the aim of pathway deregulation score shows a clear impairment of EMT in progeria subjects, the latter being in agreement with the hypothesis of an exhaustion of stem cells in these patients [7] or mesenchymal lineage differentiation defects [8]. Accordingly, the level of expression of typical mesenchymal markers such as vimentin and β-catenin nuclear localization confirms the loss of a mesenchymal phenotype in HGPS fibroblast cells in comparison to healthy subjects. Interestingly, HGPS patients show the decrease of a set of genes involved in critical cell functions related to microtubule dynamics, vascular remodeling, stem-related genes (Wnt-pathway) and protein folding.

This kind of analysis can not help in understanding the cause of the disease but is useful to highlight important hubs hit by the disease and maybe identify possible new interesting marker. In this case, EMT seems to play a critical role in the disease and therefore every treatment that could improve vascular remodeling may provide a good strategy to improve the functions of HGPS subjects. Another interesting aspect come out form our findings: we have seen a general improvement of neurotransmission and connectivity between neurons, explaining the intact brain function of HGPS subjects and the absence of neurodegenerative disease. On the pother hand, inflammation is another important aspect of this disease that lead to a severe phenotype. PTX3 and CCL2 appear to be interesting targets triggering inflammation. PTX in fact is considered an essential fluid-phase pattern recognition molecule of the innate immune system that acts as a functional ancestor of antibodies which plays a critical role in tissue repair [11] and CCL2 is involved in the recruitment of mococytes during infection and inflammation [12]. Muscle cells are also target linked to the severe phenotype of HGPS subjects and interesting target involved both in the migration and differentiation are also highlighted by our data.

The overall picture reveals an impairment of specific functions related to endothelial and muscle cells as well as a general state of inflammation that could help explain the most important symptoms displayed by HGPS subjects such as atheroscelrosis and cardiovascular disease. In contrast, brain functions appears to be preserved.

Methods

Human Fibroblasts culture growth conditions

Human fibroblasts from HGPS patient (HGSDNF167) and the relatives of this patient (HGFDNF168 and HGMDF090, father and mother, respectively) are obtained from the Progeria Foundation Cell and Tissue Bank. The HGPS patient was a male of 8 years old with the classical mutation (heterozygous LMNA Exon 11 c1824 C>T (p.Gly608Gly). The cells were maintained according to the protocol reported by The Progeria Foundation: 15% FBS, DMEM with 1% antibiotics and 1% L-glutamine. The cells were detached by trypsin EDTA 25% and are maintained in culture for no more than five passages.

Immunofluorescence

Subconfluent cells grown on glass coverslips are fixed with 3.7% parafolmaldeide in PBS for 10min, permealized with 0.5% Triton X-100 in PBS for 5min at room temperature and incubated with 10% goat serum in PBS for 1hr. The cells are stained with anti-β-catenin (anti-ActiveβCatenin, Millipore, 05-665, 1:50) or anti-vimentin (sc-53464, Santa Cruz 1:50) overnight at 4 °C. Thus, after a brief washing with PBS, the cells are incubated with the secondary antibody (anti rabbit or anti-mouse Alexa488 1:250) for 1 h. The cytoskeleton is stained with Falloidin (Acti-stain 555 Fluorescent Phalloidin, Cytoskeleton Inc, 100 nM) at room temperature for 45 min. The nuclei are counterstained with DAPI and the slides mounted with Pro-long anti fade reagent (Life technologies). The images are acquired with a Leika TCS NT confocal microscope.

Transcriptomic data pre-processing

We apply the following pre-processing steps to all transcriptomic data: 1) Probes containing missing values are excluded from the analysis. 2) Probes are mapped to Entrez ID labels if they are available in the associated platform. Otherwise the David portal is used to convert the available labels to Entrez ID labels. 3) Values corresponding to raw expression counts or gene expression intensity are log2 transformed (if necessary). 4) Probes mapping to the same Entrez ID label are averaged out. 5) Probes that cannot be mapped to a unique Entrez ID label are excluded from the analysis, as well as those that cannot be mapped to any Entrez ID label at all. 6) We apply a simple normalization in linear space, imposing that the mean of expression of each gene is constant among samples.

Batch effects removal

We use the *SVDmerge* algorithm to remove batch effects. The details of the algorithm are explained in [13]. In short, *SVDmerge* uses singular value decomposition to identify which "eigengenes" or directions in gene-expression space correspond mostly to the phenotype of interest and which can rather be associated to batch effects. In addition, by ranking the eigengenes via Kolmogorov-Smirnov tests, the algorithm can selectively filter out eigengenes associated to batch effects, minimizing the total distortion of the original data.

Calculation of Pathway Deregulation Scores

We compute Pathway Deregulation Scores (PDS) as explained in [13] for the set of 50 hallmark gene sets or pathways from the MSigDB [14]. For each pathway and each sample, PDS gives a unique value that can be associated to the overall deregulation. Taking together the PDS values of HGPS and control samples, we can confidently establish if a pathway is consistently deregulated in HGPS: it is expected that, under strong deregulation patterns, samples of the same group cluster together in terms of PDS values.

Construction of HGPS-lamins interaction network

LMNA and LMNB related datasets have been composed from genes found in the immediate neighborhood of the laminin genes in functional (STRING [15], IPA [16]) and gene co-expression (Genevestigator [17]) networks as well as proximal to LMNA and LMNB genes in their gene loci. The lists are shown in Tables 2,3 and 4. To investigate interactions between the LMN- associated genes and the genes from the defined progeria signature we have reconstructed functional networks from the combined gene sets using IPA. The Core analysis using the IPAs knowledge base gene/protein connectivity data for human and rodents was performed and the most densely interconnected and top-ranked seed networks were selected. The seed networks of directly connected gene-nodes were allowed to automatically expand up to maximal size of 70 nodes by addition of top-ranked connecting functions from the IPA knowledge base. This procedure would increase a continuity of networking within the uploaded gene set.

Centrality measures

Centrality measures are a very important set of algorithms in network science. They are used to asses the "importance" or "centrality" of nodes in a network according to different criteria. The choice of the criterion and hence of the most convenient algorithm is a delicate issue in general, and certainly has no unique answer in many cases. A common strategy is then to compute several centrality measures and look for nodes consistently identified as central by most algorithms. We compute Katz centrality [18], eigenvector centrality [19], betwenness centrality [20] and PageRank centrality [21]. We use the implementation of *graph-tool* [22], an efficient network-analysis python package. The mathematical definition of the four measures and details about the implementation can be accessed at ref.[23].

Data

A total of six transcriptomic datasets are gathered from the available literature. Here we briefly describe them, giving references to the associated original publications and accession codes from either GEO or ArrayExpress. (E-MEXP-2597): Dermal fibroblasts from five subjects with HGPS aged 1 to 4 and five age-matched dermal fibroblast control cell lines, see [24] for details. Two samples per subject are used, totaling 20 samples. (E-MEXP-3097): Primary skin fibroblasts from an autosomal recessive HGPS family, see [25] for details. Three affected homozygous samples and three healthy control samples were included in our reanalysis. Three samples from healthy heterozygote carriers were discarded. (GSE3860): Dermal fibroblasts from three HGPS cell strains and three age-matched control cell strains, see [26] for details. Three biological replicates per subject were included in the analysis. (GSE28863): Dermal fibroblast from two HGPS cell lines and three normal cell lines, see [27] for details. Two biological replicates per subject. Due to unmatching labels between [27] and GSE28863 it is not possible to determine if there is any family relationships between HGPS and control subjects. (GSE41751): Primary fibroblast cell lines from one HGPS subject, its father (normal phenotype), and one age-matched control, (two biological replicates per subject totaling 6 samples, see [28] for details). (GSE69391): A total of 12 samples obtained from primary dermal fibroblast cell lines from HGPS subjects and control dermal fibroblast cell lines.

Figures

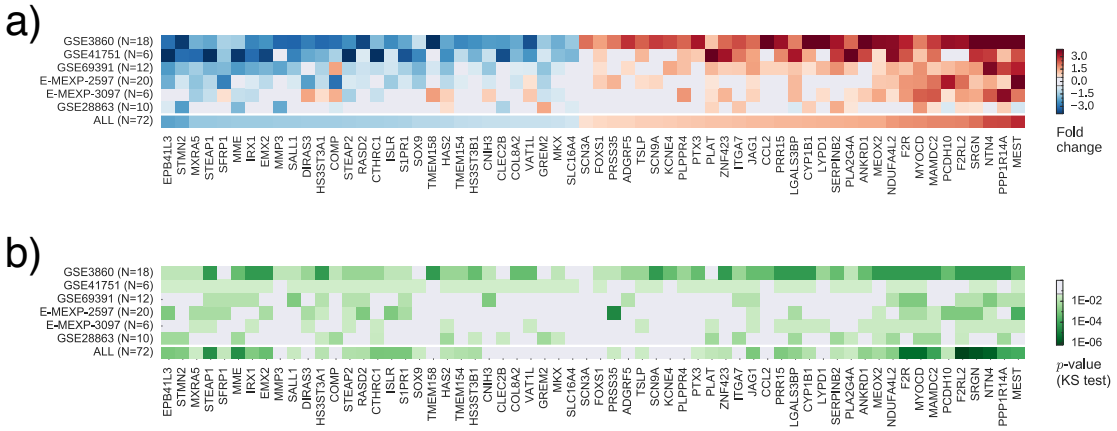

Figure 1: **A transcriptomic signature of progeria**. Overview of the 62 genes in the progeria signature among each of the 6 original datasets. (a) Fold-change values with red (blue) shades indicating over-expression (under-expression) in progeria with respect to healthy samples. Values between -0.5 and 0.5 are shown in gray. (b) P-values in a Kolmogorov-Smirnov test comparing progeria and healthy samples (FDR adjustment with Benjamini-Yekutieli method). Darker shades of green correspond to smaller p-values. Values corresponding to FDR > 0.05 are shown in gray.

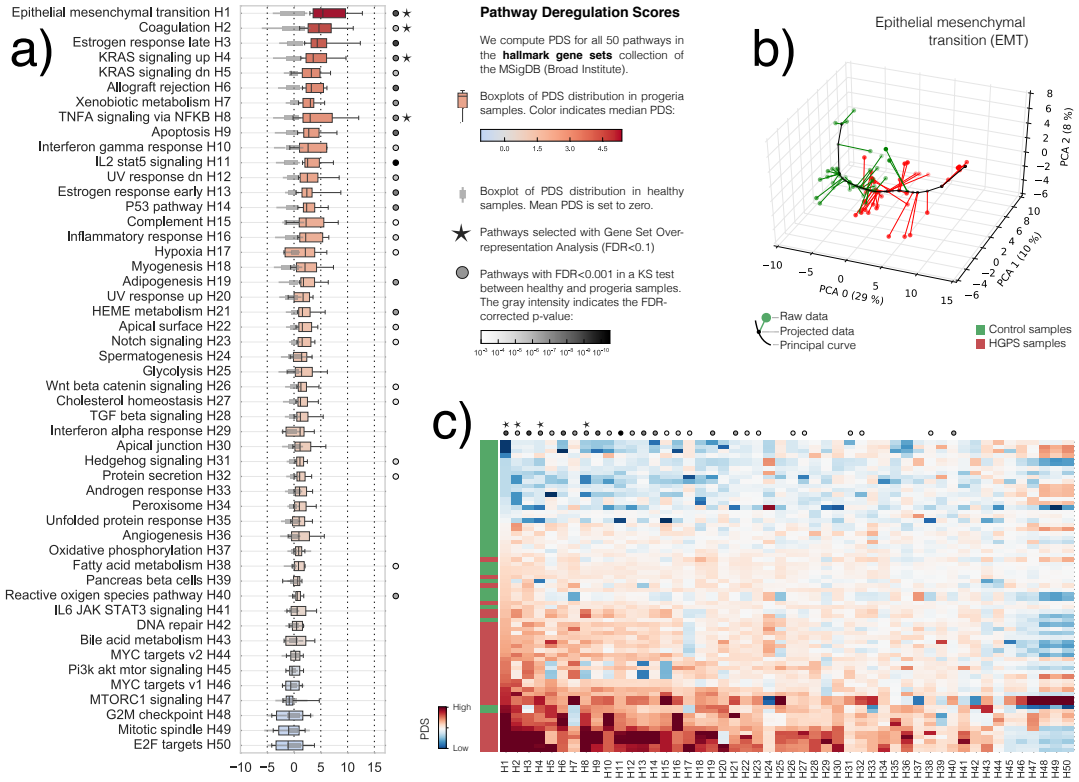

Figure 2: **Pathway Deregulation Scores (PDS)**. We compute PDS for the 50 "hallmark gene sets" from MSigDB. (a): Boxplots showing the distribution of PDS values for each pathway, both for healthy samples (gray, thin boxplots) and for progeria samples (colored,thick boxplots; coloring corresponds to median of progeria samples). Pathways are sorted by their median PDS among progeria samples. The median of healthy samples is set to zero. The gray circles placed at the right border of the boxplots indicate a FDR-corrected p-value below 10^{-3}, in a Kolmogorov-Smirnov test comparing progeria and healthy PDS values. Darker shades indicate smaller, more significant p-values. Black stars mark those pathways where the progeria signature genes are significantly over-represented (hypergeometric model, FDR-adjustment Benjamini-Yekutieli method, $FDR > 10^{-1}$). (b): Projection (black small circles) of the original transcriptomic data (colored circles) onto its principal curve (black line). The data is further projected onto its three first principal components for visualization purposes only. The panel shows that progeria and healthy samples cluster separately, indicating a strong deregulation of the "Epithelial mesenchymal transition" pathway. (c): Full PDS matrix. Pathways are place in columns and numbered H1-H50 as in panel (a). Samples are placed in rows and are sorted by their PDS value in the H1 pathway.

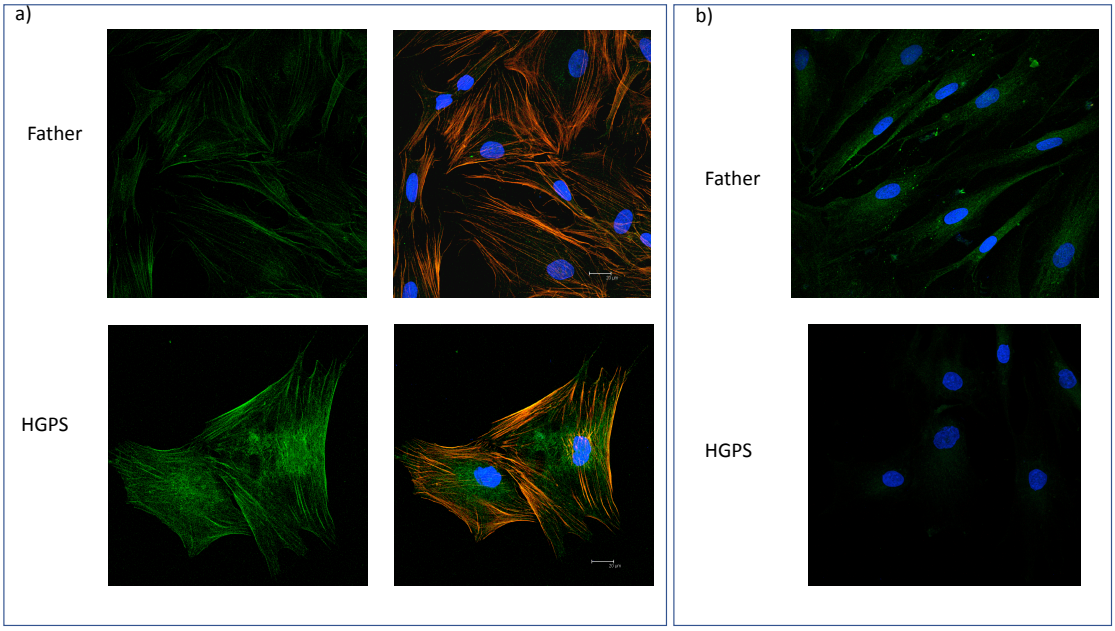

Figure 3: **Mesenchymal markers in an HGPS patient with respect to his parent**. Human fibroblasts from HGPS patient (HGSDNF167) and his father (HGFDNF168) are obtained from the Progeria Foundation Cell and Tissue Bank. Subconfluent cells grown on glass coverslips are fixed with 3.7% parafolmaldeide, permealized with 0.5% Triton X-100 and incubated with 10% goat serum in PBS for 1hr. The cells are stained with (panel a) anti-β-catenin (anti-ActiveβCatenin, Millipore, 05-665, 1:50) or (panel b) anti-vimentin (sc-53464, Santa Cruz 1:50) overnight at 4°C. Thus, the cells are incubated with the secondary antibody (anti rabbit or anti-mouse Alexa488 1:250) for 1 h. The cytoskeleton is stained with Falloidin (Acti-stain 555 Fluorescent Phalloidin, Cytoskeleton Inc, 100 nM) at room temperature for 45 min. The nuclei are counterstained with DAPI and the slides mounted with Pro-long anti fade reagent (Life technologies). The images are acquired with a Leika TCS NT confocal microscope.

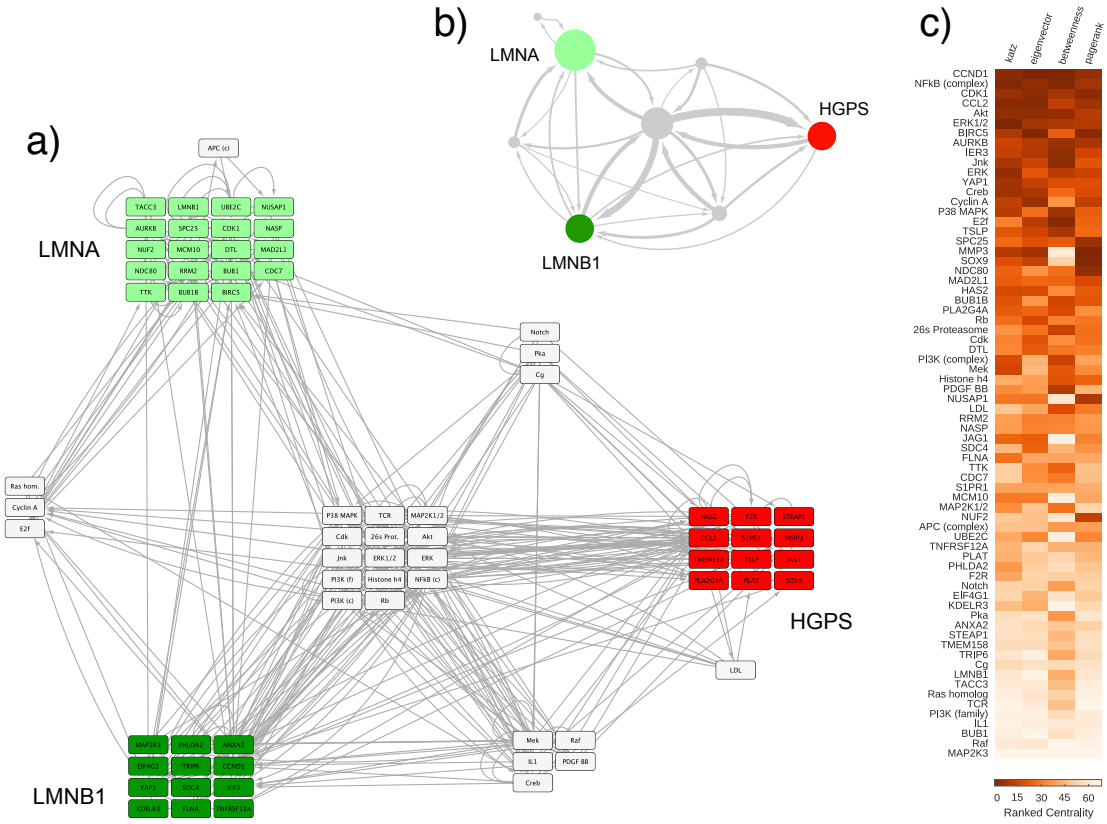

Figure 4: **Interaction network between lamins and HGPS signature**. (a): Interaction network with seed nodes colored and the rest of nodes in gray. Nodes are positioned according to which seed-nodes clusters they connect to. (b): Same, with clusters displayed as nodes (size proportional to number of elements in cluster) and arrows aggregating connections between clusters (width proportional to number of connections). direction of connections is preserved. (c): Heatmap displaying centrality measures for all nodes of the network. Darker coloring indicates more central nodes. We consider four well-known centrality measures [29]: Katz centrality [18], eigenvector centrality [19], betweenness centrality [20] and PageRank centrality [21].

rank	Gene Symbol	Entrez ID	Coefficient	rank	Gene Symbol	Entrez ID	Coefficient
1	PPP1R14A	94274	0.110724	32	CLEC2B	9976	-0.064569
2	NTN4	59277	0.105193	33	SCN3A	6328	0.064551
3	STMN2	11075	-0.099364	34	MEOX2	4223	0.063731
4	MEST	4232	0.099348	35	LYPD1	116372	0.062632
5	MMP3	4314	-0.096194	36	GREM2	64388	-0.061691
6	EPB41L3	23136	-0.086309	37	PTX3	5806	0.060865
7	COMP	1311	-0.083005	38	ANKRD1	27063	0.060542
8	SRGN	5552	0.081874	39	TSLP	85480	0.059524
9	HS3ST3A1	9955	-0.080812	40	HS3ST3B1	9953	-0.059407
10	NDUFA4L2	56901	0.080468	41	KCNE4	23704	0.05935
11	CCL2	6347	0.078802	42	MME	4311	-0.059128
12	SERPINB2	5055	0.078338	43	SLC16A4	9122	-0.058897
13	MXRA5	25878	-0.076091	44	RASD2	23551	-0.058538
14	TMEM158	25907	-0.074895	45	PRR15	222171	0.05832
15	SALL1	6299	-0.073901	46	STEAP1	26872	-0.058197
16	ITGA7	3679	0.07379	47	FOXS1	2307	0.058187
17	MAMDC2	256691	0.073285	48	IRX1	79192	-0.058006
18	PLPPR4	9890	0.072392	49	TMEM154	201799	-0.057991
19	F2R	2149	0.071678	50	CTHRC1	115908	-0.057906
20	ISLR	3671	-0.07022	51	LGALS3BP	3959	0.057905
21	VAT1L	57687	-0.070216	52	CNIH3	149111	-0.0574
22	DIRAS3	9077	-0.070214	53	S1PR1	1901	-0.057392
23	STEAP2	261729	-0.068838	54	EMX2	2018	-0.057108
24	PCDH10	57575	0.068817	55	CYP1B1	1545	0.05674
25	ZNF423	23090	0.06851	56	COL8A2	1296	-0.056338
26	MKX	283078	-0.068267	57	SFRP1	6422	-0.055354
27	ADGRF5	221395	0.067991	58	PRSS35	167681	0.055274
28	PLA2G4A	5321	0.067221	59	HAS2	3037	-0.05518
29	MYOCD	93649	0.066954	60	SOX9	6662	-0.054889
30	F2RL2	2151	0.065639	61	PLAT	5327	0.054882
31	JAG1	182	0.064746	62	SCN9A	6335	0.054334

Table 1: The 62 genes in the transcriptomic signature of HGPS and their associated coefficients. Genes are ranked by the absolute value of their coefficient. A threshold of $FDR = 10^{-4}$ was set using adjusted p-values (Benjamini/Yekutieli method).

GENEVESTIGATOR			STRING
Anatomy co-exp.	Cell lines co-exp.	Perturbation co-exp.	
SERPINH1	AHNAK	EMP1	LMNB1
TRIP6	FAM129B	FAM129B	LMNB2
RRAS	TNFRSF12A	EIF4G1	UBC
TUBB6	MYOF	FLNA	RB1
array PTRF	CD151	RNH1	RBB4
PRKCDBP	LGALS3	ARHGDIA	CTNNB1
FAM129B	RHOC	PLEC	CASP6
EMP1	ANXA2	CD151	CASP2
MYOF	CAPN2	MIR6836	SUMO1
CD151	RHBDF1	GNB2	EMERIN
RHOC	PLEC	ZYX	CDK1
TSPAN4	ITGB5	CORO1C	SYNE1
EHD2	SDC4	RHOC	SUN2
RNH1	PHLDA2	EHD4	SVIL
FAM114A1	MVP	MVP	HIVEP1
PRSS23	ANXA2P2	ACTN4	YY1
P4HA2	S100A11P1	TAGLN2P1	CENPE
FRMD6	ITPRIPL2	MAP2K3	BRCA1
EXT2	FAM114A1	CD63	H2AFX
CTNNA1	KDELR3	AP1B1	SREBPF1
GNG12	NACC2	SEC61A1	PHB
ANXA2P2	YAP1	IER3	
CCND1	GNG12	TUBB6	
	P4HA2	RRP12	
	EMP1	TMBIM1	

Table 2: Genes in the immediate neighborhood of LMNA in functional (STRING) and gene co-expression networks (GENEVESTIGATOR)

GENEVESTIGATOR			STRING
Anatomy co-exp.	Cell lines co-exp.	Perturbation co-exp.	
TACC3	BUB1B	BUB1B	LMNA
NFYA	KIF11	MCM10	MIS12
BORA	TMPO	SPC25	ZWINT
C1orf112	CCNA2	KIFC1	UBC
KNTC1	NASP	CCNA2	CASP6
ZBED4	BUB1	UHRF1	SUN1
NCAPD2	NUSAP1	TTK	SUN2
MIS18BP1	FAM72A	CKAP2L	SYCP1
BAZ1A	FAM72B	DTL	SYCP2
APAF1	FAM72C	UBE2C	TEX12
GLE1	FAM72C	PBK	SYCE2
LBR	FEN1	RAD51AP1	POT1
VRK1	HMGB2	TOP2A	REC8
NCAPG2	GINS1	BUB1	SMC3
CASP2	DTL	POLE2	H1F0
TMPO	DEPDC1B	RRM2	TINF2
HMGN2P41	MCM3	ASPM	STAG3
FANCD2	MAD2L1	BIRC5	TERF2
CCNA2	NCAPH	NUF2	CABIN1
RNF138	KIF18B	CDK1	UBN1
PRPF38A	CDCA5	AURKB	HIST3H3
NDC80	CDK1	KIF20A	HMGA1
TRA2A	FANCD2	NCAPG2	UBE2I
CKLF-CMTM1,CKLF	MND1	NDC80	TERF1
METTL21A	HELLS	HJURP	ACD
	CDC7		ASF1A
	CENPA		SMC1B
	RP11-307P22.1		SYCP3
			BRCA1
			HIVEP1
			TMPO
			YY1
			PRKCD
			CDK1
			H2AFX

Table 3: Genes in the immediate neighborhood of LMNB1 in functional (STRING) and gene co-expression networks (GENEVESTIGATOR)

GENEVESTIGATOR			STRING
Anatomy co-exp.	Cell lines co-exp.	Perturbation co-exp.	
CCNB1	KLF16	MCM2	CASP6
MIR7112	MIR7106	WHSC1	CASP2
PRC1	BAHD1	RNASEH2A	LMNB1
RNASEH2A	TRAIP	RP11-298C3.2	YY1
MELK	FZR1	MCM7	TMPO
FOXM1	AMBRA1	MCM4	PRKCD
SPDL1	GATAD2A	MCM3	GPRASP2
TPX2	PLCB3	FEN1	SVIL
UBE2C	WDR62	CDC20	HIVEP1
HMGA1	NCOA5	AURKB	
CDC20	PPIAP21	CDC45	
t DEPDC1	CWF19L1	FOXM1	
PAICSP4	DHX37	UHRF1	
TYMS	TRMT61A	MIR106B	
KIF23	CCDC94	MIR93	
CEP55	INTS5	MIR25	
TRIP13	NELFB	TIMELESS	
DLGAP5	ZNF554	TRIP13	
BUB1B	SIRT6	UBE2C	
NME1	DOHH	BIRC5	
UCK2	CASKIN2	CHEK1	
DTYMK	SUPT5H	TPX2	
KIF20A	TOP3BP1	BUB1B	
RP11-298C3.2	SLC25A22	KPNA2	
CDC6	C20orf27	RP13-104F24.2	
		RP13-104F24.1	
		MCM5	
		POLD1	
		CTD-2545M3.6	
		SNRPF	

Table 4: Genes in the immediate neighborhood of LMNB2 in functional (STRING) and gene co-expression networks (GENEVESTIGATOR)

[1] M. Eriksson, W. T. Brown, L. B. Gordon, M. W. Glynn, J. Singer, L. Scott, M. R. Erdos, C. M. Robbins, T. Y. Moses, P. Berglund, et al., Recurrent de novo point mutations in lamin A cause Hutchinson–Gilford progeria syndrometchinson–gilford progeria syndrome, Nature 423 (6937) (2003) 293–298.

[2] K. Cao, B. C. Capell, M. R. Erdos, K. Djabali, F. S. Collins, A lamin A protein isoform overexpressed in Hutchinson-Gilford progeria syndrome interferes with mitosis in progeria and normal cells, Proc Natl Acad Sci U S A 104 (12) (2007) 4949–54. doi:10.1073/pnas.0611640104.

[3] R. D. Goldman, D. K. Shumaker, M. R. Erdos, M. Eriksson, A. E. Goldman, L. B. Gordon, Y. Gruenbaum, S. Khuon, M. Mendez, R. Varga, F. S. Collins, Accumulation of mutant lamin A causes progressive changes in nuclear architecture in Hutchinson-Gilford progeria syndrome, Proc Natl Acad Sci U S A 101 (24) (2004) 8963–8. doi:10.1073/pnas.0402943101.

[4] M. Sinensky, T. McLain, K. Fantle, Expression of prelamin A but not mature lamin A confers sensitivity of DNA biosynthesis to lovastatin on F9 teratocarcinoma cells, J Cell Sci 107 (Pt 8) (1994) 2215–8.

[5] F. Kilic, J. Salas-Marco, J. Garland, M. Sinensky, Regulation of prelamin A endoprotease activity by prelamin A, FEBS Lett 414 (1) (1997) 65–8.

[6] N. J. Ullrich, L. B. Gordon, Hutchinson-Gilford progeria syndrome, Handb Clin Neurol 132 (2015) 249–64. doi:10.1016/B978-0-444-62702-5.00018-4.

[7] J. Halaschek-Wiener, A. Brooks-Wilson, Progeria of stem cells: stem cell exhaustion in Hutchinson-Gilford progeria syndrome, J Gerontol A Biol Sci Med Sci 62 (1) (2007) 3–8.

[8] P. Scaffidi, T. Misteli, Lamin A-dependent misregulation of adult stem cells associated with accelerated ageing, Nat Cell Biol 10 (4) (2008) 452–9. doi:10.1038/ncb1708.

[9] P. R. Musich, Y. Zou, Genomic instability and DNA damage responses in progeria arising from defective maturation of prelamin A, Aging (Albany NY) 1 (1) (2009) 28–37. doi:10.18632/aging.100012.

[10] V. L. R. M. Verstraeten, J. Y. Ji, K. S. Cummings, R. T. Lee, J. Lammerding, Increased mechanosensitivity and nuclear stiffness in Hutchinson-Gilford progeria cells: effects of farnesyltransferase inhibitors, Aging Cell 7 (3) (2008) 383–93. doi:10.1111/j.1474-9726.2008.00382.x.

[11] A. Doni, C. Garlanda, A. Mantovani, Innate immunity, hemostasis and matrix remodeling: Ptx3 as a link, Semin Immunol 28 (6) (2016) 570–577. doi:10.1016/j.smim.2016.10.012.

[12] C. Shi, E. G. Pamer, Monocyte recruitment during infection and inflammation, Nat Rev Immunol 11 (11) (2011) 762–74. doi:10.1038/nri3070.

[13] F. Font-Clos, S. Zapperi, C. A. M. L. Porta, Integrative analysis of pathway deregulation in obesity, npj Systems Biology and Applications (in press).

[14] A. Liberzon, C. Birger, H. Thorvaldsdóttir, M. Ghandi, J. P. Mesirov, P. Tamayo, The molecular signatures database hallmark gene set collection, Cell Systems 1 (6) (2015) 417–425. doi:10.1016/j.cels.2015.12.004.
URL `https://doi.org/10.1016/j.cels.2015.12.004`

[15] STRING, https://string-db.org/.

[16] IPA, https://www.qiagenbioinformatics.com.

[17] GeneInvestigator, https://genevestigator.com.

[18] L. Katz, A new status index derived from sociometric analysis, Psychometrika 18 (1) (1953) 39–43.

[19] P. Bonacich, Factoring and weighting approaches to status scores and clique identification, The Journal of Mathematical Sociology 2 (1) (1972) 113–120. doi:10.1080/0022250x.1972.9989806.
URL https://doi.org/10.1080/0022250x.1972.9989806

[20] A. Bavelas, A mathematical model for group structures, Human Organization 7 (3) (1948) 16–30. doi:10.17730/humo.7.3.f4033344851gl053.
URL https://doi.org/10.17730/humo.7.3.f4033344851gl053

[21] L. Page, S. Brin, R. Motwani, T. Winograd, The pagerank citation ranking: Bringing order to the web., Technical Report 1999-66, Stanford InfoLab (November 1999).

[22] T. P. Peixoto, The graph-tool python library, figsharedoi:10.6084/m9.figshare.1164194.
URL http://figshare.com/articles/graph_tool/1164194

[23] Graph Tool, https://graph-tool.skewed.de/static/doc/centrality.html.

[24] J. Marji, S. I. O'Donoghue, D. McClintock, V. P. Satagopam, R. Schneider, D. Ratner, H. J. Worman, L. B. Gordon, K. Djabali, Defective lamin A-Rb signaling in Hutchinson-Gilford progeria syndrome and reversal by farnesyltransferase inhibition, PLoS ONE 5 (6) (2010) e11132. doi:10.1371/journal.pone.0011132.
URL https://doi.org/10.1371/journal.pone.0011132

[25] M. Plasilova, C. Chattopadhyay, A. Ghosh, F. Wenzel, P. Demougin, C. Noppen, N. Schaub, G. Szinnai, L. Terracciano, K. Heinimann, Discordant gene expression signatures and related phenotypic differences in lamin A- and A/C-related Hutchinson-Gilford progeria syndrome (HGPS), PLoS ONE 6 (6) (2011) e21433. doi:10.1371/journal.pone.0021433.
URL https://doi.org/10.1371/journal.pone.0021433

[26] A. B. Csoka, S. B. English, C. P. Simkevich, D. G. Ginzinger, A. J. Butte, G. P. Schatten, F. G. Rothman, J. M. Sedivy, Genome-scale expression profiling of Hutchinson-Gilford progeria syndrome reveals widespread transcriptional misregulation leading to mesodermal/mesenchymal defects and accelerated atherosclerosis, Aging Cell 3 (4) (2004) 235–243. doi:10.1111/j.1474-9728.2004.00105.x.
URL https://doi.org/10.1111/j.1474-9728.2004.00105.x

[27] K. Cao, C. D. Blair, D. A. Faddah, J. E. Kieckhaefer, M. Olive, M. R. Erdos, E. G. Nabel, F. S. Collins, Progerin and telomere dysfunction collaborate to trigger cellular senescence in normal human fibroblasts, Journal of Clinical Investigation 121 (7) (2011) 2833–2844. doi:10.1172/jci43578.
URL https://doi.org/10.1172/jci43578

[28] R. P. McCord, A. Nazario-Toole, H. Zhang, P. S. Chines, Y. Zhan, M. R. Erdos, F. S. Collins, J. Dekker, K. Cao, Correlated alterations in genome organization, histone methylation, and DNA-lamin A/C interactions in Hutchinson-Gilford progeria syndrome, Genome Research 23 (2) (2012) 260–269. doi:10.1101/gr.138032.112.
URL https://doi.org/10.1101/gr.138032.112

[29] M. Newman, Networks: An Introduction, Oxford University Press, Inc., New York, NY, USA, 2010.

Effects of Progerin on nuclear cell plasticity

Maria Chiara Lionetti[a], Federico Mutti[a], Maria Rita Fumagalli[b], Francesc Font-Clos[b], Giulio Costantini[b], Stefano Zapperi[b], Caterina A. M. La Porta[a,1]

[a] *Center for Complexity and Biosystems University of Milano, Department of Environmental Science and Policy, via Celoria 26, 20133 Milano, Italy*

[b] *Center for Complexity and Biosystems University of Milano, Department of Physics, via Celoria 16, 20133 Milano, Italy*

Abstract

Physical connection between the nucleus and the cytoskeleton is essential for a broad range of cellular functions. In this study, we developed an inducible HeLa Tet-On 3G cellular model to investigate how the most common Lamin A mutation (Gly608Gly, Progerin) that causes HGPS impacts on nucleus to cytoskeleton coupling. Altogether, our findings show that Progerin expression significantly modifies the complex interaction between nucleus and the cytoskeleton. Promoting Fascin phosphorylation at Serine 39 regulatory site results in a stronger Actin- Giant Neprin2 interaction. Moreover, in Progerin overexpressing cells the nuclear structure appears to be more rigid. In addition, we have also investigated the effects of lamin A mutation on the cellular epigenetic landscape. Our results revealed that Progerin presence influences Polycomb repressor complex 2 activity by preventing physiologic SUZ12 binding to the wild type form of Lamin A.

Introduction

Nuclear lamina (NL) is an evolutionary well conserved cell structure, present in all the Metazoa [24]. It is a dense fibrillar protein meshwork that covers all the inner surface of the nuclear envelope (NE). It mainly consists of A-type and B-type lamins, which are type V intermediate filaments, and lamin-associated proteins (LAP) [11].

Besides providing mechanical support to the cells acting as nuclear framework, nuclear lamina functions as scaffold for the binding of chromatin) [11] and interacts with several different proteins related to the nucleoskeleton [8], the nuclear pore complex and factors whose role is to regulate gene expression [40]. Therefore, lamins participate in almost all nuclear activities and all the fundamental cellular processes such as mitosis, cell signalling, mechanotransduction [8], proliferation, and differentiation [13] [17].

The LINC (Linker of Nucleoskeleton and Cytoskeleton) complex consists of two major lamin-interacting transmembrane proteins SUN1/SUN2 and Nesprin family proteins [30] [8]. SUN1 and SUN2 are inner nuclear membrane (INM) proteins that work as a bridge across the nuclear envelope: while their amino-terminal domains interact with Lamin A on the nucleoplasmic face of the NE, their carboxy-terminus binds to neprins in the perinuclear space (see Fig. 1). Nesprins are high molecular weight proteins associated with the nuclear membrane (Fig.1). Four different Nesprin proteins isoforms have been currently described: Nesprin-1, Nesprin-2, Nesprin-3 and

*Caterina A. M. La Porta

Email address: caterina.laporta@unimi.it (Caterina A. M. La Porta)

Nesprin-4. Nesprins can associate with the inner or outer nuclear membrane depending on their size. In particular, the larger isoforms also called "Giant"-Nesprin-1 and -2, associate with the outer nuclear membrane exposing their N-term domain towards the cytoplasm where it binds cytoskeletal microfilaments [41], intermediate filaments [42], actin-bundling proteins and microtubules [38]. In particular, Nesprin-2 has been recently reported to recruit Fascin, an actin-bundling protein, to the NE both in vitro and in vivo [34]. Fascin is made up of 4 b-trefoil repeats separated by short flexible linker regions and it has 2 major binding sites for actin, one within the βt1-βt2 domains and the second within βt3-βt4 [34]. Serine 39 (S39) on βt1 is an important regulatory site for the actin-bundling activity of Fascin as its phosphorylation by PKCα results in Fascin binding to Nesprin-2 promotion [34, 1]. More precisely, Nesprin-2 binds directly to the Fascin β-trefoil3 domain through spectrin repeats (SRs) 5153 at its C-terminal domain, modulating nuclear localization in fibroblasts and nuclear deformation in cancer cells [19]. In this way, Giant Nesprins ensure nucleusto-cytoskeleton connection [16], providing a strong anchorage of the nuclear membrane to the cytoskeleton that is essential for cell migration and correct localization of the nucleus inside the cell. On the other hand, smaller Nesprins isoforms are present at the inner nuclear membrane where directly bind to lamin A/C and Emerin, a nuclear envelope transmembrane protein involved in NL-chromatin interaction [31].

In the last decades, hundreds of mutations in genes encoding for Lamins, in particular Lamina A, or Lamins functional-related genes have been reported to be responsible for the onset of a range of disorders, termed laminopathies. Laminopathies encompass apparently disparate phenotypes with a broad clinical spectrum. Among these diseases, the most interesting one is Hutchinson-Gilford Progeria Syndrome (HGPS) [36]. HGPS is an accelerating-aging genetic disorder due to a point mutation in LMNA genes that leads to the production of an aberrant form of Lamina A protein, lacking of 50 amminoacids, called Progerin [12]. Several studies reported that Progerin persistence in HGPS has a dominant-negative effect on nuclear structure and functions, the most noticeable defect being aberrant nuclear morphology [5, 15].

In this paper, we build up an inducible HeLa Tet-On 3G cellular model to investigate how the most common Lamin A mutation (Gly608Gly, Progerin) that causes HGPS, modifies the shape of the nucleus and why there is an impact from the functional point of view. Altogether, our data clearly show that presence of Progerin modifies the complex interaction between nucleus and the cytoskeleton and in particular increases the phosphorylated form of Fascin. The consequence of this phosphorylation is that Fascin is more linked to giant Nesprin-2 and the nucleus appears more rigid.

We have also investigated if under the expression of Progerin there is a different organization of chromatin and lamins.

In fact, nuclear lamina has been widely reported to be involved in gene expression regulation, and in particular in gene repression, since the discovery of lamin-associated domains (LADs)[22, 33]. LADs are heterochromatic and transcriptionally repressed large genomic regions marked by H3K9me2, H3K9me3 or H3K27me3, that bind nuclear lamina [35]. the association between NL and chromatin could be directly mediated by A-type lamins or indirectly by other lamins functional related proteins such as Emerin. Emerin is a lamin-binding nuclear membrane protein that has two distinct functional domains: the LEM-domain at the N-terminus, which mediates binding to chromatin, and a second functional domain in the central region, which mediates a direct binding to lamin A[23, 27]. Recent studies reported the presence of a strong functional interaction between Lamin A and Polycomb complex group proteins (PcG) [29]. PcG proteins are transcriptional regulators, mainly present in the nucleus as multimeric protein complexes named Polycomb repressive complexes (PRCs)[6, 7]. The two complexes PCR1 and PCR2 are able to

post-translationally modify histones and silence target genes acting as key epigenetic regulators of the most important cellular processes. PRC1 and PRC2 have different roles: PRC2 imposes high levels of H3K27me3 [3] as a repressive mark for chromodomains of PRC1, PRC1 recognizes H3K27me3 and inhibits transcriptional elongation through H2A ubiquitylation [43] in order to compact the chromatin structure [10, 14]. We characterized the PcG expressed under Progerin expression observing no significant changes in protein expression levels. On the other hand, we found that Progerin presence prevents the physiologic binding of SUZ12, a core component of PCR2, to the Lamin A.

Material and Methods

Human Fibroblasts culture growth conditions

Human fibroblasts from HGPS patient (HGSDNF167) and the relatives of this patient (HGFDNF168 and HGMDF090, father and mother, respectively) are obtained from the Progeria Foundation Cell and Tissue Bank. The HGPS patient was a male of 8 years old with the classical mutation (heterozygous LMNA Exon 11 c1824 $C > T$ (p.Gly608Gly). The cells were maintained according to the protocol reported by The Progeria Foundation: 15% FBS, DMEM with 1% antibiotics and 1% L-glutamine. The cells were detached by trypsin EDTA 0.25% and are maintained in culture for no more than five passages.

Plasmids and Subcloning

Δ50-Lamin A plasmid was obtained by Addgene (pEGFP Δ50LaminA, Addgene, cod.17653). Plasmid expressing pTRE3G-mCherry vector was obtained by Clontech (cod. 631165). E. coli One Shot TOP10 bacteria (Invitrogen, C404006) were used for transformation with pEGFP Δ50LaminA and pTRE3G-mCherry vector. Competent cells were expanded and selected in Luria Broth medium (Invitrogen, 12795-027) containing Kanamicin for pEGFP Δ50-Lamin A (Sigma Aldrich, K13747) and 100 μg/mL Ampicillin (Sigma Aldrich, A5354) for pTRE3G-mCherry vector for 18h 37°C.

AfeI/BamHI fragment containing the coding reading sequence of Δ50 Lamin A was excised by pEGFP-Δ50LaminA plasmid (AfeI cod.R0652S, New England Biolabs) and subcloned into pTRE3G-mCherry vector linearised with EcorV (cod. R1095S, New England Biolabs) and BamHI (cod. R0136SS, New England Biolabs) restriction enzymes according to the manufacturer's instructions. DNA fragments and vectors were routinely analysed by electrophoresis on 1% agarose gel in 1X TAE (Euroclone GellyPhor EMR010100). Low Melting agarose gel (Euroclone Gellyphor EMR911100) was used for the recovery of DNA fragments after electrophoresis. DNA fragments were purified using agarose gels QIAquick Gel Extraction Kit. To recover DNA digested fragments and linearised vectors after electrophoresis and proceed with subcloning, Promega T4 DNA ligase (cod. M1801) was used to allow ligation step in according to manufacturer's protocols.

DNA fragments and vectors were routinely analysed by electrophoresis on 1% agarose gel (Euroclone GellyPhor EMR010100), in 1X TAE while Low Melting agarose gel (Euroclone Gellyphor EMR911100) was used for the recovery of DNA fragments after electrophoresis. To purify DNA fragments from agarose gels QIAquick Gel Extraction Kit was used. To recover DNA digested fragments and linearised vectors after electrophoresis and proceed with subcloning, Promega T4 DNA ligase (cod. M1801, Promega) was used to allow ligation step in according to manufacturer's protocols. Promega PureYield Plasmid Miniprep and Midiprep (cod.A1330 and A2492, Promega) were used to purify plasmidic DNA.

Progerin Tet-On HeLa cells : transfection and culture methods

HeLa Tet-On 3G cells (Clontech cod. 631183) were cultured in DMEM (Euroclone cod. ECB7501L) supplemented with 10% v/v Tet-free FBS (Euroclone, cod. ECS01821) 1% Penincillin/Streptomycin and 1% L-Glutamine at 37°C and 5% CO_2 in humidified incubator immediately upon thawing without selective resistance. To create a double stable inducible HeLa 3G cell line expressing Δ50 lamin A, HeLa 3G cells were co-transfected with 5μg of pTRE3G-mCherry-Δ50-Lamin A using Xfect reagent (Clontech, cod.631317) and 250 ng of puromycin linear selection marker (Clontech cod.631626) in according to the manufacturer's instructions.

After 48h post-transfection, the cells were splitted into 4 x 10cm dishes and 0,5 μg/ml of Puromycin (Life Technologies cod. A11138-03) and 200μg/ml G418 (Sigma, cod. A1720) was added to select the positive clones. Drug-resistant colonies appeared 2 weeks after selection. Single clones were isolated using cloning cylinder (Sigma cod. C1059). When they reached the confluence, the cells were splitted in 6-well plate for testing the expression of Δ50 lamin A and for further maintenance. In order to express Δ50-Lamin A in dose dependent manner, the cells were induced with doxycycline (Clontech cod.631311) at the concentration indicated in the figures and analysed 48h after the induction. HeLa 3G cells expressing Δ50-Lamin A were rountinely maintained in culture in DMEM (Euroclone cod. ECB7501L) supplemented with 10% v/v Tet-free FBS (Euroclone cod.ECS01821), 200μ/ml G418 and 0.25μg/ml Puromycin, 1% Penincillin/Streptomycin and 1% L-Glutamine at 37°C and 5% CO_2.

Δ50 lamin A and WT lamin A transient trasfection

Plasmid containing the human Lamin A-C-18 (Addgene, cod. 55068) or Progerin (pEGFP-Δ50 lamin A, Addgene, cod.17653) were purchased by Addgene. E. coli One Shot TOP10 bacteria (Invitrogen, cod.C404006) were transformed with plasmids, expanded and selected in Luria Broth medium (Invitrogen, cod. 12795-027) containing 50 μg/mL Kanamicin. PureYield Plasmid Miniprep and Midiprep (Promega, cod.A1330 and A2492) were used to purify plasmidic DNA.

HeLa cells were maintained in DMEM (Euroclone, cod. ECM0060L) medium with 10% fetal bovine serum (Euroclone, ECS0180L), 100 U/ml penicillin, 100 mg/ml streptomycin sulphate (Euroclone,cod. ECB3001D) and 2mM L-Glutamine (Euroclone, cod. ECB3000D-20) at 37°C in an atmosphere of 5% CO2 and 95% humidity. Cells seeded at an 70% confluent onto 6-well plates were transiently transfected with pEGFP Δ50LaminA (Addgene, cod.17653) or mEmerald-WT-LaminA (Addgene, cod.54139) using Xfect transfection reagent (Clontech, cod 631317). After 48 h from transfection cells were used for cytosckeleton pharmacological perturbation experiment (see Materials and Methods).

Immunofluorescence

Subconfluent cells grown on glass coverslips are fixed with ice cold methanol for 5 minutes at -20°C, permeabilized and blocked with 1% BSA /10% Goat Serum/0.3M glycine/0.1% Tween 20 in PBS for 1 hr at room temperature.

The cells are stained with anti-Panlamin (1:50 mouse, Abcam ab207404) or anti-Lamin A (1:100 mouse, Abcam ab8980) or anti-Lamin B1(1:200 rabbit, Abcam ab16048) or Anti-Progerin overnight at 4°C. Thus, after a brief washing with PBS, the cells are incubated with the secondary antibody (anti rabbit or anti-mouse Alexa488 1:250) for 1 h. The nuclei are counterstained with DAPI and the slides mounted with Pro-long anti fade reagent (Life technologies). The images are acquired with a Leika TCS NT confocal microscope.

Duolink assay

Duolink assay involve a pair of oligonucleotide labeled secondary antibodies (PLA probes) that generates a fluorescent signal when the two PLA probes, bound to two primary antibodies raised in different species, recognized two antigens in close proximity (less than 40nm). Subconfluent cells were fixed on slides with ice cold 100% methanol for 5 min at at -20°C and incubated with Duolink Blocking Solution for 60 minutes at 37°C in a humidity chamber. Slides were then incubated in a humidity chamber overnight at 4°C with Lamin A (1:100 Abcam mouse, ab8980) or Panlamin (1:50 mouse, Abcam ab207404) and SUZ12 (1:800, Rabbit mAb 3737, Cell Signaling) or BMI1 (1:600, Rabbit mAb 6964, Cell signaling) antibodies were diluted in the Duolink Antibody Diluent and the slides were incubated with antibodies solution in a humidity chamber overnight at 4°C. After washing, anti-rabbit PLUS and anti-mouse MINUS PLA probes were diluted 1:5 in the Duolink Antibody Diluent and samples were incubated in a pre-heated humidity chamber for 1 hour at 37°C.

Ligation and amplification steps were performed according to manufacturer's instructions. Slides were mounted with Duolink In Situ Mounting Medium with DAPI (DUO82040, Sigma-Aldrich). The images were acquired with a Leika TCS NT confocal microscope.

Western blot

Confluent cells were lysed by boiling in a modified Laemmli sample buffer (2% SDS, 20% glycerol, and 125 mM Tris-HCl, pH6.8). The protein concentration was measured by DC Protein Assay Kit (BioRad). Equal amount of proteins were loaded on gel, separated by SDS-PAGE and transferred to a PVDF membrane (Trans-Blot Turbo ini PVDF, BioRad) using Trans-blot turbo system (BioRad). After blocking with 5% BSA/0.1% Tween20 in PBS for 1h at RT, primary and HRP-linked secondary antibodies specific bindings were detected by chemiluminescence system (Clarity Western Blotting ECL substrate, Biorad).

Mouse monoclonal antibody anti-nesprin 2 (1:1000, MABC86) or rabbit anti-SUN1 (1:1000, Abcam ab103021) or anti-Emerin (1:200 rabbit, Abcam ab40688) or anti-SUZ12 (1:1000, Rabbit mAb 3737, Cell Signaling) or rabbit anti- Ezh2 (1:1000, Rabbit mAb 5246 , Cell Signaling) or rabbit anti- Ring1A (1:1000, Rabbit mAb 13069, Cell signaling) or rabbit anti-RING1B (1:1000, Rabbit mAb 5694, Cell Signaling) or rabbit anti- Bmi1 (1:1000, Rabbit mAb 6964, Cell signaling) or rabbit anti- H3K27met3 (Rabbit mAb 9733, Cell signaling) were used overnight at 4°C.

Mouse anti-vinculin (1:10000, V9264, Sigma) or rabbit anti-GAPDH(1:5000, Sigma G9545) or Anti β-tubulin (1:5000mouse, Sigma T0198) for 1h at room temperature was used as housekeeping. Secondary antibodies (anti-rabbit or anti-mouse-HRP 1:3000 in 5% milk/0.1% Tween20 in PBS, Biorad) were used for 1h at room temperature to detect chemiluminescence.

Fascin immunoprecipitation with Protein A-Agarose

Confluent cells weere detached from the culture plates using a cell lifter in cold PBS, collected in a 1,5 ml eppendorf and the cell suspension was centrifuged at $3.5{\cdot}10^3$ x g for 5 min at 4°C. Cell pellets were resuspended in lysis buffer (2 mM EGTA,0.5 mM EDTA, 0.5 mM PMSF, 1X TRITONX100, 1X protease cocktail Sigma Aldrich P8340) and incubated on ice for 30 min with periodic agitation. The lysate was centrifuged at $14{\cdot}10^3$xg for 10 min at 4°C, the supernatant transferred to a fresh tube and proteins concentration was measured by DC Protein Assay Kit (BioRad). 500 μg of total proteins in lysis buffer were incubated with anti-fascin antibody (1:100, AbCam, ab126772) overnight at 4°C under agitation and following 50% beads slurry of Protein A-Agarose (Sigma-Aldrich, P9269) was added to the lysate. The mixture of beads and lysate was incubated with gentle rocking for 2 hours at 4°C and then centrifuged at $14{\cdot}10^3$ x g for 10 min

at 4°C. After three washes with 500μl of lysis buffer the sample was resuspended in 30μl of 2X Laemmli sample buffer(2% SDS, 20% glycerol, and 125 mM Tris-HCl, pH 6.8).

Finally, samples were heated to 90°C for 5 minutes. 15 μl per sample were loaded on SDS-PAGE gel (7.5%) and transferred to a PVDF membrane using Trans-blot turbo system (BioRad). After blocking with 5% BSA/0.1% TWEEN20 in PBS for 1h at RT, anti Phospho-Fascin antibody (1:10000, Abcam ab90618) or anti-fascin antibody (1:100, AbCam, ab126772) and HRP-linked secondary antibody specific bindings were detected by chemiluminescence system (Clarity Western Blotting ECL substrate, Biorad).

Cytosckeleton Pharmacological Perturbation

To study the role of cytoskeleton in this context, actin and myosin organization were perturbed by exposing pEGFP-Δ50LaminA or mEmerald-WT-LaminA overexpressing cells to Blebbistatin, a myosin inhibitor, or to a cell-permeable inhibitor of formin-mediated actin nucleation and formin-mediated elongation of actin filaments, SMIFH2. Subconfluent Hela cells expressing WT or Δ50 Lamin A were exposed to 25μM Blebbistatin (Sigma-Aldrich, B0560) for 30 min or to 20μM SMIFH2 (Sigma-Aldrich, S4826) for 1 hour at 37°C and 5% CO_2 in humidified incubator. Five minutes prior the end of the treatment, Hoechst (1:1000, Life technology, H3570) was added to the cell medium to counterstain nuclei. Immediately after the end of each treatment, medium containing drugs was replaced with fresh medium and cells were time-lapse imaged (1 shoot every 15 minutes) for 1h using a Leica TCS NT confocal microscope (63X) with a z-stack of 0.5 μm.

Image analysis

Immunofluorescence images were analyzed using existing and customized ICY plugins (v.1.9.4 and 1.9.5 [9]) and custom python scripts. In all the analyzed frames nuclei close to the borders or superimposed were manually discarded.

Duolink assay analysis. Reconstruction of nuclear envelope was performed on all the Z-stacks with ICY Icy HK-Means and ActiveContour plugin using DAPI signal and the resulting 3D meshes were exported as VTK files. A wide range of parameters was explored in order to ensure that our result were not affected by the specific parameters chosen for reconstruction. Duolink spot recognition was performed separately on each nucleus with a semi-automatic protocol involving HK-means tresholding (ICY Thresholder plugin). The minimum size of each accepted spot was set to 70 px. Center of mass (CM) was used to determine the relative position of the duolink spot respect to the nuclear envelope, and spots inside reconstructed nuclear mesh were counted.

Cytosckeleton Pharmacological Perturbation analysis. Reconstruction of nuclear envelope was performed on all the Z-stacks was performed using images with the nuclei and over-expressed lamin skeletons. We applied the Icy HK-Means plug-in to obtain three dimensional (3D) nuclear regions of interest (ROIs) for each temporal acquisition. This segmentation method uses, in fact, a K-Means classification to detect clustered objects corresponding, in our case, to the nucleus structures. The final 3D meshes of the outer nuclear membrane have been obtained thanks to the Icy Active Contours plug-in. The parameters used for the reconstruction are the default ones except for the values of contour smoothness, contour sampling and region sensitivity. For these three parameters we used, respectively, the values in the ranges 0.028-0.032, 1.9-2.1 and 2-3.

Total volume change between two meshes M_0, M_1 of a given cell at different time-points can reveal key information in some situations, but most local morphological changes can take place at fixed volume. To circumvent this issue and detect local morphological changes, we develop the

concept of local displacements d_j, which can be interpreted as the distance each face of M_0 should move to turn M_0 into M_1.

Briefly, the local displacements d_j of a triangular face j of a mesh M_0 with respect to a mesh M_1 are computed as follows. We find the matching μ that minimizes the total distance:

$$\mu = \text{argmin}_m \sum_i ||m(v_i) - v_i|| \tag{1}$$

where $m : \mathcal{V}_0 \to \mathcal{V}_1$ is a one-to-one correspondence between the vertices of M_0 and those of M_1. If $|\mathcal{V}_0| \neq |\mathcal{V}_1|$, we resort to subsampling the mesh with the largest number of vertices. We solve the equation using the Hungarian algorithm as implemented by the *scipy.optimize.linear_sum_assignment* function from the SciPy library . We computed the displacement vectors $\vec{q_i} = \mu(v_i) - v_i$ of each vertex, the normal vectors to all faces $\vec{n}_j$ and the projections of q_i on n_j. The local displacement d_j is the average of $q_i \cdot n_j$ over the vertices i that form face j:

$$d_j = \vec{n}_j \cdot \left(\frac{1}{3} \sum_{i=0}^{2} \vec{q_i} \right) \tag{2}$$

For each cell, the standard deviation $\sigma(d)$ of local displacements d_j over all the faces can be used as a proxy of deformation. Large values of $\sigma(d)$ are associated with heterogenous morphological changes such as bleb formation, while low values of $\sigma(d)$ are obtained when the changes are homogenous over the nucleus surface. In particular, volume changes due to a uniform shrinking/expansion would entail a value of $\sigma(d) \ll 1$.

Results

Progerin expression in TetON HeLa cells

We have developed a Δ50-Lamin A inducible expression HeLa model using Tetracycline controlled gene activation system (Tet-On system). Tetracycline controlled transcription activation is a method of inducible gene expression where transcription is reversibly turned on or off depending on the presence of the antibiotic tetracycline. Briefly, we cloned Δ50-Lamin A insert under the control of tetracycline inducible promoter (TRE3G), that only in presence of Doxycycline (Dox), a tetracycline analogous, promotes Δ50-Lamin A transcription in a Dox dose-dependent manner.

In Figure2 is shown Δ50-Lamin A expression increase with increasing in Dox concentration, after 48h of exposure. As appreciable, we achieved a significant increase of Progerin expression levels at 10 ng/ml of Dox, that resulted to be best experimental condition since allow us to completely avoid Dox off-target effects, such as aspecific Progerin fluorescent signal observed in cells exposed to 20 ng/ml Dox (Fig.2b). Notably, 48h after Progerin expression induction with Dox 10 ng/ml, we observed the presence of dysmorphic nuclei displaying a cellular phenotype very similar to those of HGPS derived cells (Fig.2c). Therefore, at least for the morphological point of view, our model faithfully resembles pathologic cell morphology. For all the subsequent experiments we used the induction with 10ng/ml Dox. Then, we have checked the levels of Lamin A and Lamin B in Tet-On expressing Progerin HeLa. As shown in Figure 3, no significant changes occur for both Lamin A and Lamin B at all the concentration of Dox.

Impact of Progerin on Lamina-Cytoskeleton interactions

Cell nucleus is not to be considered an entity by itself, detached from the context in which it resides. Indeed, it is physically and thus functionally connected both with the cytoskeleton via

nuclear lamina components and linkers proteins interactions, and with the residing DNA via lamins and Nuclear envelope transmembrane proteins (NETs) indirect bindings. In order to evaluate the impacts of Progerin expression on the complex protein network that ensure nuclear lamina connection both with extranuclear compartment and chromatin, we investigate the expression of one the most important NET protein, Emerin that mediates nuclear lamina-chromatin binding, and LINC complex components, SUN1 and Nesprin2, responsible for nucleus-cytoskeleton coupling.

As shown in Figure 4, no significant changes in the expression of both Emerin and SUN1 occur in HeLa Tet-On Progerin-expressing cells. Nesprins are transmembrane proteins associated with the nuclear membrane [19, 39], belonging to the LINC complex. In particular, the larger isoforms called giant-nesprin-2 [21], associate with the outer nuclear membrane exposing their N-term domain towards the cytoplasm where it binds cytoskeletal actin and their C-term domain towards the perinuclear space where it binds to SUN1/2. In Figure 4 is shown that the level of expression of Giant-nesprin 2 does not change in Tet-On expressing Progerin HeLa cells. Considering that nesprin- 2 interaction with actin is regulated by phosphorylated ser39 fascin [19], we checked by immunoprecipitation the status of phosphorylation of Fascin in ser39. Interestingly, we found an increase of fascin serine 39 phosphorylated in Tet-On expressing Progerin HeLa cells (Fig.4, panel b). This data suggests a more stable coupling between the nucleus and cytoskeleton in the presence of Progerin.

Effect of Progerin on morphological changes due to drug targeting cytoskeleton

To better understand the possible functional changes due to the expression of Progerin in HeLa cells we transiently transfected these cells with GFP-Δ50 Lamin A (Progerin) or GFP-WT Lamin A plasmids and then we treated the cells with two different drugs which act on the cytoskeleton: blebbistatin, a myosin inhibitor [25] and SMIFH2, an inhibitor of formin-mediated actin nucleation [18] for 30min and 1h, respectively. After each treatment, we put the cells in fresh drug-free growth medium and we took a snapshot with a confocal microscope in time lapse of the cells treated or untreated, every 15 minutes up to an hour. The nucleus 3D mesh has been then reconstructed with Icy according to Material and Methods section.

Figure 7 shows distribution of nuclear envelope displacement standard deviation that is an indicator of nuclear deformation as function of the time, after actin or myosin inhibitors exposure and in untreated cells. As shown in Figure 7a, the treatment with blebbistatin significantly inhibits the physiological nuclear fluctuations in cells expressing Progerin with respect to untreated cells. In contrast, a negligible effect occur in cells expressing wt Lamin A (Fig.7a). Similar results occur with SMIFH2 treatment (Fig.7b) All together, these results suggest that the cell nuclei of Progerin-overexpressing cell are more rigid/stiffer and less plastic in comparison with those overexpressing WT Lamin A. Moreover, our data seem to indicate that in Δ50 Lamin A overexpressing cells nuclear fluctuations are mainly dependent on cytoskeleton coupling, since cytoskeleton components pharmacological inhibition results in a complete suppression of nuclear physiological fluctuations in time.

Expression of Prgerin prevents Polycomb Repressor Complex 2 binding to Lamin A

Nuclear lamina can be considered a regulator of chromatin status and thus gene expression since it works as dynamic platform that binds residing DNA, a large number of transcription factors and epigenetic regulators such as Polycomb complex group proteins (PcGs). In order to investigate the impact of Progerin overexpression on cellular epigenetic landscape, we analysed the expression levels of PcG proteins in our cellular model. In particular, we evaluated whether Progerin presence interferes in PcG protein-nuclear lamins interaction.

First we characterized the level of expression of the main PcGs in TetON Progerin expressing HeLa cells. As shown in Figure 8, we found that these cells express the main important PcGs. Then, we performed a proximity ligation assay which allows the detection of a fluorescent spot if two different primary are in close proximity (less than 40 nm), such as when they bind one to another.

Figure 9 shows the quantification of the number of dots obtained with proximity ligation assay. While there is no significant changes in the number of dots between PanLamin or Lamin A bindings BM1 In contrast, we found a significant decrease in the number of dots between PanLamin A and SUZ12 with respect to Lamin A and SuZ12 (Fig.9b).

Discussion

Nuclear lamina is involved in almost all fundamental cells functions since it is a dynamic platform that, besides providing mechanical support to the nucleus, takes contacts with a large number of proteins with different functions, termed lamin-associated proteins (LAP), and the residing DNA [37]. Mutations in lamins and lamin-associated proteins cause human diseases termed laminopathies [4]. Among these, there is the premature ageing disease HGPS, whose most prominent feature is the presence of aberrant nuclei. Progeria patients derived cells might be, in principle, the best biological tool to study in vitro the impact of Progerin on nuclear architecture and functions. Unluckily, these primary cells are not researchers friendly since these are obtained from very rare bioptic samples, have a very slow rate of doubling and can be maintained in culture for very few passages. The canonical approach used to bypass these experimental problems, is building cellular models that try to mimic the pathologic condition by overexpressing or silencing Lamin A or Progerin. This kind of models, although informative, most of the time are exasperation of the reality. Thus, in order to perturb nuclear lamina architecture in a more controlled way, with fine tuning of gene expression, we developed a Progerin-inducible expression cellular model using Tetracycline controlled gene activation system (TetOn system). Our model resembles the typical morphological changes of HGPS nuclei: under Progerin induced expression, indeed, we observed the presence of dysmorphic, disrupted, blebbed nuclei very similar to those of HGPS patients derived cells. One of the prominent structural role of NL consists in the formation of a physical and functional link between the lamina and the cytoskeleton [8]. These links, fundamental for the proper nuclear positioning in the cell and for mechanotransduction processes, are mediated by Lamin A and SUN 1/2 at the inner nuclear membrane, and SUN1 and Giant nesprin 1/2 in the perinuclear space [28]. Giant Nesprin-1/2 association with actin [41] is mediated by Fascin, an actin bundling-protein, whose phosphorylation at S39 by PKCα promotes its binding to Nesprin-2 [34, 1]. Notably, nuclear envelope localized Fascin has been reported to be crucial in maintaining the nuclear morphology and it allows nuclear deformability in physiologic conditions [19]. Our data clearly show that, the expression of progerin in TetOn Hela cells does not induce any significant changes in the level of expression of SUN1, emerin and Giant Nesprin2 expression, but promotes the phosphorylation of Serine-39 residue of Fascin. Therefore, this data suggest that the nucleus is more tightly linked to the cytoskeleton in the presence of progerin. Confirming this view, we found that progerin expression reduced the capability of the nucleus to ripristinate its morphology after inhibition of the cytoskeleton by blebbistatin or SMIFH2. Therefore in addition to the reported importance of the ratio of A-type lamins and B-type lamins for nuclear stiffness and plasticity [26], Progerin also contributes to the rigidity of the nucleus in agreement with other evidences [2]. Finally we checked the possible effect of progerin on the interaction between Polycomb group complex proteins (PgC). PcG proteins are transcriptional regulators that associate in

multimeric complexes termed Polycomb repressor complex 1 and 2 [6, 7]: key epigenetic regulators that post-transcriptionally modify histones leading to chromatin compactation [10, 14]. It has been reported that PcGs directly bind to Lamin A [29]. Moreover, the reduction of Lamin A/C levels causes PcGs dispersion in the nucleoplasm, accompanied by a relaxation of PcG-mediated higher-order chromatin structure which become more prone to transcriptional reactivation [29]. In progerin expressing cells we found an interesting decrease of LaminA-Suz12 interaction. Suz 12 is a core component of PCR2 that is required for an efficient H3K27 methylation [32]. Therefore, we speculate that the reduction of Suz12 and Lamin A interaction observed in the presence of progerin might contribute to the widely reported heterochromatin loss observed in HGPS derived cells [20]. Altogether, our findings revealed the peculiar role of Progerin in the changes of mechanical interaction between lamins and the cytoskeleton and in epigenetic regulation of chromatin status.

Figures

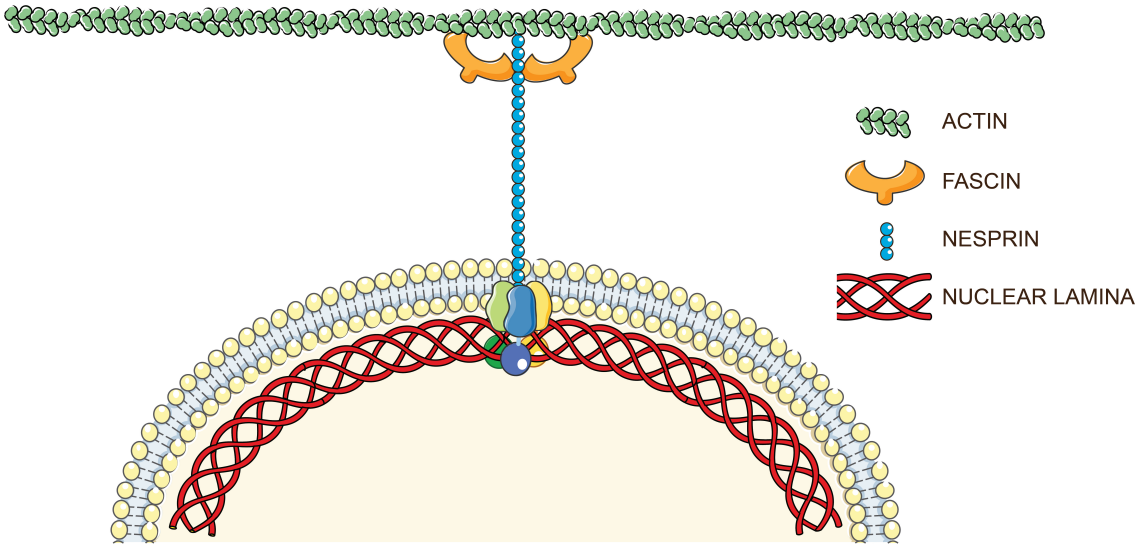

Figure 1: **Schematic representation of Nuclear membrane outer.**

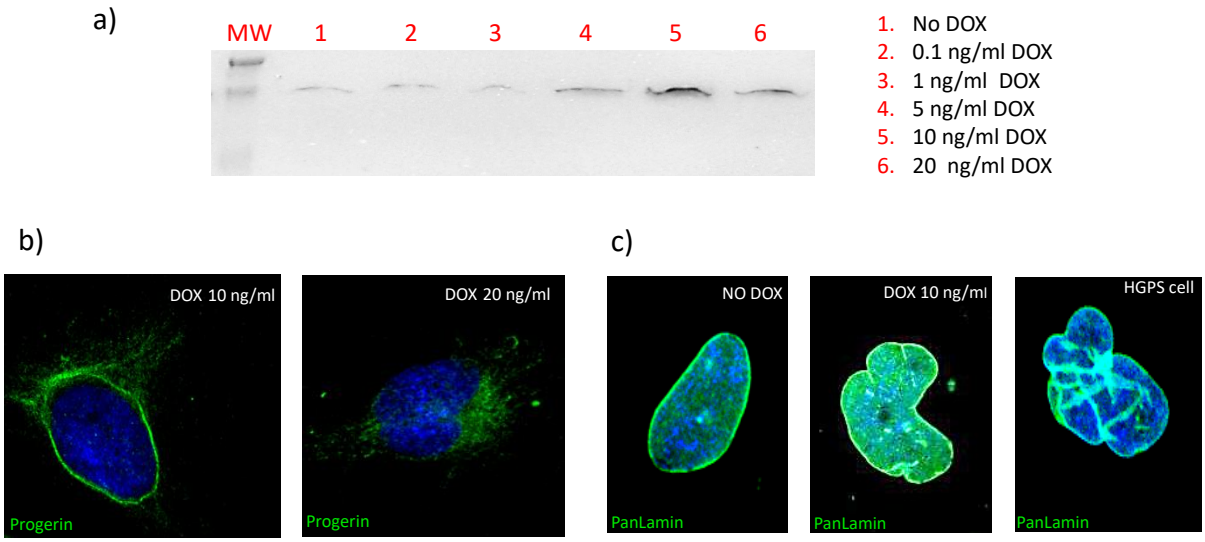

Figure 2: Panel a) Western blot of Progerin in HeLa TetON Progerin-expressing cells exposed to increasing dose of Dox. 20μg total protein were loaded on 10% polyacrylamide gel, transferred on PVDF and incubated with rabbit anti-Progerin (1:1000 rabbit, Abcam ab66587) overnight at 4°C. Mouse anti-Vinculin antibody (1:5000, Sigma) for 1 h at room temperature was used as housekeeping. Panel b) Progerin expression of HeLa TetON Progerin-expressing cells. Subconfluent cells were fixed with ice-cold methanol and incubated with anti-Progerin (1:20 rabbit, Abcam ab66587) overnight at 4°C. Then, the cells are incubated with anti-rabbit AlexaFluo488 for 1 h, at room temperature. Nuclei are stained with DAPI. Images are acquired by Leica SP2 laser scanning confocal microscope. Panel c) Example of HeLa TetON Progerin-expressing cells morphology before Dox induction, after 48h of Dox-Progerin induction and a HGPS derived cell. Subconfluent were cells fixed with ice-cold methanol, incubated with anti-PanLamin (1:50 mouse, Abcam ab207404) at 4°C and following with anti-mouse AlexaFluo488 for 1 h, at room temperature.

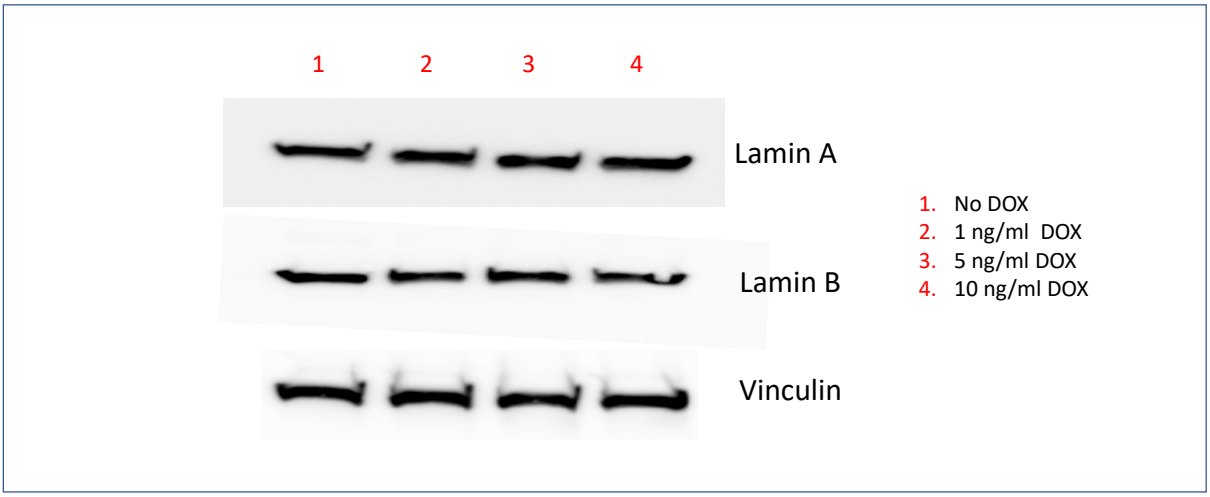

Figure 3: **Lamin A and B in TetON expressing Progerin HeLa cells** Western blot of Lamina A and Lamin B in HeLa cells untreated and after 2 days of increasing dose of Dox exposure. 20μg total protein were loaded on 10% polyacrylamide gel, transferred on PVDF and incubated or anti-Lamin A (1:1000 mouse, Abcam ab8980) or anti-Lamin B (1:1000 rabbit, Abcam ab16048) overnight at 4°C. Mouse anti-Vinculin antibody (1:5000, Sigma) for 1 h at room temperature was used as housekeeping.

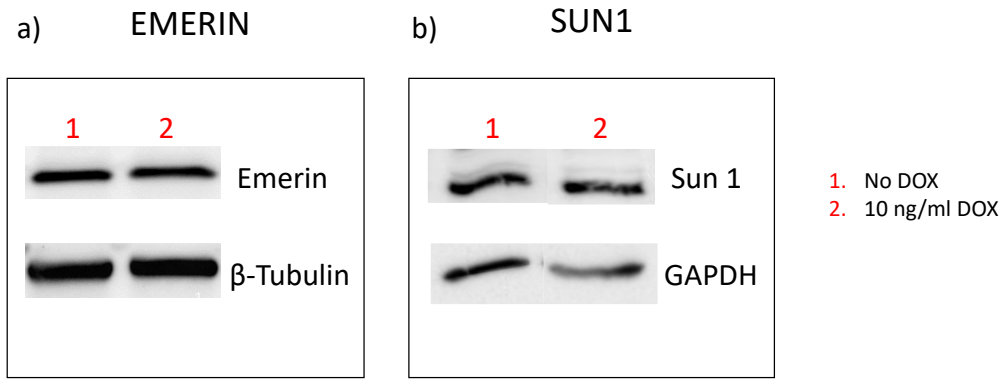

Figure 4: Levels of expression of Emerin and SUN1 in Δ50-laminA inducible cellular model after Progerin induced expression (10 ng/ml Dox) and in control condition. Western blot of Emerin (panel a) and SUN1 (panel b) in HeLa TetOn Progerin expressing cells. 20 μg total protein were loaded on 10% polyacrylamide gel, transferred on PVDF and incubated with anti-SUN1 (1:1000, Abcam ab103021) or anti-Emerin (1:1000 rabbit, Abcam ab40688) overnight at 4°C. Rabbit anti-GAPDH(1:5000, Sigma G9545) or mouse anti β-tubulin (1:5000, Sigma T0198) for 1h, at room temperature was used as housekeeping. Secondary antibodies (anti-rabbit or anti-mouse-HRP 1:3000 in 0.1% Tween20 / 5% milk in PBS, Biorad) were used for 1h at room temperature to detect chemiluminescence.

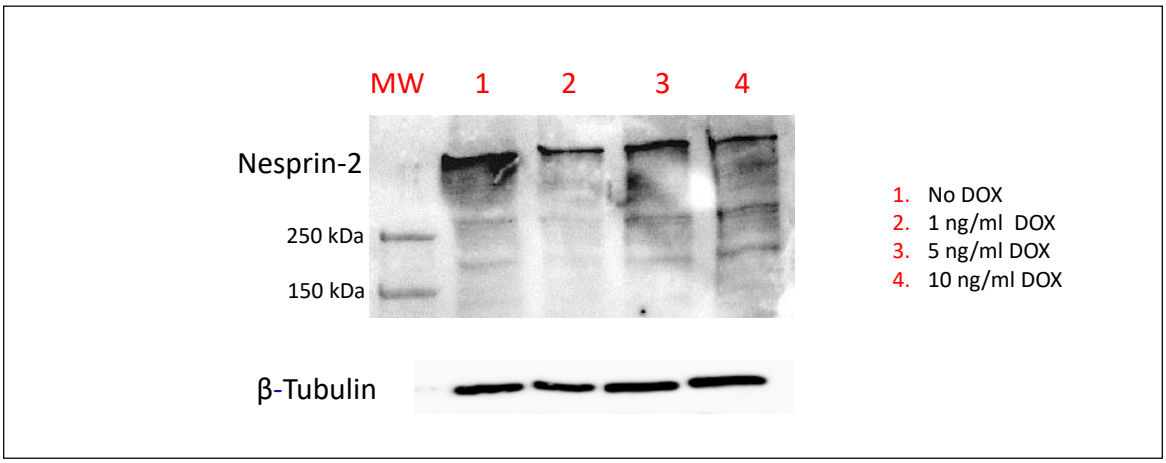

Figure 5: **Giant Nesprin-2 and S39-P-Fascin expression levels in Δ50-laminA inducible cellular model.** Western blot of Giant-Nesprin2 in HeLa TetOn Progerin expressing cells. 20 μg total protein were loaded on 10% polyacrylamide gel, transferred on PVDF and incubated with mouse monoclonal antibody anti-nesprin 2 (1:1000, MABC86) overnight at 4°C. Mouse anti β-tubulin (1:5000, Sigma T0198) for 1h at room temperature was used as housekeeping. Secondary antibodies (anti-mouse-HRP 1:3000 in 5% milk/0.1% Tween20 in PBS, Biorad) was used for 1h at room temperature to detect chemiluminescence.

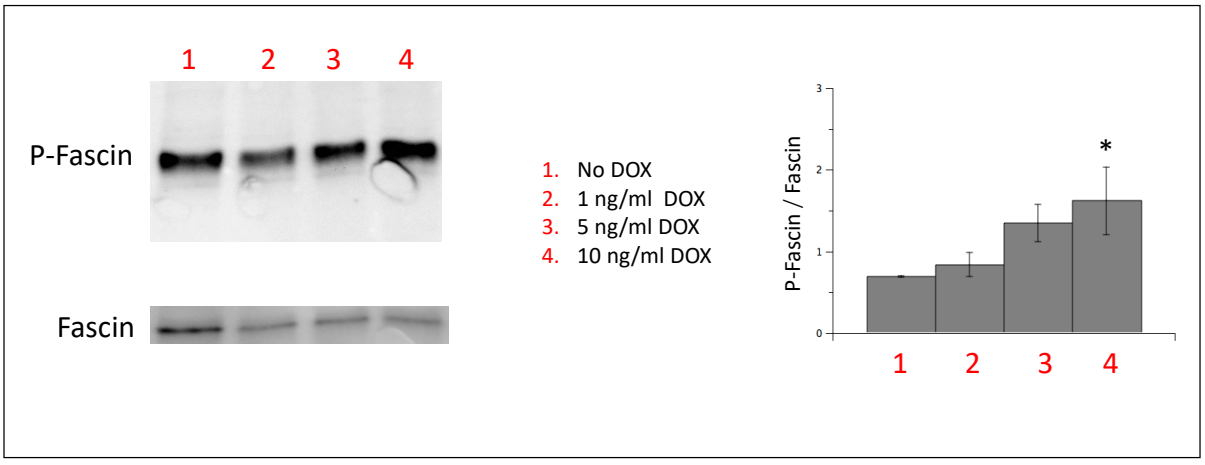

Figure 6: Western blot of S39-P-Fascin in HeLa TetOn Progerin expressing cells. 500 μg of total proteins were incubated with anti-Fascin antibody (1:100, Abcam ab126772) overnight at 4°C under agitation and following immune-precipitated with Protein A-Agarose (Sigma-Aldrich) beads. 15μl of immunoprecipitated protein solution per sample were loaded on SDS-PAGE gel (7.5%) and transferred to a PVDF membrane using Trans-blot turbo system (BioRad). After blocking with 5% BSA/0.1% TWEEN20 in PBS for 1h at RT, anti Phospho-Fascin antibody (1:10000, Abcam ab90618), anti-Fascin (1:1000, Abcam ab126772) and HRP-linked secondary antibody specific bindings were detected by chemiluminescence system (Clarity Western Blotting ECL substrate, Biorad).

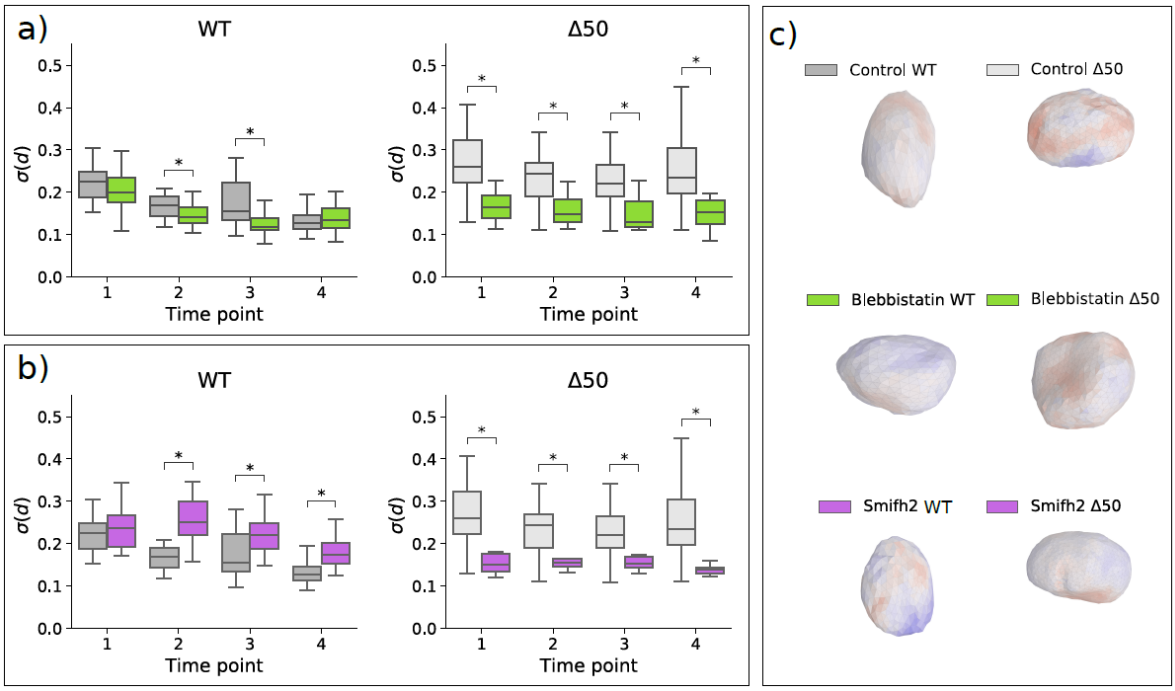

Figure 7: **Fluctuations of local displacements $\sigma(d)$ over time for WT and Δ50 Lamin A overexpressing cells**. Cells were treated with the myosin inhibitor, Blebbistatin (a) or actin an inhibitor of formin-mediated actin nucleation, SMIFH2 (b) for 30 min and 1h respectively. At the end of treatment, cells returned in routinely fresh growth medium and imaged every 15 min, for 1h. Timepoint i refers to local displacements from time point $i-1$ to time point i. Time points are taken for 1h, every 15 minutes, after the end of both treatments. Statistical significance is assessed through a Kolmogorov-Smirnov test at the significance level of $\alpha = 0.01$. (c) Representative images of nuclear reconstruction in all the analyzed experimental condition.

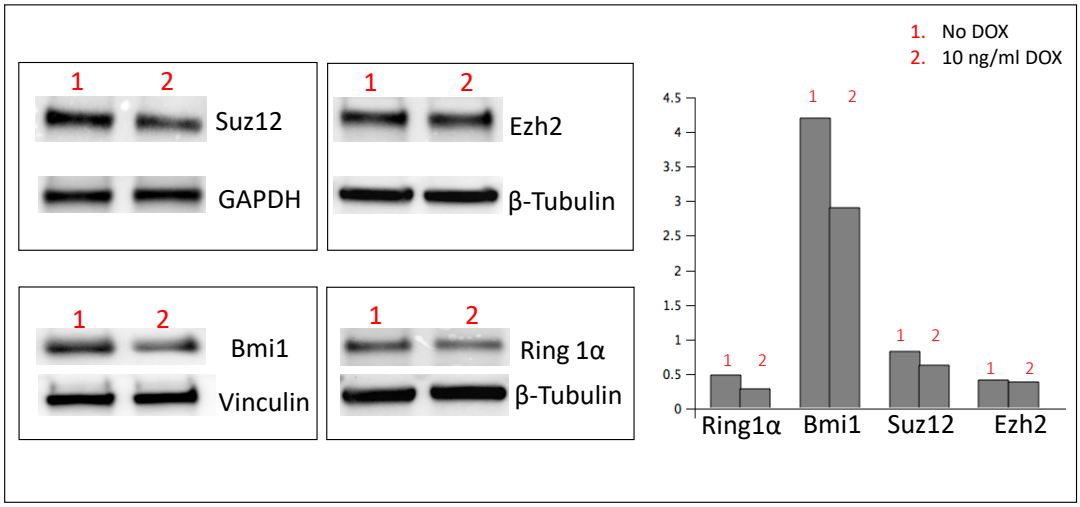

Figure 8: Western blot of PcG protein expression in HeLa TetOn Progerin expressing cells. 20 μg total protein were loaded on 10% polyacrylamide gel, transferred on PVDF and incubated with anti-SUZ12 (1:1000, Rabbit mAb 3737, Cell Signaling) or rabbit anti- Ezh2 (1:1000, Rabbit mAb 5246, Cell Signaling) or rabbit anti- Ring1A (1:1000, Rabbit mAb 13069, Cell signaling) or rabbit anti- Bmi1 (1:1000, Rabbit mAb 6964, Cell signaling), overnight at 4°C. Mouse anti-vinculin (1:10000, V9264, Sigma) or rabbit anti-GAPDH (1:5000, Sigma G9545) or Anti β-tubulin (1:5000mouse, Sigma T0198) for 1h at room temperature was used as housekeeping. Secondary antibodies (anti-rabbit or anti-mouse-HRP 1:3000 in 5% milk/0.1% Tween20 in PBS, Biorad) were used for 1h at room temperature to detect chemiluminescence.

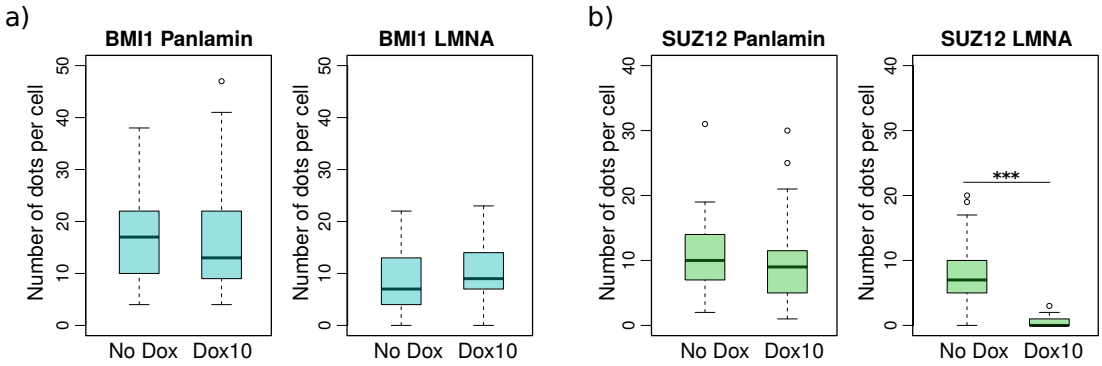

Figure 9: **Quantification of the number of foci per cell identifying lamins and BMI1 or SUZ12 interactions.** Number of dots per cell was estimated using customized ICY pipeline [9]. Progerin induction (Dox 10) does not influence BMI1 interaction with the lamins (a). At the opposite, we can observe slight decrease of dots SUZ12-Panlamin dots and a significative decrease of interactions for SUZ12-Lamin A (panel b, *** p-value ¡0.01, assessed through a Kolmogorov-Smirnov test).

[1] S. Antoku and G.G. Gundersen. Analysis of nesprin-2 interaction with its binding partners and actin. *Methods in Molecular Biology*, 1840:35–43, 2018.

[2] Elizabeth A Booth, Stephen T Spagnol, Turi A Alcoser, and Kris Noel Dahl. Nuclear stiffening and chromatin softening with progerin expression leads to an attenuated nuclear response to force. *Soft Matter*, 11(32):6412–6418, 2015.

[3] J. Boros, N. Arnoult, V. Stroobant, J.-F. Collet, and A. Decottignies. Polycomb repressive complex 2 and h3k27me3 cooperate with h3k9 methylation to maintain heterochromatin protein 1α at chromatin. *Molecular and Cellular Biology*, 34(19):3662–3674, 2014.

[4] B.C. Capell and F.S. Collins. Human laminopathies: Nuclei gone genetically awry. *Nature Reviews Genetics*, 7(12):940–952, 2006.

[5] Y.-H. Chi, Z.-J. Chen, and K.-T. Jeang. The nuclear envelopathies and human diseases. *Journal of Biomedical Science*, 16(1), 2009.

[6] E.C. Chittock, S. Latwiel, T.C.R. Miller, and C.W. Mller. Molecular architecture of polycomb repressive complexes. *Biochemical Society Transactions*, 45(1):193–205, 2017.

[7] C. Ciferri, G.C. Lander, A. Maiolica, F. Herzog, R. Aebersold, and E. Nogales. Molecular architecture of human polycomb repressive complex 2. *eLife*, 2012(1), 2012.

[8] M. Crisp, Q. Liu, K. Roux, J.B. Rattner, C. Shanahan, B. Burke, P.D. Stahl, and D. Hodzic. Coupling of the nucleus and cytoplasm: Role of the linc complex. *Journal of Cell Biology*, 172(1):41–53, 2006.

[9] Fabrice de Chaumont, Stphane Dallongeville, Nicolas Chenouard, Nicolas Herv, Sorin Pop, Thomas Provoost, Vannary Meas-Yedid, Praveen Pankajakshan, Timothe Lecomte, Yoann Le Montagner, Thibault Lagache, Alexandre Dufour, and Jean-Christophe Olivo-Marin. Icy: an open bioimage informatics platform for extended reproducible research. *Nature Methods*, 9:690–, June 2012.

[10] M. de Napoles, J.E. Mermoud, R. Wakao, Y.A. Tang, M. Endoh, R. Appanah, T.B. Nesterova, J. Silva, A.P. Otte, M. Vidal, H. Koseki, and N. Brockdorff. Polycomb group proteins ring1a/b link ubiquitylation of histone h2a to heritable gene silencing and x inactivation. *Developmental Cell*, 7(5):663–676, 2004.

[11] T. Dechat, K. Pfleghaar, K. Sengupta, T. Shimi, D.K. Shumaker, L. Solimando, and R.D. Goldman. Nuclear lamins: Major factors in the structural organization and function of the nucleus and chromatin. *Genes and Development*, 22(7):832–853, 2008.

[12] M. Eriksson, W.T. Brown, L.B. Gordon, M.W. Glynn, J. Singer, L. Scott, M.R. Erdos, C.M. Robbins, T.Y. Moses, P. Berglund, A. Dutra, E. Pak, S. Durkin, A.B. Csoka, M. Boehnke, T.W. Glover, and F.S. Collins. Recurrent de novo point mutations in lamin a cause hutchinson-gilford progeria syndrome. *Nature*, 423(6937):293–298, 2003.

[13] R. Foisner. Cell cycle dynamics of the nuclear envelope. *TheScientificWorldJournal [electronic resource]*, 3:1–20, 2003.

[14] N.J. Francis and R.E. Kingston. Mechanisms of transcriptional memory. *Nature Reviews Molecular Cell Biology*, 2(6):409–421, 2001.

[15] Farhana Haque, Daniela Mazzeo, Jennifer T Patel, Dawn T Smallwood, Juliet A Ellis, Catherine M Shanahan, and Sue Shackleton. Mammalian sun protein interaction networks at the inner nuclear membrane and their role in laminopathy disease processes. *Journal of Biological Chemistry*, 285(5):3487–3498, 2010.

[16] F. Houben, F.C.S. Ramaekers, L.H.E.H. Snoeckx, and J.L.V. Broers. Role of nuclear lamina-cytoskeleton interactions in the maintenance of cellular strength. *Biochimica et Biophysica Acta - Molecular Cell Research*, 1773(5):675–686, 2007.

[17] P. Isermann and J. Lammerding. Nuclear mechanics and mechanotransduction in health and disease. *Current Biology*, 23(24):R1113–R1121, 2013.

[18] Tadamoto Isogai, Rob Van Der Kammen, and Metello Innocenti. Smifh2 has effects on formins and p53 that perturb the cell cytoskeleton. *Scientific reports*, 5:9802, 2015.

[19] A. Jayo, M. Malboubi, S. Antoku, W. Chang, E. Ortiz-Zapater, C. Groen, K. Pfisterer, T. Tootle, G. Charras, G.G. Gundersen, and M. Parsons. Fascin regulates nuclear movement and deformation in migrating cells. *Developmental Cell*, 38(4):371–383, 2016.

[20] B. Jones. Ageing: Heterochromatin disorganization associated with premature ageing. *Nature Reviews Genetics*, 16(6):p318, 2015.

[21] Sebastian Kandert, Yvonne Lüke, Tobias Kleinhenz, Sascha Neumann, Wenshu Lu, Verena M Jaeger, Martina Munck, Manfred Wehnert, Clemens R Müller, Zhongjun Zhou, et al. Nesprin-2 giant safeguards nuclear envelope architecture in lmna s143f progeria cells. *Human molecular genetics*, 16(23):2944–2959, 2007.

[22] Jop Kind, Ludo Pagie, Havva Ortabozkoyun, Shelagh Boyle, Sandra S de Vries, Hans Janssen, Mario Amendola, Leisha D Nolen, Wendy A Bickmore, and Bas van Steensel. Single-cell dynamics of genome-nuclear lamina interactions. *Cell*, 153(1):178–192, 2013.

[23] A.J. Koch and J.M. Holaska. Emerin in health and disease. *Seminars in Cell and Developmental Biology*, 29:95–106, 2014.

[24] L. Koreny and M.C. Field. Ancient eukaryotic origin and evolutionary plasticity of nuclear lamina. *Genome Biology and Evolution*, 8(9):2663–2671, 2016.

[25] Mihály Kovács, Judit Tóth, Csaba Hetényi, András Málnási-Csizmadia, and James R Sellers. Mechanism of blebbistatin inhibition of myosin ii. *Journal of Biological Chemistry*, 279(34):35557–35563, 2004.

[26] J. Lammerding, L.G. Fong, J.Y. Ji, K. Reue, C.L. Stewart, S.G. Young, and R.T. Lee. Lamins a and c but not lamin b1 regulate nuclear mechanics. *Journal of Biological Chemistry*, 281(35):25768–25780, 2006.

[27] Kenneth K Lee, Tokuko Haraguchi, Richard S Lee, Takako Koujin, Yasushi Hiraoka, and Katherine L Wilson. Distinct functional domains in emerin bind lamin a and dna-bridging protein baf. *Journal of Cell Science*, 114(24):4567–4573, 2001.

[28] W. Lu, M. Schneider, S. Neumann, V.-M. Jaeger, S. Taranum, M. Munck, S. Cartwright, C. Richardson, J. Carthew, K. Noh, M. Goldberg, A.A. Noegel, and I. Karakesisoglou. Nesprin interchain associations control nuclear size. *Cellular and Molecular Life Sciences*, 69(20):3493–3509, 2012.

[29] F. Marullo, E. Cesarini, L. Antonelli, F. Gregoretti, G. Oliva, and C. Lanzuolo. Nucleoplasmic lamin a/c and polycomb group of proteins: An evolutionarily conserved interplay. *Nucleus*, 7(2):103–111, 2016.

[30] P. Meinke and E.C. Schirmer. Linc'ing form and function at the nuclear envelope. *FEBS Letters*, 589(19):2514–2521, 2015.

[31] J.M.K Mislow, J.M. Holaska, M.S. Kim, K.K. Lee, M. Segura-Totten, K.L. Wilson, and E.M. McNally. Nesprin-1α self-associates and binds directly to emerin and lamin a in vitro. *FEBS Letters*, 525(1-3):135–140, 2002.

[32] D. Pasini, A.P. Bracken, M.R. Jensen, E.L. Denchi, and K. Helin. Suz12 is essential for mouse development and for ezh2 histone methyltransferase activity. *EMBO Journal*, 23(20):4061–4071, 2004.

[33] Daan Peric-Hupkes, Wouter Meuleman, Ludo Pagie, Sophia WM Bruggeman, Irina Solovei, Wim Brugman, Stefan Gräf, Paul Flicek, Ron M Kerkhoven, Maarten van Lohuizen, et al. Molecular maps of the reorganization of genome-nuclear lamina interactions during differentiation. *Molecular cell*, 38(4):603–613, 2010.

[34] K. Pfisterer, A. Jayo, and M. Parsons. Control of nuclear organization by f-actin binding proteins. *Nucleus*, 8(2):126–133, 2017.

[35] T. Shimi, K. Pfleghaar, S.-I. Kojima, C.-G. Pack, I. Solovei, A.E. Goldman, S.A. Adam, D.K. Shumaker, M. Kinjo, T. Cremer, and R.D. Goldman. The a- and b-type nuclear lamin networks: Microdomains involved in chromatin organization and transcription. *Genes and Development*, 22(24):3409–3421, 2008.

[36] N.J. Ullrich and L.B. Gordon. Hutchinson-gilford progeria syndrome. *Handbook of Clinical Neurology*, 132:249–264, 2015.

[37] S. Vlcek and R. Foisner. A-type lamin networks in light of laminopathic diseases. *Biochimica et Biophysica Acta - Molecular Cell Research*, 1773(5):661–674, 2007.

[38] K. Wilhelmsen, S.H.M. Litjens, I. Kuikman, N. Tshimbalanga, H. Janssen, I.D. Van Bout, K. Raymond, and A. Sonnenberg. Nesprin-3, a novel outer nuclear membrane protein, associates with the cytoskeletal linker protein plectin. *Journal of Cell Biology*, 171(5):799–810, 2005.

[39] Gavin S Wilkie, Nadia Korfali, Selene K Swanson, Poonam Malik, Vlastimil Srsen, Dzmitry G Batrakou, Jose de las Heras, Nikolaj Zuleger, Alastair RW Kerr, Laurence Florens, et al. Several novel nuclear envelope transmembrane proteins identified in skeletal muscle have cytoskeletal associations. *Molecular & Cellular Proteomics*, 10(1):M110–003129, 2011.

[40] K.L. Wilson and R. Foisner. Lamin-binding proteins. *Cold Spring Harbor perspectives in biology*, 2(4), 2010.

[41] Q. Zhang, J.N. Skepper, F. Yang, J.D. Davies, L. Hegyi, R.G. Roberts, P.L. Weissberg, J.A. Ellis, and C.M. Shanahan. Nesprins: A novel family of spectrin-repeat-containing proteins that localize to the nuclear membrane in multiple tissues. *Journal of Cell Science*, 114(24):4485–4498, 2001.

[42] Y.-Y. Zhen, T. Libotte, M. Munck, A.A. Noegel, and E. Korenbaum. Nuance, a giant protein connecting the nucleus and actin cytoskeleton. *Journal of Cell Science*, 115(15):3207–3222, 2002.

[43] W. Zhou, P. Zhu, J. Wang, G. Pascual, K.A. Ohgi, J. Lozach, C.K. Glass, and M.G. Rosenfeld. Histone h2a monoubiquitination represses transcription by inhibiting rna polymerase ii transcriptional elongation. *Molecular Cell*, 29(1):69–80, 2008.

Sulforaphane can not protect the cells to a repeated, short and sublethal treatment with hydrogen peroxide

Maria Chiara Lionetti[a], Federico Mutti[a], Erica Soldati[a], Maria Rita Fumagalli[b], Valentina Coccé[b], Graziano Colombo[c], Emanuela Astori[c], Aldo Milzani[c], Isabella Dalle Donne[c], Emilio Ciusani[d], Giulio Costantini[b], Caterina A. M. La Porta[a,1]

[a] *Center for Complexity and Biosystems University of Milano, Department of Environmental Science and Policy, via Celoria 26, 20133 Milano, Italy*
[b] *Center for Complexity and Biosystems University of Milano, Department of Physics, via Celoria 16, 20133 Milano, Italy*
[c] *Department of Biosciences, via Celoria 26, 20133 Milano, Italy*
[d] *Istituto Besta, Via Celoria 11, 20133 Milano, Italy*

Abstract

A delicate balance of reactive oxygen species (ROS) exists inside the cell: when the mechanisms that controls the level of ROS fail, the cell is in an oxidative stress state, a condition that can help aging processes. To contrast the pro-aging effect of ROS, the supplementation of antioxidants has been recently proposed. Sulforaphane (SNF), is an isothiocyanate isolated from Brassica plants that has been shown to modulate many critical factors inside the cells that seems to help in contrasting aging. In the present work, we have used a short, subletal and repeated exposure for 8 days to hydrogen peroxide without or in combination with low concentration of low concentration of SNF in human dermal fibroblasts. Hydrogen peroxide treatments do not affect the oxidative status of the cells, without any significant change of the intracellular ROS levels or the number of mitochondria or thiols in total proteins. However, our regime promotes cell cycle progression and cell viability, increases the anti-apoptotic factor survivin, decreases Lamin B and increase DNA damage, measured as number of foci positive for γH2AX. Therefore this kind of treatment, despite the fact that the oxidative status of the cells appears to be restored, is able to alter the delicate balance of the cells helping DNA damage. On the other hand, the treatment with SNF alone does not affect significantly the cells and seems to exert a protective effect increasing the level of p53 than can block the expansion of possible DNA damaged cells. However, continuos exposure to SNF is not able, at this concentration, to protect cells against hydrogen peroxide induced oxidative stress.

Keywords: oxidative stress, sulforaphane, fibrobalsts, lamins

Introduction

Senescence is a complex process where the integrity and the structure of the nuclear scaffold changes [1]. The nuclear envelope involves a complex network of intermediate filaments including Lamina A/C and Lamin B which affect chromatin architecture and topology of chromosomal domains [2]. One important factor contributing to cell senescence is oxidative stress [3]. Reactive

*Caterina A. M. La Porta
Email address: caterina.laporta@unimi.it (Caterina A. M. La Porta)

oxygen species (ROS) are physiological by-products of mitochondria metabolism. Oxidative stress is due to the level of reactive oxidative species (ROS) produced by the cells that could cause damage at the level of DNA, membrane lipids and proteins. ROS level regulates physiological functions, including signal transduction, gene expression, and proliferation, therefore they underline physiological and pathological events [4]. For example, mitochondrial ROS may activate an adaptive response which promotes health to extend the lifespan through diseases prevention [5]. ROS overproduction, on the other hand, hampers damaged nuclear and mitochondrial DNA repair at multiple steps, contributing to cell genomic instability [6]. Interestingly, ROS, including hydrogen peroxide, can inhibit cell growth and induce cell death and senescence in a context-dependent manner [7]. Accordingly, a recent paper showed that low levels of ROS can improve the defense mechanisms by inducing adaptive responses, which in turn contributes to stress resistance and longevity [8]. In contrast, high levels of ROS induced insufficient adaptive responses, contributing to aging onset and progression [8]. Interventions to keep low the level of ROS, by both scavenging free radicals and enhancing antioxidant factors, are widely proposed as an anti-aging state.

The main goal of the present paper was to investigate the impact of short and repeated sublethal treatments with hydrogen peroxide, commonly used to mimic oxidative stress [3], alone or in combination with sulforaphane (SFN) on human primary dermal fibroblasts (hSDF) focusing on critical biological functions of the cells. Recent evidence in fibroblasts showed that concentrations between 90-360μM of hydrogen peroxide is sufficient to induce oxidative stress and premature cellular senescence in vitro, recapitulating an aging process profile [3]. SNF is a well tolerate natural compounds obtained from cruciferous vegetables which has been shown to have a protective effect on the cells through Nrf2-mediated induction of phase 2 detoxification enzymes that elevate cell defense against oxidative damage and promote the removal of potential carcinogens [9]. However, it is becoming clear that multiple mechanisms are activated in response to SFN, including the suppression of cytochrome P450 enzymes, the induction of apoptotic pathways, the suppression of cell cycle progression, the inhibition of angiogenesis and anti-inflammatory activity [9]. Another important biological activity of SFN is the negative control of HDAC activity [9].

Altogether, our findings show two interesting aspects: first low and pro-longer exposure with sublethal stress of hydrogen peroxide leads to a significant decrease of Lamin B expression and the treatment with SNF is able to contrast this effect. Long treatment with SNF alone increases p53 level of expression suggests that alone it plays a protective role inside the cell versus DNA damage to DNA. However, this is not sufficient to protect against hydrogen peroxide, since DNA damage occurs in cells treated with both SNF and hydrogen peroxide.

Results

Effect of short and repeated sublethal treatment with hydrogen peroxide without or in combination with SNF on the oxidative status of hSDF cells after 8 days

H2DCFDA is a chemically reduced form of fluorescein used as an indicator for reactive oxygen species (ROS) in cells. The short treatment (30min) with hydrogen peroxyde repeated 48 h for 8 days with sublethal concentrations (15μM or 25μM of H_2O_2) (see Fig. S1) according to [3] alone or in combination with 1μM SNF does not affect the levels of ROS measured using H2CDF assay or the numbers of mitochondria quantified by flow cytometry (Fig.1). These data suggests that during the 48 h recovery, the cells are able to recover possible damages.

It is known that oxidative stress leads to the formation of unwanted disulphide bonds in the cytoplasm resulting in protein folding leading to the end to impair proteins function. To face this, the cells have several mechanisms to increase the intracellular levels of thiol[10]. Notably, It has

been recently reported that the intracellular increased of thiols are strongly associated with an increased tolerance to an oxidant stress [10] since they act as extraordinarily efficient antioxidants protecting the cells against consequences of damage induced by free radicals [11]. Conversely, large increase in free thiols on the circulation are associated with toxic effects [12]. Under our experimental conditions, the levels of reduced thiols in total proteins measured by biotin maleimide assay, do not show any significant changes (Fig. 1).

SNF and oxidative stress decrease cell viability but promote cell cycle progression and regulation of apoptosis

The short treatment (30min) with H_2O_2 repeated 48 h for 8 days with sublethal concentrations (15μM or 25μM) (see without or in combination with SFN Fig. S1), promotes cell cycle progression as shown Fig. 2a. In fact, we detected an increase in the number of cells into G2-M phase (Fig. 2a). On the other hand, the treatment with SFN alone does no effect the cell cycle progression (Fig. 2a). We also detected the viability of the cells with SRB assay. As shown in Fig. 3b, hSDF cells viability decrease significantly with 25μM of H_2O_2 only while 1μM SNF does not affect it (Fig. 3b). This data suggests that the cells receive a damage at higher concentration of hydrogen peroxide even if this is sublethal and the oxidative status of the cell appears recovered .

To investigate if the treatments affects apoptosis, we detected a well known anti-apoptotic factors, survivin. Fig.3c shows an increased level of expression of survivin in cells treated with both concentration of hydrogen peroxide without or in the presence of SNF. Moreover, the treatment with SNF alone does not affect survivin expression Fig.3c.

Finally, we checked p53, a well known factor which controls the genome by orchestrating a variety of DNA-damage-response to restore genome stability and that plays a critical role in triggering apoptotic pathways in damaged cells [13]. Interestingly, the treatment with 1μM SNF alone increases significantly the level of expression of total p53 (Fig. 2d). This effect disappears when the cells are submitted to both SNF and oxidative stress (Fig. 2d).

Effect of SNF alone or with oxidative stress on gamma-H2AX positive cells

Histone γH2AX is the most sensitive marker of double-stranded DNA breaks (DSB) and telomere shortening [14]. Herein we have quantified the number of foci γ-H2AX positive cells in hSDF cells after 8 day of oxidative stress induction with or without 1μM SFN. As shown in Fig. 3, there is a significant increase in the number of γH2AX positive foci increasing the concentration of hydrogen peroxide. In SNF treated cells there is no significant change in comparison to the untreated cells(Fig. 3)

SNF contrast the loss of nuclear Lamin B due to H_2O_2 treatment

The treatment with H_2O_2 (15 or 25μM) induces a significant decrease of Lamin B without any significant changes in the level of expression of Lamin A (Fig. 4). Loss of Lamin B has already been reported in the literature to be associated with the prolongation of S phase and oxidative stress condition [15, 16]. Interestingly, the treatment with 1μM SNF is able to contrasts this effect at both concentration of H_2O_2, leaving Lamin A levels unchanged (Fig. 4).

Discussion

Sulforaphane (SFN) is mainly present in Brassica plants such as broccoli sprouts and cabbages. It is a very well tolerate factor, showing antioxidant properties and inhibiting histone deacetylase enzymes (HDAC) [9]. In a recent study, it has been investigated the effect of SNF on human

mesenchymal stem cells (MSCs) at low or high concentration [17], giving opposite effects. In fact, while low doses of SNF (1μM) for 3 days enhanced the cellular proliferation and protected the cells toward apoptosis and senescence, higher concentration (5μM) had a cytotoxic effect, leading to the induction of cell cycle arrest, programmed cell death and senescence [17]. SNF seems to have a double face effect: on one side acts as anti-tumorigenic factor targeting cancer stem cells (CSC) [18] and on the other hand helps the clearance of progerin in accelerating ageing [19].

The main two goals of this paper were to investigate the effect of sublethal concentration and long-term exposure with SFN on human normal cells (hSDF) on critical functions of the cells and the possible protective role of SFN. Our experimental approach leads to faithfully mimic physiologic conditions allowing the cells to recover possible damages. In fact, in most of the studies reported in the literature, the experimental induction of oxidative stress condition is achieved by short exposure of the cells to high concentration of exogenous ROS, or by long and continuous exposure to moderate concentration of exogenous ROS. Both of these models are unlikely to reproduce physiologic conditions, where stimuli are discontinuous and ROS exposure limited. Indeed, excluding particular pathological conditions, it is very rare to find, a prolonged increase of ROS levels but rather occasional and short increase of ROS levels, albeit for a long time.

It is known that sublethal concentration of ROS acts mainly as second messengers in signaling cascade and it is involved in cell proliferation and differentiation [20]. The sublethal exposure repeated for 30 min every 48 h up to 8 days does not change the oxidative status of the cell measured as levels of ROS, the number of mitochondria and levels of reduced thiols in total proteins. This suggest that the cells under this treatment can compensate and recover the oxidative status. In this connection, higher concentration (90-360 μM) has been reported to increase the number of mitochondria in fibroblasts [21].

However, hydrogen peroxide alone or in combination with SNF, modify the complex and delicate physiology of the cells since they starting to promote the cell cycle, to contrast apoptosis increasing survivin without any significant changes in p53. Lamin B is also affected.

This picture is consistent with the presence of higher number of foci gamma H2AX positive DNA damage detected in hydrogen peroxide treated cells. Two interesting results are related to SNF. Firstly, SNF induces alone an increase of p53 and itself does not induce any DNA damage, playing a protective role. Consistently, it is known that p53 by SNF can promote the stabilization of p53 oscillatory behavior [22],[23]. Moreover, p53 prevents the accumulation of oxidative damage in cells and thus maintain genomic stability by direct transcriptional regulation of genes involved in oxidative-stress responses or modulating other pathways important in oxidative-stress responses[24]. The second interesting resulkt is that SNF can not contrast the effect of hydroen peroxide in hSDF cells. On the other hand, higher levels of SNF (higher than 5mM) was shown to induce apoptosis via an incraese of ROS[25]

Methods

Cell lines and treatments

Human primary dermal fibroblasts (hSDF) were obtained as previously described by [26] and cultured in EMEM (Euroclone) containing 1% L-Glutamine, 1% Penicillin/Streptomycin and 10% FBS (basal medium) at 37°C in 5% CO_2 for no more than 10 passages[26]. The cells are treated at sublethal concentration of H_2O_2 for short (30min) and repeated time according to [3].

Briefly, subconfluent cells were plated and exposed to 15 or 25μM H_2O_2 (Fluka cod.95302) for 30 minutes at 37°C, this treatment was repeated every 48 h for four times Fig. S1. Untreated cells were plated and grown in basal medium for all the time of the experiment (8 days) Fig. S1.

After every treatment with H_2O_2, the cells were washed twice with sterile PBS and maintained in basal medium until the other treatment. Subconfluent cells were treated with sulforaphane (SNF, cod.S4441, Sigma) at a final concentration of 1μM for 8 days after plating (see Fig. S1). In combined experiments with H_2O_2 and SNF, the cells were maintained with H_2O_2 for 30min without SNF, then replaced with fresh medium containing SNF Fig. S1.

Cell proliferation assay by SRB

Sulforhodamine B (SRB) assay allow to quantify cellular protein content according to (Sulforhodamine B (SRB) Assay in Cell Culture to Investigate Cell Proliferation 2017). Briefly, the cells were fixed with 10% Trichloroacetic acid (Sigma, cod.T6399) for 2 hours at 4°C and 0.04% (wt/vol) SRB protein-bound dye (Sulforhodamine B Sigma, cod. S1402, dissolved in 10 mMTris base solution) was added to each well and incubated at RT for 1hour. After four washes with 1% (vol/vol) acetic acid, the samples were left to air-dry at room temperature. 100μl of 10 mM Tris base solution (pH 10.5) was added to each well and shake the plate on an orbital shaker for 10 min to solubilize the protein-bound dye. The absorbance at 510nm was detected using an microplate reader (BioRad) at 510nm.

Cell Cycle Analysis

Subconfluent cells were harvested by trypsinization, pelleted and fixed in 70% cold ethanol and subsequently stained with propidium iodide (PI, cod. P4864, Sigma) for 30 minutes at 4°C. PI fluorescence was analyzed using FACS Vantage SE Becton Dickinson flow cytometry. The percentages of cells in each phase of the cell cycle were calculated using FlowJO software.

p53 level of expression by flow cytometry

Subconfluent cells were fixed 15 minutes in methanol at -20°C, and than incubated with primary antibody p53 linked to FITC at 4°C (1:500, Abcam, ab156030) for 1h and then immediately analysed using FACS Vantage SE Becton Dickinson flow cytometry. Analysis were conducted using FlowJo software and the expression of p53 for each sample is reported as the ratio between the intensity of fluorescence with respect to unstained cells due to autofluorescence.

Quantification of intracellular ROS by H2DCFDA

To detect ROS in cells, the cell-permeant 2',7'-dichlorodihydrofluorescein diacetate (H2DCFDA)(Thermo Fisher, cod.D399) has been used. The latter is converted into the highly fluorescent 2',7'-dichlorofluorescein (DCF) by the cleavage of acetate groups due to intracellular esterases and oxidation. Briefly, acetylated dyes has been reconstituted in anhydrous dimethylsulfoxide (DMSO) at stock concentration of 100μM just prior to use. Cells have been incubated in 10μM dye solution in pre-warmed PBS for 1h at 37°C in 5% CO_2, protected from light. Following, loading buffer has been removed and cells returned to prewarmed growth medium and incubate at the optimal temperature, for 1h at 37°C in 5% CO_2 in order to allow esterases to hydrolyze the acetate groups and render the dye responsive to oxidation. Fluorescence has been determined using Ensight microplate fluorescence reader (Perkin Elmer) using and Ex/Em: 492495/517527nm. Results are reported as mean fluoresce values for each sample.

goat-serum/0.3% glycine/0.1% Tween in PBS) for 1h at RT. The cells were incubated overnight at 4°C with the primary antibody as following:Lamin A (1:100, Abcam ab8980), Lamin B1 (1:200, Abcam ab16048), γH2AX (1:700, Abcam, ab2893-Phosho139), anti-survivin (1:250, NB500-201, Novus Biological). The samples were incubated with secondary antibodies FITC anti-Rabbit (1:250, ab150077, AbCam) or anti-Mouse (1:250, MAP501F, Millipore) for 1h at RT and then mounted with Pro-long anti-fade reagent (P7481, Life Technologies) with DAPI to stain the nuclei. The images were acquired with a Leica TCS NT confocal microscope.

0.1. γH2AX spots counting

γH2AX spots inside the nuclei were counted using spot detector tool of ICY Software as described in our previous paper [27]. Briefly, we computed the intensity of the marker used to spot the damage inside the nuclei. After the treatment we created a script with Matlab which was able to quantify the intensity of every pixel and to divide the intensities into a bin according to the scale. All the nuclei taken into account were split from the original images and elaborated (this to reduce the noise of non-specific signal). The script uses the imhist function to quantify all the pixels and divide them into a range 255 bin wide. To plot the value we chose a semi-logarithmic scale plot. All the resulting values are normalized with the total number of pixels of their image, to make possible the comparison of all the nuclei, one with each other.

Figures

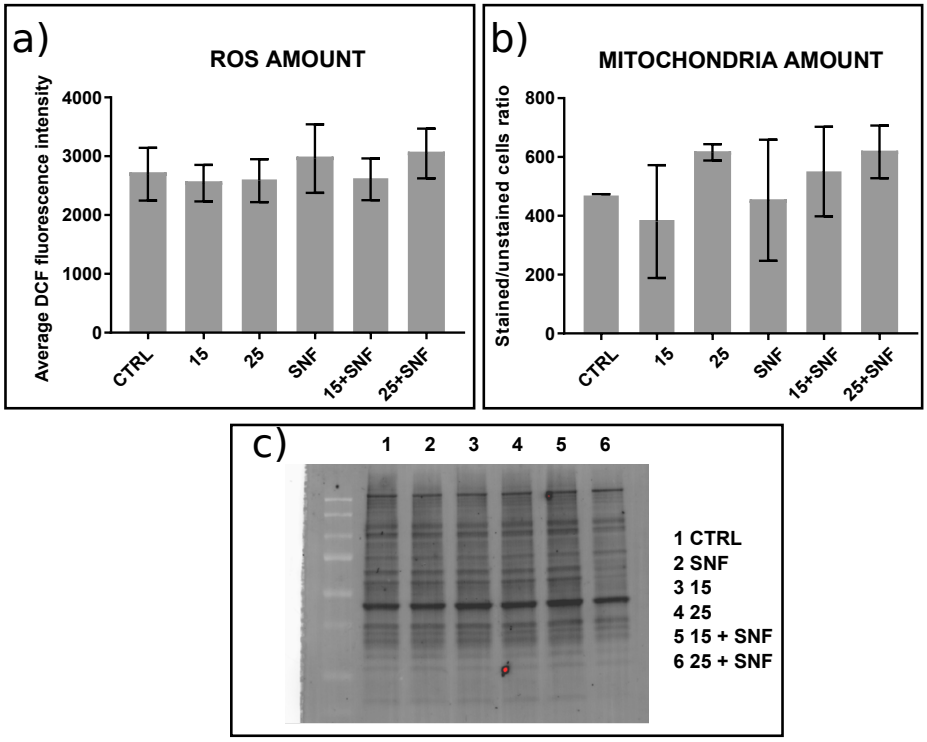

Figure 1: **Evaluation of oxidative status after treatment with sublethal concentration, short and repeated exposure with hydrogen peroxide without or with 1μM SNF** a) ROS detection. Subconfluent cells treated as described in Fig. S1 and Material and Methods section, are incubated in 10μM H2DCFDA (Thermo Fisher, cod.D399) in pre-warmed PBS for 1h at 37°C in 5% CO_2. Fluorescence has been determined using Ensight microplate fluorescence reader (Perkin Elmer) using and Ex/Em: 492495/517527nm. Results are reported as mean fluoresce values for each sample. b) Number of Mitochondria. Cells treated as described in (a) are quantified using MitoTracker probe, which passively diffuses across the plasma membrane and accumulates in active mitochondria. Subconfluent cells were incubated with 250nM MitoTracker (Thermo Fisher, cod. M7512) for 45min at 37°C in 5% CO_2. Fluorescence has been detected using FACS Vantage SE Becton Dickinson flow cytometry and the data were analyzed by FlowJo. Results are reported as the ratio between the intensity of fluorescence of each sample with respect to unstained cells due to autofluorescence. c) Reduced thiols into total protein. Total cellular proteins were obtained by cell homogenization with ice-cold lysis buffer. The lysate was incubated on ice for 30 min and centrifuged at 10000rpm, for 10 min at 4°C to remove cell debris. The concentration of protein was assessed using BCA protein assay. To detect thiols present into proteins a biotin-maleimide assay was carried out. 1mg/mL of protein was incubated with 75μM biotin-maleimide solution for 1 hour at RT and then mixed to Laemmli sample buffer, boiled for 5 min at 90°C and immediately loaded on 12% SDSPAGE gel. The protein were then electroblotted onto a low-fluorescence polyvinylidene difluoride (LF-PVDF) membrane. Biotin tag was revealed using streptavidin-HRP assay. Biotinylated proteins were visualized by ECL detection (cod.1705061, Biorad) using Chemidoc Touch Imaging System (Biorad). ECL signals has been normalized with respect to PVDF stain free.

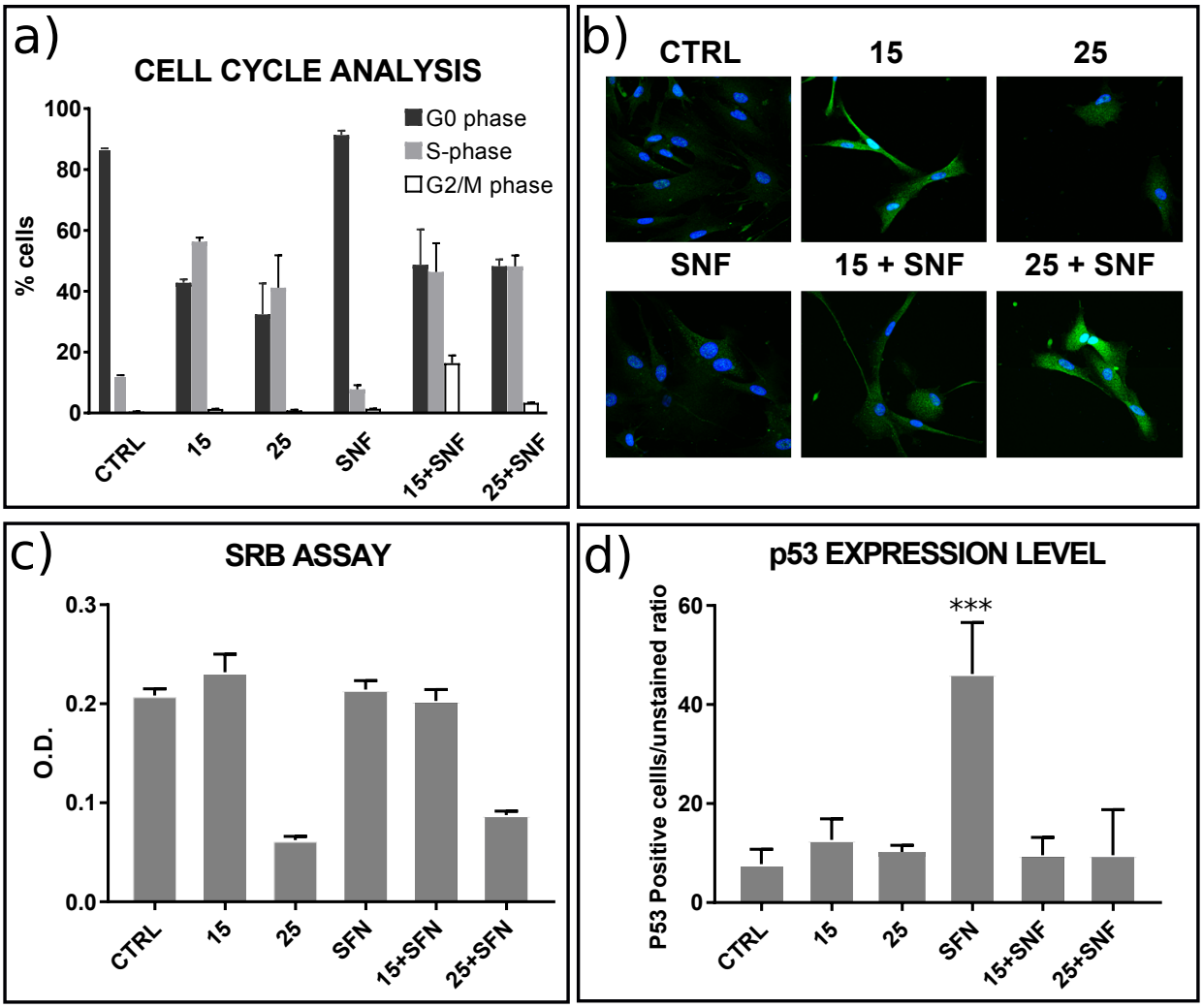

Figure 2: **Effect on cell vitality, cell cycle and survivin expression after the treatment after the treatment with sublethal concentration, short and repeated exposure with hydrogen peroxide without or with 1μM SNF.** a) Sulforhodamine B (SRB) assay. Briefly, cells (see Fig. S1) were fixed with 10% Trichloroacetic acid (Sigma, cod.T6399) for 2 hours at 4°C. 0.04% (wt/vol) SRB protein-bound dye was added to each well and incubated at RT for 1hour. 100μl of 10 mM Tris base solution (pH 10.5) was added to each well and the plate placed on an orbital shaker for 10 min to solubilize the protein-bound dye. The absorbance was detected using a Ensight microplate reader (Perkin Elmer) at 510nm. (b) Cell cycle. Subconfluent cells were fixed in 70% cold ethanol and stained with propidium iodide (PI, cod. P4864, Sigma) for 30 minutes at 4°C. PI fluorescence was analyzed using FACS Vantage SE Becton Dickinson flow cytometry. The percentages of cells in each phase of the cell cycle were calculated using FlowJO software. (c) Immunofluorescence on survivin. Subconfluent cells plated on coverslips were fixed with 3.7% paraformaldehyde, permeabilized with 0.1%TRITOX-100 in PBS for 15min at RT, and incubated overnight at 4°C with anti-survivin (1:250, NB500-201, Novus Biological). The samples were incubated with secondary antibodies FITC anti-Rabbit (1:250, ab150077, AbCam) and then mounted with Pro-long anti-fade reagent (P7481, Life Technologies) with DAPI to stain the nuclei. The images were acquired with a Leica TCS NT confocal microscope. d) Quantification of p53 by flow cytometry. Subconfluent cells were fixed 15 minutes in ice cold methanol at -20°C, and then incubated with primary antibody anti-p53 FITC-conjugated at 4°C (1:500, Abcam, ab156030 Mouse) for 1h and then immediately analysed using FACS Vantage SE Becton Dickinson flow cytometry. Analysis were conducted using FlowJo software and the expression of p53 for each sample is reported as the ratio between the intensity of fluorescence with respect to unstained cells due to autofluorescence.

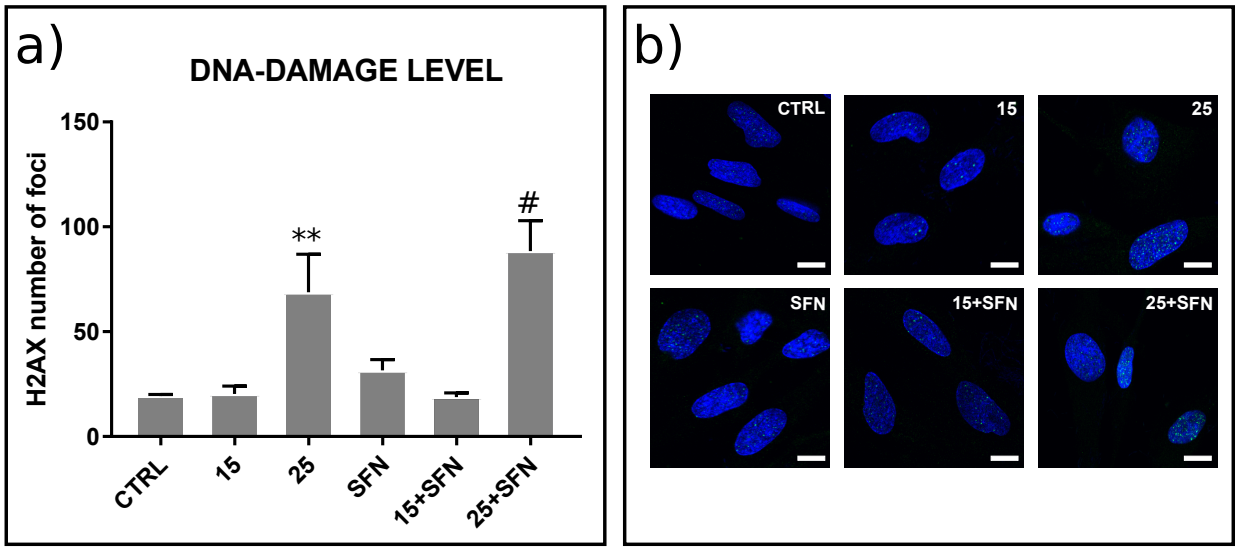

Figure 3: **Effects of SFN alone or in combination with oxidative stress on DNA-damage** a) Subconfuent cells plated on coverslips were fixed with 3.7% paraformaldehyd, permeabilized with 0.1%TRITOX-100 in PBS for 15min at RT and incubated with incubated overnight at 4°C with the γH2AX (1:700, Abcam, ab2893-Phosho139), The samples were then incubated with FITC anti-Rabbit (1:250, ab150077, AbCam) for 1h at RT and then mounted with Pro-long anti-fade reagent (P7481, Life Technologies) with DAPI to stain the nuclei. The images were acquired with a Leica TCS NT confocal microscope. γH2AX spots inside the nuclei were counted using spot detector tool of ICY Software as described in the Materials and Method section All the resulting values are normalized with the total number of pixels of their image, to make possible the comparison of all the nuclei, one with each other.

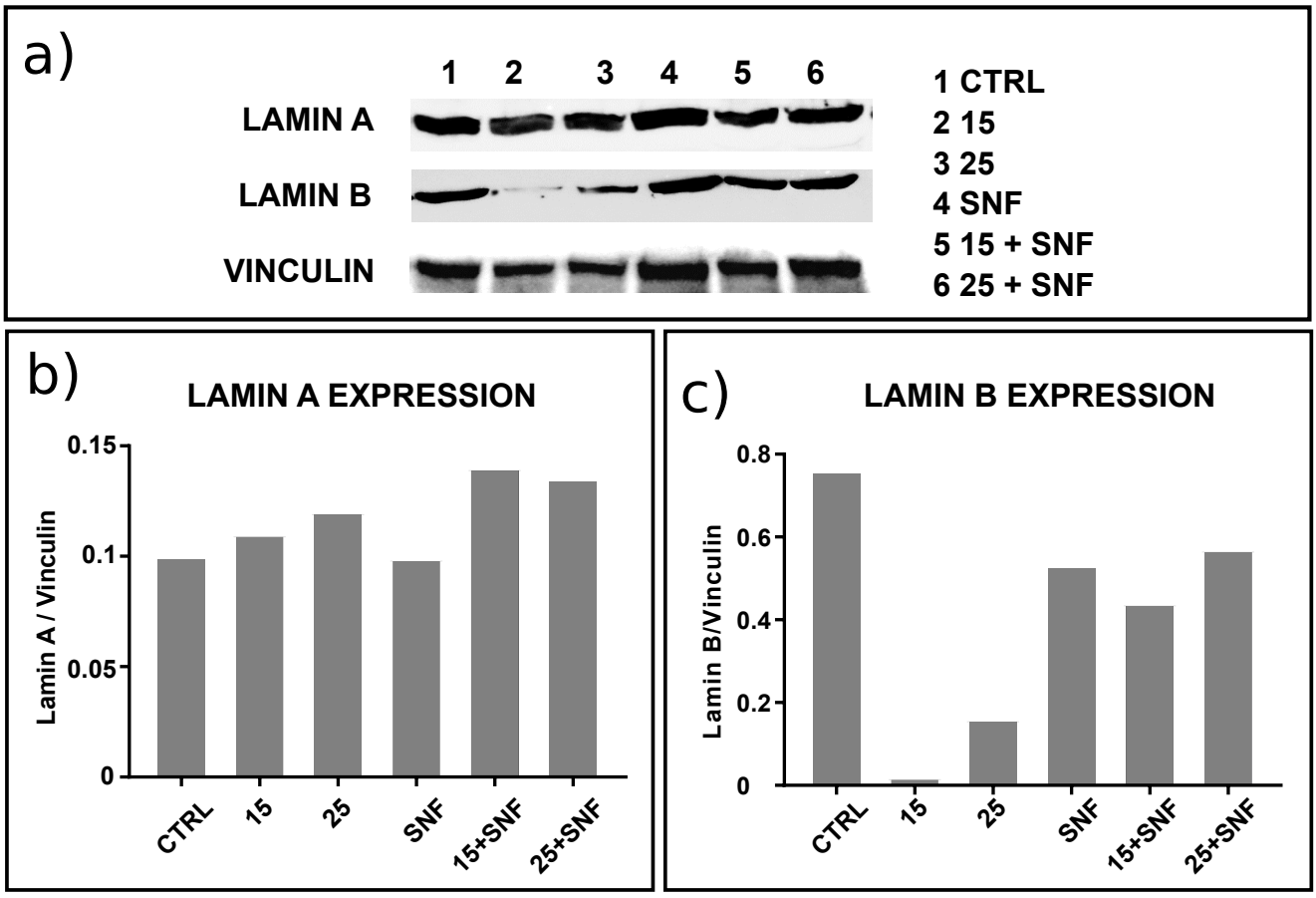

Figure 4: Effect of short and repeated sublethal treatment with H_2O_2 and 1μM SNF alone or in combination on the level of expression of Lamin A and B. Panel a. 15μg protein were loaded on 12% SDS-PAGE gel and transferred on PVDF using the TranBlot Turbo Transfer System Bio-Rad. The membrane was incubated overnight at 4°C with primary antibodies: anti- Lamin B1 (Abcam ab16048 1:1.000 Rabbit) or anti-Lamin A (Abcam, ab8980 Mouse 1:1000) and then with secondary antibody (anti-Mouse HRP (Bio-Rad 1: 3000) for 1h. ECL Blotting reagents were used at room temperature to detect chemioluminescence. The signal has been acquired using Chemidoc Touch. Panels b,c. Densitometric analysis was performed with ImageJ.

Supplementary Information

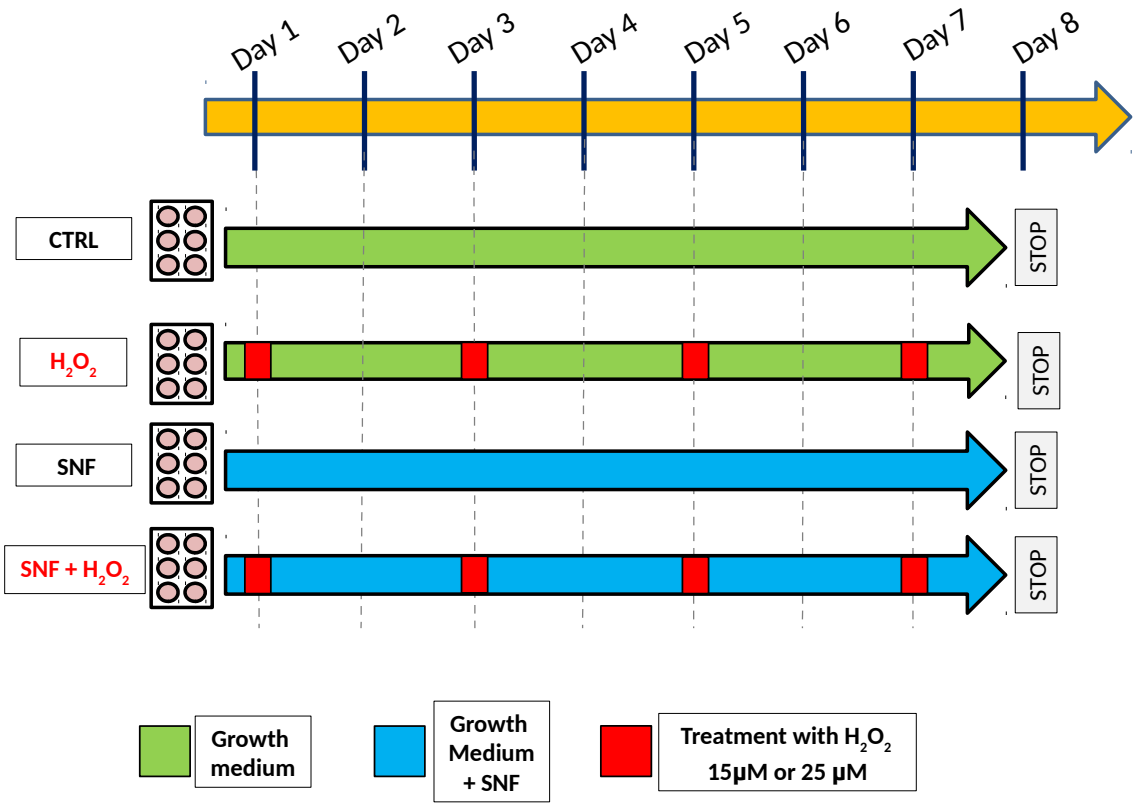

Figure S1: Schematic time line of the treatments with hydrogen peroxide alone or in combination with SNF

[1] N. Lebrasseur, T. Tchkonia, J. Kirkland, Cellular senescence and the biology of aging, disease, and frailty, Nestlé Nutrition Institute workshop series 83 (2015) 11–18.

[2] J. D. Robin, F. Magdinier, Physiological and pathological aging affects chromatin dynamics, structure and function at the nuclear edge, Front Genet 7 (2016) 153. doi:10.3389/fgene.2016.00153.

[3] R. Caldini, M. Chevanne, A. Mocali, D. Tombaccini, F. Paoletti, Premature induction of aging in sublethally h2o2-treated young mrc5 fibroblasts correlates with increased glutathione peroxidase levels and resistance to dna breakage, Mech Ageing Dev 105 (1-2) (1998) 137–50.

[4] P. Davalli, T. Mitic, A. Caporali, A. Lauriola, D. D'Arca, Ros, cell senescence, and novel molecular mechanisms in aging and age-related diseases, Oxid Med Cell Longev 2016 (2016) 3565127. doi:10.1155/2016/3565127.

[5] M. Ristow, S. Schmeisser, Extending life span by increasing oxidative stress, Free Radic Biol Med 51 (2) (2011) 327–36. doi:10.1016/j.freeradbiomed.2011.05.010.

[6] J. Cachat, C. Deffert, S. Hugues, K.-H. Krause, Phagocyte nadph oxidase and specific immunity, Clin Sci (Lond) 128 (10) (2015) 635–48. doi:10.1042/CS20140635.

[7] C. Lawless, D. Jurk, C. S. Gillespie, D. Shanley, G. Saretzki, T. von Zglinicki, J. F. Passos, A stochastic step model of replicative senescence explains ros production rate in ageing cell populations, PLoS One 7 (2) (2012) e32117. doi:10.1371/journal.pone.0032117.

[8] L.-J. Yan, Positive oxidative stress in aging and aging-related disease tolerance, Redox Biol 2 (2014) 165–9. doi:10.1016/j.redox.2014.01.002.

[9] M. Russo, C. Spagnuolo, G. L. Russo, K. Skalicka-Woźniak, M. Daglia, E. Sobarzo-Sánchez, S. F. Nabavi, S. M. Nabavi, Nrf2 targeting by sulforaphane: a potential therapy for cancer treatment, Critical reviews in food science and nutrition 58 (8) (2018) 1391–1405.

[10] S. M. Deneke, Thiol-based antioxidants, in: Current topics in cellular regulation, Vol. 36, Elsevier, 2001, pp. 151–180.

[11] L. Wlodek, Beneficial and harmful effects of thiols, Pol. J. Pharmacol 54 (2002) 215–223.

[12] P. Svoboda, M. Harms-Ringdahl, Protection or sensitization by thiols or ascorbate in irradiated solutions of dna or deoxyguanosine, Radiation research 151 (5) (1999) 605–616.

[13] J. Fridman, S. Lowe, Control of apoptosis by p53, Oncogene 22 (56 REV. ISS. 8) (2003) 9030–9040. doi:10.1038/sj.onc.1207116.

[14] M. G. Hovest, N. Brüggenolte, K. S. Hosseini, T. Krieg, G. Herrmann, Senescence of human fibroblasts after psoralen photoactivation is mediated by atr kinase and persistent dna damage foci at telomeres, Mol Biol Cell 17 (4) (2006) 1758–67. doi:10.1091/mbc.E05-08-0701.

[15] A. S. Balajee, C. R. Geard, Replication protein a and γ-h2ax foci assembly is triggered by cellular response to dna double-strand breaks, Experimental cell research 300 (2) (2004) 320–334.

[16] T. Shimi, V. Butin-Israeli, S. A. Adam, R. B. Hamanaka, A. E. Goldman, C. A. Lucas, D. K. Shumaker, S. T. Kosak, N. S. Chandel, R. D. Goldman, The role of nuclear lamin b1 in cell proliferation and senescence, Genes Dev 25 (24) (2011) 2579–93. doi:10.1101/gad.179515.111.

[17] F. Zanichelli, S. Capasso, M. Cipollaro, E. Pagnotta, M. Cartenì, F. Casale, R. Iori, U. Galderisi, Dose-dependent effects of r-sulforaphane isothiocyanate on the biology of human mesenchymal stem cells, at dietary amounts, it promotes cell proliferation and reduces senescence and apoptosis, while at anti-cancer drug doses, it has a cytotoxic effect, Age (Dordr) 34 (2) (2012) 281–93. doi:10.1007/s11357-011-9231-7.

[18] J. P. Burnett, G. Lim, Y. Li, R. B. Shah, R. Lim, H. J. Paholak, S. P. McDermott, L. Sun, Y. Tsume, S. Bai, et al., Sulforaphane enhances the anticancer activity of taxanes against triple negative breast cancer by killing cancer stem cells, Cancer letters 394 (2017) 52–64.

[19] D. Gabriel, D. Roedl, L. B. Gordon, K. Djabali, Sulforaphane enhances progerin clearance in h utchinson-g ilford progeria fibroblasts, Aging cell 14 (1) (2015) 78–91.

[20] H. Sauer, M. Wartenberg, J. Hescheler, Reactive oxygen species as intracellular messengers during cell growth and differentiation, Cellular Physiology and Biochemistry 11 (4) (2001) 173–186. doi:10.1159/000047804.

[21] H.-C. Lee, P.-H. Yin, C.-W. Chi, Y.-H. Wei, Increase in mitochondrial mass in human fibroblasts under oxidative stress and during replicative cell senescence, Journal of Biomedical Science 9 (5-6) (2002) 517–526. doi:10.1007/BF02254978.

[22] A. Rufini, P. Tucci, I. Celardo, G. Melino, Senescence and aging: the critical roles of p53, Oncogene 32 (43) (2013) 5129–43. doi:10.1038/onc.2012.640.

[23] A. Chicas, X. Wang, C. Zhang, M. McCurrach, Z. Zhao, O. Mert, R. A. Dickins, M. Narita, M. Zhang, S. W. Lowe, Dissecting the unique role of the retinoblastoma tumor suppressor during cellular senescence, Cancer Cell 17 (4) (2010) 376–87. doi:10.1016/j.ccr.2010.01.023.

[24] V. Gambino, G. De Michele, O. Venezia, P. Migliaccio, V. Dall'Olio, L. Bernard, S. P. Minardi, M. A. Della Fazia, D. Bartoli, G. Servillo, et al., Oxidative stress activates a specific p53 transcriptional response that regulates cellular senescence and aging, Aging cell 12 (3) (2013) 435–445.

[25] H. Lan, H. Yuan, C. Lin, Sulforaphane induces p53-deficient sw480 cell apoptosis via the ros-mapk signaling pathway, Molecular medicine reports 16 (5) (2017) 7796–7804.

[26] V. Coccè, A. Vitale, S. Colombo, A. Bonomi, F. Sisto, E. Ciusani, G. Alessandri, E. Parati, P. Brambilla, M. Brambilla, C. A. La Porta, A. Pessina, Human skin-derived fibroblasts used as a 'trojan horse' for drug delivery, Clin Exp Dermatol 41 (4) (2016) 417–24. doi:10.1111/ced.12811.

[27] C. Giampietro, M. Lionetti, G. Costantini, F. Mutti, S. Zapperi, C. Porta, Cholesterol impairment contributes to neuroserpin aggregation, Scientific Reports 7. doi:10.1038/srep43669.

Concluding remarks and future perspectives

The research reported in this thesis is the results of 3 years of works spent investigating different aspects of Nuclear lamina biology. Taking into consideration Hutchinson-Guilford Progeria Syndrome as an extreme example of what nuclear lamina aberration entails, we studied the effect of nuclear lamina alteration on global gene expression regulation, on cell mechanics, and the interconnection existing between nuclear lamina integrity, ageing and oxidative stress. In Chapter 1, we performed a bioinformatics study to study the impact of Lamin A mutation on global gene expression regulation, in HGPS patients. We analysed all the public available transcriptomic data sets of HGPS and compared them with those of healthy matched controls. Once identified genes that are differentially expressed in the analysed groups, we identified the pathways in which genes differentially expressed in HGPS patients are involved using pathway deregulation score analysis. This kind of analysis shows a clear impairment of Epithelial to Mesenchymal Transition (EMT) pathway in HGPS subjects. EMT is a physiologic process during which epithelial cell undergo to a phenotypic switching that involved the loss of cell polarity and cell-to-cell adhesion but also the gain of migratory and invasive properties, typical of mesenchymal stem cells. EMT impairment, reported by our study, is in agreement with the hypothesis of a stem cells exhaustion in these patients or mesenchymal lineage differentiation defects. Given all the obtained results, we can conclude that mutation in Lamin A gene strongly impact on global gene expression regulation. Chapter 2 deals with the investigation of how nuclear lamina alterations impact on its physical and functional connections with extra-nuclear and nuclear elements. To do this, we developed an inducible cellular model of the mutated form of Lamin A responsible for HGPS. Our model faithfully resembles the typical HGPS-patients' nuclear phenotype. Our results clearly show that Progerin presence makes cell nucleus stiffer and less plastic. Furthermore, our data revealed that Progerin expression induces modifications

of the complex interactions present between nuclear lamina and the cytoskeleton. These mainly consist in the establishment of a stronger and more stable coupling between nucleus and cytoskeleton. Nevertheless, we also investigated whether Progerin expression somehow influences the physiologic interaction occurring between nuclear lamina and PcGs protein, components of Polycomb Repressor Complexes 1 and 2. These are key epigenetic regulators of the chromatin status that in physiologic conditions directly bind to wild type Lamin A. We found that Progerin expression significantly interferes in Lamin A-PRC2 interactions, opening up new possible scenarios to further investigate. Physiological ageing and HGPS share some clinical and biological features, among which nuclear shape defects and deterioration, proliferation impairment, progerin and reactive oxygen species accumulation. Moreover, expression and stability of lamins proteins are altered in response to oxidative stress, that is in turn strongly linked to ageing process and the consequent nuclear morphology alterations. Finally, in Chapter 3 we investigated the interdependence between ROS, ageing and lamins in a novel oxidative stress cellular model developed in our laboratory, that is also efficient in recapitulating typical ageing profile. Our findings revealed, that oxidative stress impacts differently on Lamin A and Lamina B1: while it has no effects on Lamin A expression, it induces a significant Lamin B loss which can be rescued by anti-oxidant supplementation. Overall, this study contributes to shed light on the role of the nuclear lamina in health and disease providing new insight but also opening up to new scenarios that need to be further investigated. In the future, indeed, it would be of great interest to study deeper the functional effect of the reduced interaction between wild type Lamin A and PCR2 observed in presence of Progerin, since this could be linked to heterochromatin loss in HGPS. Intriguingly, the latter is another common feature between Progeria and normal aging. Our group is now going on to study lamins focusing on the impact of progerin in tumor cells. In fact, it has been reported that in tumor cells progerin is expressed and we are now investigating the impact of this aberrant lamin in the contest of a tumor cell instead of a normal cell like happens in HGPS.

Final report

Seminars

- Mathematical Modelling Of Cell Migration , Rhoda Hawkins , 13rd November 2015 - University of Milan
- Can theory help us understand cancer metastasis?. Herbert Levine , 18th November 2016 University of Milan
- T memory stem cells in health and disease: new insights and therapeutic opportunities., Dr. M. Gattinoni , 15th September 2016, University of Milan
- On the molecular mechanisms of chromatin modification., Dr. A. Mattevi, 12nd April 2016, University of Milan
- Mechanical guidance of collective cell migration and invasion, Dr. X. Trepat, 27th May 2016 , University of Milan
- Quantitative methods in gene regulation, Dr. M. Caselle, 21st January 2016, University of Milan
- Modelling chemotactic motion of cells in biological tissues, Dr. Bakhtier Vasiev, 29th January 2016, University of Milan
- Inside-out the skin, Dr.ssa Elena Donetti, 14thFebruary 2017, University of Milan
- Susceptibility to particle health effects, mirna and extracellular vesicles, Valentina Bollati, 6th March 2017, University of Milan
- Comparative genomics of 500 species reveal new insights about superpowers, drugs and human diseases, Y. Tabach , 10th March 2017 , University of Milan
- Molecular determinants of cell-to-cell variability in the cellular response to anti-mitotic drugs, Andrea Ciliberto , 6th April 2017, University of Milan
- The translational impact of molecular pathology for healthcare providers. Nicola Fusco , 24th May 2017
- Sleep and synapsis, Michele Bellesi , 21st June 2017, University of Milan

- Mechanical guidance of collective cell migration and invasion, Dr. X. Trepat , 27th May 2016 University of Milan

- Quantitative methods in gene regulation, Dr. M. Caselle, 21st Hanuary 2016, University of Milan

- Cancer: bad luck or environment? The contribution of exposome research, Paolo Vineis, 24th November 2017 , University of Milan

- Quantitative systems biophysiology for precision personalized medicine: from data mining through signal processing to mathematical modeling , Diego Liberati, 30th November 2017, University of Milan

- Exploring the effects of social influence on flocking dynamics, M.Carmen Miguel , 12th December 2017, University of Milan

- Next-Generation Sequencing to uncover the pre-clinical evolution of multiple myeloma, Niccoloò Bolli, 14th December 2017, University of Milan

- Active mechanics in a model biological tissue,Daniel Matoz Fernandez, 26th January 2018, University of Milan

- Linking mechanochemistry with protein folding with single bond resolution, Sergi Garcia-Manyes, 9th February 2018, University of Milan

- On the entropy of the human transcriptome, Giulio Pavesi, 27th February 2018 , University of Milan

Courses

- Comunicare la scienza , M. Bellone - M. Franceschini - P. Morandini , 16th June 2017 University of Milan
- Corso di Statistica, Dott. Roberto Ambrosini, 4th September – 5th October, University of Milan
- Competenze trasversali: La valutazione della ricerca, 21st September 2016, University of Milan
- Competenze trasversali: Placement e mercato del lavoro, 18th November 2016, University of Milan
- Competenze trasversali: Come scrivere un progetto di ricerca: . Le 100 cose che avrei voluto sapere quando ero un dottorando (First Part), 22nd February 2017, University of Milan
- Competenze trasversali: Come scrivere un progetto di ricerca (second Part). Le 100 cose che avrei voluto sapere quando ero un dottorando, 16th June 2017, University of Milan
- Tossicologia ambientale: dall'esposizione all'effetto biologico, Prof. Fustinoni, 20th June – 6th July 2017, University of Milan
- Competenze trasversali: Research integrity, 29th September 2017, University of Milan
- Competenze trasversali: Valorizzare creando impresa: fare spin o in unimi (First Part). 20th April 2018 , University of Milan
- Competenze trasversali: Valorizzare creando impresa: fare spin o in unimi (Second Part), 23rd April 2018 , University of Milan
- Corso di Matematica (ottimizzazione in piuvariabili), Dr. Paola Morando, 10th May-21st June 2016, University of Milan
- Corso Teorico-Pratico : Comunicare la scienza, organized by Prof. Caterina La Porta, 20th April 2018 , University of Milan
- Competenze trasversali: Open access, 17thJune 2016, University of Milan
- Competenze trasversali: Evaluation of research,21st September 2016, University of Milan

Congresses

- Physicists working on cancer at Weizmann Institute of Science, Israel, 1st-12th July 2018
- Neuronest, University of Milan, 8th March 2018
- PhD Meeting in Neuroscience at Università Federico II di Napoli, 24th February 2017

Summer Schools and traineeships

- Advances in Complex Systems - Como Lake Summer School 3rd-7th July 2017
- Visiting Ph.D. Student at Institute of Integrative Biology, University of Liverpool, June-July 2016
- Erasmus Plus traineeship - Ecole Normale Superieure de Lyon, 23rd April-23rd July 2018

Publications

- **Cholesterol impairment contributes to Neuroserpin aggregation**

Maria Chiara Lionetti, C.Giampietro, G. Costantini, Federico Mutti,Stefano Zapper and Caterina A.M. La Porta
Scientic Reports, 2017 Mar 3;7:43669. doi: 10.1038/srep43669.

- **From jamming to collective cell migration though a boundary induced transition**

Olekasandr Chepizhko, Maria Chiara Lionetti, Chiara Malinverno, Giorgio Scita, Stefano Zapperi and Caterina A.M.La Porta
Soft Matter, 2018 May 16;14(19):3774-3782. doi: 10.1039/c8sm00128f.

- **Cellular pathways affected by carbon nanopowder-benzo(a)pyrene complex in human skin broblasts identied by proteomics**

Binelli A,Magni S., La Porta C., Bini L., Della Torre C., Ascagni M.,Maggioni D, Ghilardi A, Armini A, Landi C, Santo N, Madaschi L,Cocce V, Mutti F, Lionetti MC, Ciusani E, Del Giacco L.
Ecotoxicol Environ Saf, 2018 Sep 30;160:144-153. doi: 10.1016/j.ecoenv.2018.05.027. Epub 2018 May 26.

- **Metamaterial architecture from a self-shaping carnivorous plant**

  Caterina A.M. La Porta, Milan S., Bonfanti S.,Ferrario C., Maria Chiara Lionetti, et al.

  under revision Nature Physics

- **Pathway deregulation analysis in Hutchinson-Gilford Progeria Syndrome**

  Francesc Font-Clos, Maria Chiara Lionetti, Stefano Zapperi and Caterina A.M.La Porta

  under revision Scientic Reports

- **Sulforaphane can not protect the cells to a repeated, short and sublethal treatment with hydrogen peroxide**

  Maria Chiara Lionetti, Federico Mutti, Erica Soldati, Maria Rita Fumagalli, Graziano Colombo,

  Emanuela Astori, Aldo Milzani, Isabella Dalle Donne, Emilio Ciusani, Giulio Costantini, Caterina A. M. La Porta

  under revision Journal of Nutrition Biochemistry

Bibliography

[1] Asifa Akhtar and Susan M Gasser. The nuclear envelope and transcriptional control. *Nature Reviews Genetics*, 8(7):507, 2007.

[2] Jason M Berk, Kathryn E Tifft, and Katherine L Wilson. The nuclear envelope lem-domain protein emerin. *Nucleus*, 4(4):298–314, 2013.

[3] B.P. Berman, D.J. Weisenberger, J.F. Aman, T. Hinoue, Z. Ramjan, Y. Liu, H. Noushmehr, C.P.E. Lange, C.M. Van Dijk, R.A.E.M. Tollenaar, D. Van Den Berg, and P.W. Laird. Regions of focal dna hypermethylation and long-range hypomethylation in colorectal cancer coincide with nuclear laminag-associated domains. *Nature Genetics*, 44(1):40–46, 2012.

[4] Gisèle Bonne, Marina Raffaele Di Barletta, Shaida Varnous, Henri-Marc Bécane, El-Hadi Hammouda, Luciano Merlini, Francesco Muntoni, Cheryl R Greenberg, Françoise Gary, Jon-Andoni Urtizberea, et al. Mutations in the gene encoding lamin a/c cause autosomal dominant emery-dreifuss muscular dystrophy. *Nature genetics*, 21(3):285, 1999.

[5] J.L.V. Broers and F.C.S. Ramaekers. The role of the nuclear lamina in cancer and apoptosis. *Advances in Experimental Medicine and Biology*, 773:27–48, 2014.

[6] Francine Bruston, Erwan Delbarre, Cecilia Östlund, Howard J Worman, Brigitte Buendia, and Isabelle Duband-Goulet. Loss of a dna binding site within the tail of prelamin a contributes to altered heterochromatin anchorage by progerin. *FEBS letters*, 584(14):2999–3004, 2010.

[7] Henian Cao and Robert A Hegele. Nuclear lamin a/c r482q mutation in canadian kindreds with dunnigan-type familial partial lipodystrophy. *Human molecular genetics*, 9(1):109–112, 2000.

[8] Kan Cao, Cecilia D Blair, Dina A Faddah, Julia E Kieckhaefer, Michelle Olive, Michael R Erdos, Elizabeth G Nabel, and Francis S Collins. Progerin and telomere dysfunction collaborate to trigger cellular senescence in normal human fibroblasts. *The Journal of clinical investigation*, 121(7):2833–2844, 2011.

[9] Kan Cao, John J Graziotto, Cecilia D Blair, Joseph R Mazzulli, Michael R Erdos, Dimitri Krainc, and Francis S Collins. Rapamycin reverses cellular phenotypes and enhances mutant protein clearance in hutchinson-gilford progeria syndrome cells. *Science translational medicine*, 3(89):89ra58–89ra58, 2011.

[10] Brian C Capell and Francis S Collins. Human laminopathies: nuclei gone genetically awry. *Nature reviews genetics*, 7(12):940, 2006.

[11] Brian C Capell, Michael R Erdos, James P Madigan, James J Fiordalisi, Renee Varga, Karen N Conneely, Leslie B Gordon, Channing J Der, Adrienne D Cox, and Francis S Collins. Inhibiting farnesylation of progerin prevents the characteristic nuclear blebbing of hutchinson-gilford progeria syndrome. *Proceedings of the National Academy of Sciences*, 102(36):12879–12884, 2005.

[12] Elisa Cesarini, Chiara Mozzetta, Fabrizia Marullo, Francesco Gregoretti, Annagiusi Gargiulo, Marta Columbaro, Alice Cortesi, Laura Antonelli, Simona Di Pelino, Stefano Squarzoni, et al. Lamin a/c sustains pcg protein architecture, maintaining transcriptional repression at target genes. *J Cell Biol*, 211(3):533–551, 2015.

[13] Fabio Coppedè. The epidemiology of premature aging and associated comorbidities. *Clinical interventions in aging*, 8:1023, 2013.

[14] L.S. Cox and G.H. Leno. Extracts from eggs and oocytes of xenopus laevis differ in their capacities for nuclear assembly and dna replication. *Journal of Cell Science*, 97(1):177–184, 1990.

[15] Melissa Crisp, Qian Liu, Kyle Roux, JB Rattner, Catherine Shanahan, Brian Burke, Phillip D Stahl, and Didier Hodzic. Coupling of the nucleus and cytoplasm: role of the linc complex. *J Cell Biol*, 172(1):41–53, 2006.

[16] Kris Noel Dahl, Adam J Engler, J David Pajerowski, and Dennis E Discher. Power-law rheology of isolated nuclei with deformation mapping of nuclear substructures. *Biophysical journal*, 89(4):2855–2864, 2005.

[17] Brandon SJ Davies, Loren G Fong, Shao H Yang, Catherine Coffinier, and Stephen G Young. The posttranslational processing of prelamin a and disease. *Annual review of genomics and human genetics*, 10:153–174, 2009.

[18] Franklin L DeBusk. The hutchinson-gilford progeria syndrome: report of 4 cases and review of the literature. *The Journal of pediatrics*, 80(4):697–724, 1972.

[19] T. Dechat, S.A. Adam, and R.D. Goldman. Nuclear lamins and chromatin: When structure meets function. *Advances in Enzyme Regulation*, 49(1):157–166, 2009.

[20] T. Dechat, K. Pfleghaar, K. Sengupta, T. Shimi, D.K. Shumaker, L. Solimando, and R.D. Goldman. Nuclear lamins: Major factors in the structural organization and function of the nucleus and chromatin. *Genes and Development*, 22(7):832–853, 2008.

[21] Travis A Dittmer and Tom Misteli. The lamin protein family. *Genome biology*, 12(5):222, 2011.

[22] Agnieszka Dobrzynska, Susana Gonzalo, Catherine Shanahan, and Peter Askjaer. The nuclear lamina in health and disease. *Nucleus*, 7(3):233–248, 2016.

[23] Patrick Dumont, Maggi Burton, Qin M Chen, Efstathios S Gonos, Christophe Frippiat, Jean-Baptiste Mazarati, François Eliaers, José Remacle, and Olivier Toussaint. Induction of replicative senescence biomarkers by sublethal oxidative stresses in normal human fibroblast. *Free Radical Biology and Medicine*, 28(3):361–373, 2000.

[24] Don W Fawcett. On the occurrence of a fibrous lamina on the inner aspect of the nuclear envelope in certain cells of vertebrates. *American Journal of Anatomy*, 119(1):129–145, 1966.

[25] R. Foisner. Cell cycle dynamics of the nuclear envelope. *TheScientificWorldJournal [electronic resource]*, 3:1–20, 2003.

[26] Peter Friedl, Katarina Wolf, and Jan Lammerding. Nuclear mechanics during cell migration. *Current opinion in cell biology*, 23(1):55–64, 2011.

[27] Diana Gabriel, Daniela Roedl, Leslie B Gordon, and Karima Djabali. Sulforaphane enhances progerin clearance in h utchinson–g ilford progeria fibroblasts. *Aging cell*, 14(1):78–91, 2015.

[28] Kevin Gesson, Philipp Rescheneder, Michael P Skoruppa, Arndt von Haeseler, Thomas Dechat, and Roland Foisner. A-type lamins bind both hetero-and euchromatin, the latter being regulated by lamina-associated polypeptide 2 alpha. *Genome research*, 2016.

[29] Hastings Gilford. Progeria: a form of senilism. *Practitioner*, 73:188–217, 1904.

[30] M.W. Goldberg and T.D. Allen. Structural and functional organization of the nuclear envelope. *Current Opinion in Cell Biology*, 7(3):301–309, 1995.

[31] Ignacio Gonzalez-Suarez, Abena B Redwood, Stephanie M Perkins, Bart Vermolen, Daniel Lichtensztejin, David A Grotsky, Lucia Morgado-Palacin, Eric J Gapud, Barry P Sleckman, Teresa Sullivan, et al. Novel roles for a-type lamins in telomere biology and the dna damage response pathway. *The EMBO journal*, 28(16):2414–2427, 2009.

[32] David M Graham and Keith Burridge. Mechanotransduction and nuclear function. *Current opinion in cell biology*, 40:98–105, 2016.

[33] John J Graziotto, Kan Cao, Francis S Collins, and Dimitri Krainc. Rapamycin activates autophagy in hutchinson-gilford progeria syndrome: implications for normal aging and age-dependent neurodegenerative disorders. *Autophagy*, 8(1):147–151, 2012.

[34] Lars Guelen, Ludo Pagie, Emilie Brasset, Wouter Meuleman, Marius B Faza, Wendy Talhout, Bert H Eussen, Annelies de Klein, Lodewyk Wessels, Wouter de Laat, et al. Domain organization of human chromosomes revealed by mapping of nuclear lamina interactions. *Nature*, 453(7197):948, 2008.

[35] Farshid Guilak. Compression-induced changes in the shape and volume of the chondrocyte nucleus. *Journal of biomechanics*, 28(12):1529–1541, 1995.

[36] Gregg G Gundersen and Howard J Worman. Nuclear positioning. *Cell*, 152(6):1376–1389, 2013.

[37] Michelle L Hamilton, Holly Van Remmen, Jessica A Drake, Hong Yang, Zhong Mao Guo, Kristen Kewitt, Christi A Walter, and Arlan Richardson. Does oxidative damage to dna increase with age? *Proceedings of the National Academy of Sciences*, 98(18):10469–10474, 2001.

[38] Farhana Haque, David J Lloyd, Dawn T Smallwood, Carolyn L Dent, Catherine M Shanahan, Andrew M Fry, Richard C Trembath, and Sue Shackleton. Sun1 interacts with nuclear

lamin a and cytoplasmic nesprins to provide a physical connection between the nuclear lamina and the cytoskeleton. *Molecular and cellular biology*, 26(10):3738–3751, 2006.

[39] Denham Harman. Free radical theory of aging. *Mutation Research/DNAging*, 275(3-6):257–266, 1992.

[40] Raoul CM Hennekam. Hutchinson–gilford progeria syndrome: review of the phenotype. *American journal of medical genetics Part A*, 140(23):2603–2624, 2006.

[41] Christopher Hine, Eylul Harputlugil, Yue Zhang, Christoph Ruckenstuhl, Byung Cheon Lee, Lear Brace, Alban Longchamp, Jose H Treviño-Villarreal, Pedro Mejia, C Keith Ozaki, et al. Endogenous hydrogen sulfide production is essential for dietary restriction benefits. *Cell*, 160(1):132–144, 2015.

[42] Ian Holt, Nguyen Thuy Duong, Qiuping Zhang, Le Thanh Lam, Caroline A Sewry, Kamel Mamchaoui, Catherine M Shanahan, and Glenn E Morris. Specific localization of nesprin-1-α2, the short isoform of nesprin-1 with a kash domain, in developing, fetal and regenerating muscle, using a new monoclonal antibody. *BMC cell biology*, 17(1):26, 2016.

[43] F Houben, FCS Ramaekers, LHEH Snoeckx, and JLV Broers. Role of nuclear lamina-cytoskeleton interactions in the maintenance of cellular strength. *Biochimica et Biophysica Acta (BBA)-Molecular Cell Research*, 1773(5):675–686, 2007.

[44] Jonathan Hutchinson. Congenital absence of hair and mammary glands with atrophic condition of the skin and its appendages, in a boy whose mother had been almost wholly bald from alopecia areata from the age of six. *Medico-chirurgical transactions*, 69:473, 1886.

[45] Hélene Karcher, Jan Lammerding, Hayden Huang, Richard T Lee, Roger D Kamm, and Mohammad R Kaazempur-Mofrad. A three-dimensional viscoelastic model for cell deformation with experimental verification. *Biophysical journal*, 85(5):3336–3349, 2003.

[46] J. Kind, L. Pagie, H. Ortabozkoyun, S. Boyle, S.S. De Vries, H. Janssen, M. Amendola, L.D. Nolen, W.A. Bickmore, and B. Van Steensel. Single-cell dynamics of genome-nuclear lamina interactions. *Cell*, 153(1):178–192, 2013.

[47] Jop Kind, Ludo Pagie, Sandra S de Vries, Leila Nahidiazar, Siddharth S Dey, Magda Bienko, Ye Zhan, Bryan Lajoie, Carolyn A de Graaf, Mario Amendola, et al. Genome-

wide maps of nuclear lamina interactions in single human cells. *Cell*, 163(1):134–147, 2015.

[48] Jan Lammerding, Janet Hsiao, P Christian Schulze, Serguei Kozlov, Colin L Stewart, and Richard T Lee. Abnormal nuclear shape and impaired mechanotransduction in emerin-deficient cells. *J cell biol*, 170(5):781–791, 2005.

[49] G Lattanzi, S Marmiroli, A Facchini, and NM Maraldi. Nuclear damages and oxidative stress: new perspectives for laminopathies. *European journal of histochemistry: EJH*, 56(4), 2012.

[50] Thi Thanh Huong Le. Molecular genetic studies in hereditary laminopathies of man. 2010.

[51] Kenneth K Lee, Tokuko Haraguchi, Richard S Lee, Takako Koujin, Yasushi Hiraoka, and Katherine L Wilson. Distinct functional domains in emerin bind lamin a and dna-bridging protein baf. *Journal of Cell Science*, 114(24):4567–4573, 2001.

[52] Thorsten Libotte, Hafida Zaim, Sabu Abraham, VC Padmakumar, Maria Schneider, Wenshu Lu, Martina Munck, Christopher Hutchison, Manfred Wehnert, Birthe Fahrenkrog, et al. Lamin a/c–dependent localization of nesprin-2, a giant scaffolder at the nuclear envelope. *Molecular biology of the cell*, 16(7):3411–3424, 2005.

[53] Baohua Liu, Shrestha Ghosh, Xi Yang, Huiling Zheng, Xinguang Liu, Zimei Wang, Guoxiang Jin, Bojian Zheng, Brian K Kennedy, Yousin Suh, et al. Resveratrol rescues sirt1-dependent adult stem cell decline and alleviates progeroid features in laminopathy-based progeria. *Cell metabolism*, 16(6):738–750, 2012.

[54] J. Liu, T.R. Ben-Shahar, D. Riemer, M. Treinin, P. Spann, K. Weber, A. Fire, and Y. Gruenbaum. Essential roles for caenorhabditis elegans lamin gene in nuclear organization, cell cycle progression, and spatial organization of nuclear pore complexes. *Molecular Biology of the Cell*, 11(11):3937–3947, 2000.

[55] Yiyong Liu, Antonio Rusinol, Michael Sinensky, Youjie Wang, and Yue Zou. Dna damage responses in progeroid syndromes arise from defective maturation of prelamin a. *J Cell Sci*, 119(22):4644–4649, 2006.

[56] Maria L Lombardi, Diana E Jaalouk, Catherine M Shanahan, Brian Burke, Kyle J Roux, and Jan Lammerding. The interaction between nesprins and sun proteins at the nuclear

envelope is critical for force transmission between the nucleus and cytoskeleton. *Journal of Biological Chemistry*, pages jbc–M111, 2011.

[57] Carlos López-Otín, Maria A Blasco, Linda Partridge, Manuel Serrano, and Guido Kroemer. The hallmarks of aging. *Cell*, 153(6):1194–1217, 2013.

[58] Eivind Lund, Anja R Oldenburg, Erwan Delbarre, Christel T Freberg, Isabelle Duband-Goulet, Ragnhild Eskeland, Brigitte Buendia, and Philippe Collas. Lamin a/c-promoter interactions specify chromatin state–dependent transcription outcomes. *Genome research*, 2013.

[59] Eivind G Lund, Isabelle Duband-Goulet, Anja Oldenburg, Brigitte Buendia, and Philippe Collas. Distinct features of lamin a-interacting chromatin domains mapped by chip-sequencing from sonicated or micrococcal nuclease-digested chromatin. *Nucleus*, 6(1):30–39, 2015.

[60] Barbie M Machiels, Antoine HG Zorenc, Jorike M Endert, Helma JH Kuijpers, Guillaume JJM van Eys, Frans CS Ramaekers, and Jos LV Broers. An alternative splicing product of the lamin a/c gene lacks exon 10. *Journal of Biological Chemistry*, 271(16):9249–9253, 1996.

[61] Andrew J Maniotis, Christopher S Chen, and Donald E Ingber. Demonstration of mechanical connections between integrins, cytoskeletal filaments, and nucleoplasm that stabilize nuclear structure. *Proceedings of the National Academy of Sciences*, 94(3):849–854, 1997.

[62] F Marullo, E Cesarini, L Antonelli, F Gregoretti, G Oliva, and C Lanzuolo. Nucleoplasmic lamin a/c and polycomb group of proteins: An evolutionarily conserved interplay. *Nucleus*, 7(2):103–111, 2016.

[63] N. Maus, N. Stuurman, and P.A. Fisher. Disassembly of the drosophila nuclear lamina in a homologous cell-free system. *Journal of Cell Science*, 108(5):2027–2035, 1995.

[64] Patrizia Mecocci, Usha MacGarvey, Allan E Kaufman, Deborah Koontz, John M Shoffner, Douglas C Wallace, and M Flint Beal. Oxidative damage to mitochondrial dna shows marked age-dependent increases in human brain. *Annals of Neurology: Official Journal of the American Neurological Association and the Child Neurology Society*, 34(4):609–616, 1993.

[65] Wouter Meuleman, Daan Peric-Hupkes, Jop Kind, Jean-Bernard Beaudry, Ludo Pagie, Manolis Kellis, Marcel Reinders, Lodewyk Wessels, and Bas van Steensel. Constitutive nuclear lamina–genome interactions are highly conserved and associated with a/t-rich sequence. *Genome research*, 23(2):270–280, 2013.

[66] Antoine Muchir, Gisèle Bonne, Anneke J van der Kooi, Mia van Meegen, Frank Baas, Pieter A Bolhuis, Marianne de Visser, and Ketty Schwartz. Identification of mutations in the gene encoding lamins a/c in autosomal dominant limb girdle muscular dystrophy with atrioventricular conduction disturbances (lgmd1b). *Human molecular genetics*, 9(9):1453–1459, 2000.

[67] A. Muñoz-Alarcón, M. Pavlovic, J. Wismar, B. Schmitt, M. Eriksson, P. Kylsten, and M.S. Dushay. Characterization of lamin mutation phenotypes in drosophila and comparison to human laminopathies. *PloS one*, 2(6), 2007.

[68] Ashwin S Nathan, Brendon M Baker, Nandan L Nerurkar, and Robert L Mauck. Mechano-topographic modulation of stem cell nuclear shape on nanofibrous scaffolds. *Acta biomaterialia*, 7(1):57–66, 2011.

[69] Xavier Nissan, Sophie Blondel, Claire Navarro, Yves Maury, Cécile Denis, Mathilde Girard, Cécile Martinat, Annachiara De Sandre-Giovannoli, Nicolas Levy, and Marc Peschanski. Unique preservation of neural cells in hutchinson-gilford progeria syndrome is due to the expression of the neural-specific mir-9 microrna. *Cell reports*, 2(1):1–9, 2012.

[70] Asao Noda, Shuji Mishima, Yuko Hirai, Kanya Hamasaki, Reid D Landes, Hiroshi Mitani, Kei Haga, Tohru Kiyono, Nori Nakamura, and Yoshiaki Kodama. Progerin, the protein responsible for the hutchinson-gilford progeria syndrome, increases the unrepaired dna damages following exposure to ionizing radiation. *Genes and Environment*, 37(1):13, 2015.

[71] Milos Pekny and E Birgitte Lane. Intermediate filaments and stress. *Experimental cell research*, 313(10):2244–2254, 2007.

[72] Vanja Pekovic, Ian Gibbs-Seymour, Ewa Markiewicz, Fahad Alzoghaibi, Adam M Benham, Robert Edwards, Manfred Wenhert, Thomas von Zglinicki, and Christopher J Hutchison. Conserved cysteine residues in the mammalian lamin a tail are essential for cellular responses to ros generation. *Aging cell*, 10(6):1067–1079, 2011.

[73] Daan Peric-Hupkes, Wouter Meuleman, Ludo Pagie, Sophia WM Bruggeman, Irina Solovei, Wim Brugman, Stefan Gräf, Paul Flicek, Ron M Kerkhoven, Maarten van Lohuizen, et al. Molecular maps of the reorganization of genome-nuclear lamina interactions during differentiation. *Molecular cell*, 38(4):603–613, 2010.

[74] Roopali Pradhan, Devika Ranade, and Kundan Sengupta. Emerin modulates spatial organization of chromosome territories in cells on softer matrices. *Nucleic acids research*, 46(11):5561–5586, 2018.

[75] Heinrich Sauer, Maria Wartenberg, and Juergen Hescheler. Reactive oxygen species as intracellular messengers during cell growth and differentiation. *Cellular physiology and biochemistry*, 11(4):173–186, 2001.

[76] Paola Scaffidi and Tom Misteli. Lamin a-dependent nuclear defects in human aging. *Science*, 312(5776):1059–1063, 2006.

[77] Eva Schmidt, Ola Nilsson, Antti Koskela, Juha Tuukkanen, Claes Ohlsson, Björn Rozell, and Maria Eriksson. Expression of the hutchinson-gilford progeria mutation during osteoblast development results in loss of osteocytes, irregular mineralization, and poor biomechanical properties. *Journal of Biological Chemistry*, 287(40):33512–33522, 2012.

[78] Katherine H Schreiber and Brian K Kennedy. When lamins go bad: nuclear structure and disease. *Cell*, 152(6):1365–1375, 2013.

[79] Wolfgang Schütz, Ricardo Benavente, and Manfred Alsheimer. Dynamic properties of germ line-specific lamin b3: the role of the shortened rod domain. *European journal of cell biology*, 84(7):649–662, 2005.

[80] Yuri B Schwartz and Vincenzo Pirrotta. Polycomb complexes and epigenetic states. *Current opinion in cell biology*, 20(3):266–273, 2008.

[81] Sue Shackleton, David J Lloyd, Stephen NJ Jackson, Richard Evans, Martinus F Niermeijer, Baldev M Singh, Hartmut Schmidt, Georg Brabant, Sudesh Kumar, Paul N Durrington, et al. Lmna, encoding lamin a/c, is mutated in partial lipodystrophy. *Nature genetics*, 24(2):153, 2000.

[82] Parisha P Shah, Greg Donahue, Gabriel L Otte, Brian C Capell, David M Nelson, Kajia Cao, Varun Aggarwala, Hazel A Cruickshanks, Taranjit Singh Rai, Tony McBryan, et al.

Lamin b1 depletion in senescent cells triggers large-scale changes in gene expression and the chromatin landscape. *Genes & development*, 2013.

[83] YY Shevelyov, SA Lavrov, LM Mikhaylova, ID Nurminsky, RJ Kulathinal, KS Egorova, YM Rozovsky, and DI Nurminsky. The b-type lamin is required for somatic repression of testis-specific gene clusters. *Proceedings of the National Academy of Sciences*, 106(9):3282–3287, 2009.

[84] Takeshi Shimi and Robert D Goldman. Nuclear lamins and oxidative stress in cell proliferation and longevity. In *Cancer Biology and the Nuclear Envelope*, pages 415–430. Springer, 2014.

[85] Mayank Singh, Clayton R Hunt, Raj K Pandita, Rakesh Kumar, Chin-Rang Yang, Nobuo Horikoshi, Robert Bachoo, Sara Sarag, Michael D Story, Jerry W Shay, et al. Lamin a/c depletion enhances dna damage induced stalled replication fork arrest. *Molecular and cellular biology*, pages MCB–01676, 2013.

[86] T. Sullivan, D. Escalante-Alcalde, H. Bhatt, M. Anver, N. Bhat, K. Nagashima, C.L. Stewart, and B. Burke. Loss of a-type lamin expression compromises nuclear envelope integrity leading to muscular dystrophy. *Journal of Cell Biology*, 147(5):913–919, 1999.

[87] Joe Swift and Dennis E Discher. The nuclear lamina is mechano-responsive to ecm elasticity in mature tissue. *J Cell Sci*, pages jcs–149203, 2014.

[88] Joe Swift, Irena L Ivanovska, Amnon Buxboim, Takamasa Harada, PC Dave P Dingal, Joel Pinter, J David Pajerowski, Kyle R Spinler, Jae-Won Shin, Manorama Tewari, et al. Nuclear lamin-a scales with tissue stiffness and enhances matrix-directed differentiation. *Science*, 341(6149):1240104, 2013.

[89] Stephen D Thorpe and David A Lee. Dynamic regulation of nuclear architecture and mechanics—a rheostatic role for the nucleus in tailoring cellular mechanosensitivity. *Nucleus*, 8(3):287–300, 2017.

[90] Julia I Toth, Shao H Yang, Xin Qiao, Anne P Beigneux, Michael H Gelb, Casey L Moulson, Jeffrey H Miner, Stephen G Young, and Loren G Fong. Blocking protein farnesyltransferase improves nuclear shape in fibroblasts from humans with progeroid syndromes. *Proceedings of the National Academy of Sciences*, 102(36):12873–12878, 2005.

[91] Jop H van Berlo, Willem G de Voogt, Anneke J van der Kooi, J Peter van Tintelen, Gisèle Bonne, Rabah Ben Yaou, Denis Duboc, Tom Rossenbacker, Hein Heidbüchel, Marianne de Visser, et al. Meta-analysis of clinical characteristics of 299 carriers of lmna gene mutations: do lamin a/c mutations portend a high risk of sudden death? *Journal of molecular medicine*, 83(1):79–83, 2005.

[92] B. van Steensel and A.S. Belmont. Lamina-associated domains: Links with chromosome architecture, heterochromatin, and gene repression. *Cell*, 169(5):780–791, 2017.

[93] Bas van Steensel and Andrew S Belmont. Lamina-associated domains: links with chromosome architecture, heterochromatin, and gene repression. *Cell*, 169(5):780–791, 2017.

[94] Gabriela Viteri, Youn Wook Chung, and Earl R Stadtman. Effect of progerin on the accumulation of oxidized proteins in fibroblasts from hutchinson gilford progeria patients. *Mechanisms of ageing and development*, 131(1):2–8, 2010.

[95] Kevin Wilhelmsen, Sandy HM Litjens, Ingrid Kuikman, Ntambua Tshimbalanga, Hans Janssen, Iman van den Bout, Karine Raymond, and Arnoud Sonnenberg. Nesprin-3, a novel outer nuclear membrane protein, associates with the cytoskeletal linker protein plectin. *The Journal of cell biology*, 171(5):799–810, 2005.

[96] Margaret K Willer and Christopher W Carroll. Substrate stiffness-dependent regulation of srf/mkl1 requires the inner nuclear membrane protein emerin. *J Cell Sci*, pages jcs–197517, 2017.

[97] S.G. Young, M. Meta, S.H. Yang, and L.G. Fong. Prelamin a farnesylation and progeroid syndromes. *Journal of Biological Chemistry*, 281(52):39741–39745, 2006.

[98] Magdalena Zaremba-Czogalla, Magda Dubińska-Magiera, and Ryszard Rzepecki. Laminopathies: the molecular background of the disease and the prospects for its treatment. *Cellular & molecular biology letters*, 16(1):114, 2011.

[99] Jianlin Zhang, Amanda Felder, Yujie Liu, Ling T Guo, Stephan Lange, Nancy D Dalton, Yusu Gu, Kirk L Peterson, Andrew P Mizisin, G Diane Shelton, et al. Nesprin 1 is critical for nuclear positioning and anchorage. *Human molecular genetics*, 19(2):329–341, 2009.

[100] Qiuping Zhang, Cassandra D Ragnauth, Jeremy N Skepper, Nathalie F Worth, Derek T Warren, Roland G Roberts, Peter L Weissberg, Juliet A Ellis, and Catherine M Shanahan.